# Impairment-Aware Resource Allocation in Translucent Optical Networks

by Juzi Zhao

A Dissertation submitted to

The Faculty of

The School of Engineering and Applied Science
of the George Washington University in partial satisfaction of the requirements
for the degree of Doctor of Philosophy

May 18, 2014

Dissertation Director
Suresh Subramaniam
Professor of Engineering and Applied Science

The School of Engineering and Applied Science of The George Washington University certifies that Juzi Zhao has passed the Final Examination for the degree of Doctor of Philosophy as of March 31, 2014. This is the final and approved form of the dissertation.

# Impairment-Aware Resource Allocation in Translucent Optical Networks

Juzi Zhao

Dissertation Research Committee:

Suresh Subramaniam, Professor of Engineering and Applied Science, Dissertation Director

Milos Doroslovacki, Associate Professor of Engineering and Applied Science, Committee Member

Maite Brandt-Pearce, Professor of The Charles L. Brown Department of Electrical and Computer Engineering, Committee Member

## Dedication

To my family and Lab634.

## Acknowledgement

I would like to thank my advisor, Professor Suresh Subramaniam, for his guidance and encouragement throughout the past five years. He has been involved in every step of my research and has provided me support on every detailed problem. His knowledge about the newest networking technology trends have helped me to focus on important and timely problems to solve. His technical and editorial advice and infinite patience have been essential for my research papers. I feel privileged to have the opportunity to study under him.

I thank Professors Maite Brandt-Pearce, Milos Doroslovacki, Tian Lan and Howie Huang for serving on my Ph.D. dissertation committee. I have coauthored five research papers with Professor Brandt-Pearce, and my research has benefited immensely from her insightful comments.

I gratefully acknowledge the support of NSF (through grant CNS-0915795), which sponsored my research.

I thank my friends, Yu Xiang, Qianyi Zhao, Jia Sheng, Jingxin Wu, Hang Liu, Yongbo Li, Huachuan Wang, Wenhui Zhang, Chong Liu, Xin Xu, Jie Chen, Fan Yao, Ron Chiang and all others, for their friendship and for making my stay here at GWU a wonderful and unforgettable one.

Last, but not least, I thank my parents for their selfless love and support throughout my life.

## Abstract

Impairment-Aware Resource Allocation in Translucent Optical Networks

Wavelength Division Multiplexing (WDM)-based optical networks are ideal candidates for core backbone networks because of their ability to carry large amounts of traffic. Optical amplification has increased the reach of long-haul optical links. Nevertheless, it is impossible today to construct a truly optical network without converting optical signals to electrical signals and regenerating them, because of the deleterious effects of physical impairments such as amplifier noise, dispersion, and non-linear effects such as four-wave mixing and cross-phase modulation. Regenerators (called 3R regenerators because of their function of reamplification, retiming, reshaping) can clean up the accumulated impairments by performing an Optical-Electrical-Optical (OEO) conversion and processing the electrical signal. Being expensive devices, these regenerators are expected to be sparsely located in the network, and networks with sparse regeneration capabilities are called translucent optical networks. Modern-day optical network customers (which are mainly core network routers) demand connections with heterogeneous bandwidth requirements. A Mixed Line Rate (MLR) optical network serves this purpose very well.

Next-generation optical transport networks are also likely to include multiple domains with diverse technologies, protocols, granularities, and carriers. In such networks, the problem of routing and wavelength assignment (RWA) aims to find an adequate route and wavelength(s) for lightpaths carrying end-to-end service demands subject to scalability constraints. The first part of this dissertation presents our work on resource allocation algorithms for single-domain and multi-domain translucent optical networks.

The second part of the dissertation addresses problems on a new technology - elastic optical networking through Optical Orthogonal Frequency-Division Multiplexing

(OOFDM). A specific problem that we consider is the impairment-aware embedding of virtual networks in an elastic optical network. Virtualization improves the efficiency of networks by allowing multiple virtual networks to share a single physical network's resources.

The last part of the dissertation presents new analytical models to calculate the connection blocking probability for three typical regeneration node allocation policies. The first policy allocates regeneration nodes when the lightpath needs either regeneration or wavelength conversion; while the other two allocation policies allocate regenerators only for one of the two reasons.

# Table of Contents

**Dedication** iii

**Acknowledgement** iv

**Abstract** v

**Contents** vii

**List of Figures** x

**List of Tables** xiv

**1 Introduction** 1

1.1 WDM Optical Networks . . . . . 1

1.1.1 Multi-domain Optical Networks . . . . . 1

1.1.2 Mixed Line Rate Optical Networks . . . . . 2

1.2 Network Virtualization . . . . . 2

1.3 OOFDM-based Optical Network . . . . . 3

1.4 Analytical Models for Blocking Probability . . . . . 3

1.5 Contributions . . . . . 4

**2 Cross-layer RWA in Translucent Optical Networks** 6

2.1 Related Work . . . . . 6

2.2 Network Model and Definitions . . . . . 7

2.2.1 Physical Impairment Model . . . . . 8

2.2.2 Traffic Model . . . . . 9

2.3 RWA Algorithms . . . 10
2.3.1 Selection of Candidate Path Set . . . 10
2.3.2 Routing and Wavelength Assignment Algorithms . . . 12
2.4 Simulation Results . . . 16
2.4.1 Performance Comparison of Algorithms . . . 16
2.4.2 Blocking vs. Number of OEO Converters . . . 19
2.4.3 Blocking vs. Number of Alternate Paths . . . 19
2.5 Conclusions . . . 20

**3 Inter-domain QoT-aware RWA 23**
3.1 Related Work . . . 23
3.2 Network Model and Definitions . . . 24
3.3 RWA Algorithms for Inter-Domain Connections . . . 25
3.3.1 BRPC Framework . . . 25
3.3.2 Domain Sequence Selection . . . 26
3.3.3 RWA Algorithm per Domain PCE . . . 27
3.3.4 QoT-aware BRPC . . . 29
3.3.5 Full-Info . . . 32
3.4 Simulation Results . . . 32
3.5 Conclusion . . . 33

**4 QoT-aware GRWA for MLR optical networks 36**
4.1 Related Work . . . 36
4.2 Network Model . . . 37
4.2.1 MLR Model . . . 37
4.2.2 3R Model . . . 38
4.2.3 QoT Model . . . 38
4.2.4 Grooming Model . . . 38
4.2.5 Splitting Model . . . 38
4.2.6 Performance Metrics . . . 39
4.3 Algorithms . . . 40

4.3.1 Logical Graph (LG) . . . 40
4.3.2 Shortest Path (SP) . . . 44
4.3.3 Logical Graph-single path (LG-single path) . . . 45
4.4 Simulation Results . . . 46
4.4.1 Performance Comparison of Algorithms . . . 47
4.4.2 Blocking vs. Number of OEO Converters . . . 49
4.5 Conclusion . . . 51

**5 Virtual Topology Mapping in Elastic Optical Networks 54**
5.1 Model and Problem Statement . . . 54
5.1.1 Virtual Optical Network Problems . . . 54
5.1.2 OOFDM . . . 55
5.1.3 Network Model and Notation . . . 56
5.1.4 Problem Statement . . . 56
5.2 Algorithms . . . 57
5.2.1 ILP Formulation . . . 58
5.2.2 Static Requests . . . 59
5.2.3 Dynamic Requests . . . 62
5.3 Simulation Results . . . 63
5.3.1 Static Requests . . . 64
5.3.2 Dynamic Case . . . 65
5.4 Conclusions . . . 66

**6 Analytical Performance Modeling 68**
6.1 Related Work . . . 68
6.2 Contributions . . . 69
6.3 Network and Traffic Model . . . 69
6.4 Analytical Models . . . 70
6.4.1 Assumptions . . . 71
6.4.2 Notation . . . 71
6.4.3 Reduced Load Approximation . . . 71

6.4.4 OEO Allocation Policy I: Reach and Wavelength (RW) . . . . 72
6.4.5 OEO Allocation Policy II: Wavelength Only (WO) . . . . . 79
6.4.6 OEO Allocation Policy III: Reach Only (RO) . . . . . 85
6.4.7 Independence Model . . . . . 91
6.5 Numerical Results . . . . . 94
6.6 Conclusions . . . . . 100
6.7 Appendix A . . . . . 102
6.8 Appendix B . . . . . 104
6.8.1 **Calculation of** $M(i, j, d)$ . . . . . 105
6.8.2 **Calculation of** $M'(i, j, d, k)$ . . . . . 106
6.9 Appendix C . . . . . 107
6.10 Appendix D . . . . . 111
6.11 Appendix D . . . . . 112

**7 Conclusions and Future Directions** **117**
7.1 Conclusions . . . . . 117
7.2 Future Directions . . . . . 118
7.2.1 Advanced Reservation . . . . . 118
7.2.2 Survivable Translucent Optical Networking . . . . . 119
7.2.3 Analytical Models . . . . . 120

# List of Figures


2.1 General flowchart for RWA algorithms. . . . . 11
2.2 28-node EON. . . . . 18
2.3 24-node USANET. . . . . 18
2.4 Blocking vs. Load for the EON (single domain case), 5 3R nodes. . . 19
2.5 Blocking vs. Load for the EON (single domain case), 15 3R nodes. . . 20
2.6 Blocking vs. Load for the USANET (single domain case), 15 3R nodes. 21
2.7 Blocking vs. number of OEO converters per 3R node for the EON . . 21
2.8 Blocking vs. number of alternate paths $K$ in the EON . . . . . 22
2.9 Blocking vs. number of alternate paths $K$ in the USANET . . . . . 22

3.1 A multi-domain optical network. . . . . 24
3.2 Example sub-path used to explain the BRPC-DPID algorithm. . . . . 30
3.3 9-domain and EON. . . . . 33
3.4 Blocking vs. load in EON; 3 domains. . . . . 34
3.5 Blocking vs. load in EON; 4 domains. . . . . 34
3.6 Blocking vs. load in 9-domain . . . . . 35

4.1 Path line-rate combinations for different remaining bandwidth requests after grooming. . . . . 41
4.2 Example showing (a) a physical topology and (b) the corresponding logical topology. . . . . 43
4.3 28-node EON . . . . . 47
4.4 24-node USA network (USANET) . . . . . 47
4.5 BW Blocking vs. Erlang load; 10 OEO converters per 3R node in EON 49

4.6 TH Blocking vs. Erlang load; 10 OEO converters per 3R node in EON 49
4.7 BW Blocking vs. Erlang load; 30 OEO converters per 3R node in EON 49
4.8 TH Blocking vs. Erlang load; 30 OEO converters per 3R node in EON 49
4.9 BW Blocking vs. Erlang load; 16 OEO converters per 3R node in USANET . . . . . 50
4.10 TH Blocking vs. Erlang load; 16 OEO converters per 3R node in USANET . . . . . 50
4.11 BW Blocking vs. Erlang load; 34 OEO converters per 3R node in USANET . . . . . 50
4.12 TH Blocking vs. Erlang load; 34 OEO converters per 3R node in USANET . . . . . 50
4.13 BW Blocking vs. Erlang load; 10/6 OEO converters per 3R node in EON . . . . . 52
4.14 TH Blocking vs. Erlang load; 10/6 OEO converters per 3R node in EON 52
4.15 BW Blocking vs. Erlang load; 30/20 OEO converters per 3R node in EON . . . . . 52
4.16 TH Blocking vs. Erlang load; 30/20 OEO converters per 3R node in EON. . . . . 52
4.17 BW Blocking vs. OEO converters per 3R node in EON; load=130 Erlangs . . . . . 53
4.18 TH Blocking vs. OEO converters per 3R node in EON; load=130 Erlangs 53
4.19 BW Blocking vs. OEO converters per 3R node in USANET; load=100 Erlangs . . . . . 53
4.20 BW Blocking vs. OEO converters per 3R node in USANET; load=100 Erlangs. . . . . 53

5.1 6-node network and 14-node DT. . . . . 64
5.2 Request Blocking vs. Load L for arrival rates 20 and 30. . . . . 66
5.3 Bandwidth Blocking vs. Load L for arrival rates 20 and 30. . . . . 67

6.1 An example showing OEO allocation. . . . . 72

6.2 An example showing a path with 3R nodes. . . . . 78
6.3 Example for the Reach Only policy. . . . . 88
6.4 The 28 node EON. . . . . 95
6.5 The 14 node NSFNET. . . . . 95
6.6 The 20 node ring network. . . . . 96
6.7 Comparison of the three OEO allocation policies in the EON; 10 OEOs per 3R node . . . . . 96
6.8 Comparison of the three OEO allocation policies in the NSFNET; 10 OEOs per 3R node . . . . . 97
6.9 Comparison of the three OEO allocation policies in the Ring; 10 OEOs per 3R node. . . . . 97
6.10 Model validation and comparison of Two-link and Independence models: EON; RW Policy . . . . . 98
6.11 Model validation and comparison of Two-link and Independence models: NSFNET; RW Policy. . . . . 98
6.12 Model validation and comparison of Two-link and Independence models: Ring; RW Policy. . . . . 99
6.13 Model validation and comparison of Two-link and Independence models: EON; RO Policy . . . . . 99
6.14 Model validation and comparison of Two-link and Independence models: NSFNET; RO Policy . . . . . 100
6.15 Model validation and comparison of Two-link and Independence models: Ring; RO Policy . . . . . 100
6.16 Model validation and comparison of Two-link and Independence models: EON; WO Policy . . . . . 101
6.17 Model validation and comparison of Two-link and Independence models: NSFNET; WO Policy . . . . . 101
6.18 Model validation and comparison of Two-link and Independence models: Ring; WO Policy . . . . . 102
6.19 Blocking vs. load, RW Model . . . . . 102

6.20 Blocking vs. load, RO Model . . . . . 103
6.21 Blocking vs. load, WO Model . . . . . 103

# List of Tables

2.1 Physical Parameters . . . . . 17

4.1 3R node placement and number of transponders . . . . . 46

5.1 Number of Subcarriers for ILP . . . . . 65
5.2 Number of Subcarriers for Static Traffic . . . . . 66

6.1 Basic Notation . . . . . 114
6.2 Notation for paths with two or more links . . . . . 115
6.3 Notation to calculate $\rho_r$ and $\rho_w$ . . . . . 116

# Chapter 1 Introduction

We first briefly review the technologies used in this work, and outline our contributions.

## 1.1 WDM Optical Networks

Wavelength Division Multiplexing (WDM)-based optical networks are widely deployed at the Internet's core because of their ability to carry large amounts of traffic. Optical amplification has increased the reach of long-haul optical links in WDM-based optical networks; yet, physical impairments make it impossible to construct truly optical core networks. To combat these impairments, optical signals are intermittently converted to electrical signals and regenerated, thus ridding the optical signals of accumulated impairments. Networks with sparse regeneration capabilities are called *translucent optical networks*. In physically-impaired networks, the specified Quality of Transmission (QoT) of connections (as exemplified by, say, their Bit Error Rates (BER)) must be satisfied. At the same time, network operators are interested in utilizing the network effectively, or in other words, minimizing the blocking probability of connections.

### 1.1.1 Multi-domain Optical Networks

Next generation optical networks may employ a variety of technologies, protocols, granularities, and management systems, and thus may be logically divided into multiple domains. End-to-end services are carried over lightpaths (that may be regenerated within the optical network) that may traverse multiple domains. Because of scalability constraints, the scope of network state information (e.g., topology, wavelength

availability) may be limited to within a domain. In such a case, some state information may have to be explicitly exchanged among the domains to facilitate the routing and wavelength assignment (RWA) process with the aim to find an adequate route and wavelength(s) for lightpaths carrying end-to-end service demands. The challenge is to determine which information is the most critical, and make a wise choice for the path and wavelength(s) using the limited information. There are currently three methods for inter-domain routing: Per-Domain, Backward Recursive Path Computation (BRPC) and Hierarchical-PCE (H-PCE) [1, 2]. In the Per-Domain method, path segments are computed within each intermediate domain without sharing path information with other domains. BRPC provides a framework for computing the shortest inter-domain path (with constraints) given a predetermined domain sequence with collaboration among multiple PCEs (Path Computation Elements). In H-PCE, besides the PCEs in each domain, there is a parent PCE, which knows some information about the state of inter-domain links and finds the paths for inter-domain connections.

### 1.1.2 Mixed Line Rate Optical Networks

A Mixed-Line-Rate (MLR) optical network (with 10/40/100 Gbps rates per wavelength) is a good candidate for next generation core backbone, because the multiple line rates are more suitable for heterogeneous traffic requirements; e.g., very high bit-rate demands can be carried by 100 Gbps lightpaths, while lower bit-rate traffic connections can use 10 or 40 Gbps lightpaths.

## 1.2 Network Virtualization

Network virtualization serves as an efficient method to circumvent the Internet's rigidity, in which multiple virtual networks with different topologies and requirements are allowed to share a single physical network. This concept was originally applied to the higher protocol layers, but recent efforts have turned their attention to virtualizing the physical layer [3], which has traditionally been based on Wavelength Division Multiplexing (WDM). These Virtual Optical Networks are expected to handle the

exploding traffic demands in carrier networks in the future. The concept of optical network virtualization, and its implication and challenges for optical network elements and transport technologies are presented in [3]. A possible approach for virtualization of classical wavelength-switched optical network by partitioning and aggregation of optical switching nodes and link capacity is also discussed.

### 1.3 OOFDM-based Optical Network

Concurrent with the emergence of virtualization of the optical layer, new ways of getting around the rigidity and coarseness of the wavelength spectrum in WDM-based transmission are being identified. Efforts have been underway for some time on optical orthogonal frequency division multiplexing (OOFDM), which has been proposed as a viable technology for optical transmission [4]. A novel programmable mechanism for OOFDM which utilizes advanced digital signal processing, parallel signal detection, and flexible resource management schemes for subwavelength level multiplexing and grooming is presented in [5]. OOFDM allows fiber bandwidth to be carved up into subcarriers that have much finer bandwidth granularities than wavelengths. Whereas in WDM the typical wavelength spacing is 25 GHz and wavelength bit-rates are 10, 40, or 100 Gbps, and whole wavelengths are allocated to services, the spacing between subcarriers is only a few GHz and subcarrier bit rates are a few Gbps. An attractive feature of OOFDM is that different bit rates may be achieved by using one of a variety of modulation schemes, and bands of subcarriers may be assigned to a service as needed. In this way, allocated network resources can be matched up with service requirements in a much more flexible manner than in WDM-based networks. Such optical networks have therefore been called *elastic optical networks* [6].

### 1.4 Analytical Models for Blocking Probability

The network performance of optical networks has traditionally been quantified using the connection blocking probability. This is the probability that a new connection or lightpath request is blocked due to the unavailability of resources, and is a

measure of the resources in the network as well as the quality of the resource allocation algorithm. Different resource allocation policies will have different performance. Analytical models have two advantages over simulation: 1) they can provide insight into the effect of various parameters on performance; 2) they can significantly reduce the computational complexity in approximating the blocking performance compared to simulation, especially for low values of blocking probability ($B_N$), where one may need, say, $10/B_N$ connection arrivals. For networks with many resources (e.g., regenerators and wavelengths) subjected to a low traffic load, $B_N$ could be as low as $10^{-7}$, and the simulation would take a substantially longer running time than the analysis. In addition, several simulations with different seeds must be executed in order to ensure the necessary confidence in the results, adding to the computational burden. The analytical approach only requires one computation.

### 1.5 Contributions

In this dissertation, we first address the fundamental problem of QoT-aware routing and wavelength assignment in translucent single line rate optical networks for connections with sources and destinations in a single domain (single-domain connections). The impairment metric (BER) adopted for this problem has the property that a good BER value on each transparent segment of the connection's path is not sufficient to guarantee the quality of the whole path. Several cross-layer heuristics that are based on dynamic programming to effectively allocate the Optical-Electronic-Optical (OEO) converters in sparsely placed regenerators (the placements of regenerators are given) are developed. Then we consider the Multi-Domain single line rate optical networks. The inter-domain RWA algorithm that requires limited amounts of inter-domain network state information is based on the BRPC framework to effectively route the connections across multiple domains. After that, we address the problem of dynamic QoT-aware grooming, routing, and wavelength assignment (GRWA) in MLR translucent optical networks. We propose a QoT-aware algorithm for GRWA (called Logical Graph, LG) that effectively allocates the sparsely available OEO converters to connections, so that the blocking probability is reduced.

In the second part of the dissertation, we study the intersection of two emerging research areas: virtualization and OOFDM. One of the challenges of network virtualization is the virtual topology mapping (or embedding) problem, which assigns substrate physical nodes to virtual nodes, and guarantees the bandwidth requirements of the virtual links. We consider the problem of mapping virtual topologies in elastic optical networks. We present an optimal ILP formulation suitable to small networks and two heuristic algorithms, applicable to larger systems, to map the virtual topology requests onto the physical network, and assign VMs and OFDM subcarriers to virtual network requests.

In the last part of the dissertation, we present complete analytical models for translucent optical networks considering the Transmission Reach constraint (the maximum distance that optical signals can travel before they have to be regenerated) and limited regeneration resources. The models take into account realistic algorithms for wavelength conversion and regenerator allocation. The introduction of regenerator allocation to the problem of Routing and Wavelength Assignment (RWA) brings about new and significant challenges in modeling. Our rigorously derived models strike a balance between complexity and accuracy, as demonstrated through extensive simulation results. The input to the models is the optical network topology with a limited number of OEO converters at selected 3R nodes (which can be used as wavelength converters and/or regenerators when necessary), and the number of wavelengths per fiber. Connections arrive to and depart from the network according to a stochastic process. The output of the analytical performance models is the blocking probability of a connection request.

# Chapter 2 Cross-layer RWA in Translucent Optical Networks

In this chapter, we address the RWA and OEO converter allocation problem for a single-domain translucent optical network.

## 2.1 Related Work

Some recent papers address the routing and wavelength assignment problem for intra-domain connections. The authors of [7] investigate the RWA and regeneration allocation problem by proposing an exhaustive search algorithm (that calculates all feasible lightpaths for the given source-destination, including all the possible combinations for the utilization of available regenerators of the network) with a worst-case time complexity that is exponential in the number of wavelengths and nodes. In [8], the authors propose effective dynamic routing algorithms considering physical impairments and OEO allocation with the assumption that at most one regenerator (except source and destination) can be used by each connection. The authors of [9] propose an online constraint-based routing (CBR) algorithm that allows a more accurate assessment of the (multi-channel) nonlinear degradation effects by taking into account the current network load; the regenerator pools are assumed to have enough OEO circuits, which is not the case in our dissertation. The authors of [10] consider the IA-RWA path selection and regenerator allocation problem, but only discuss the routing and not the wavelength assignment. An IA-RWA algorithm and corresponding Generalized Multi-Protocol Label Switching (GMPLS) extensions are presented in [11], with the assumption that the QoT requirement of the end-to-end lightpath is satisfied as long as the QoT requirement of each transparent segment is satisfied (this

assumption is also made in [7], [8], [12], and [13]). The authors of [14] present a three phase approach for IA-RWA in translucent optical networks, using a distributed optical control plane (some information about the network state was assumed unknown for IA-RWA). An IA-RWA algorithm is proposed in [15] that considers both the path quality and regenerator allocation. We implement this algorithm in this dissertation, and compare it with our dynamic programming method.

## 2.2 Network Model and Definitions

Some nodes in the network are 3R regenerator nodes, i.e., perform reamplification, reshaping, and retiming through an OEO conversion.[1] Each 3R node has a given limited number of OEO converters, which can be used for signal regeneration and/or wavelength conversion. The OEOs are assumed to be available for any connection passing through the 3R node. An OEO that is allocated to a connection cannot be used by another connection until the first connection is torn down. Each link consists of two fibers with $W$ wavelengths each, oriented in opposite directions. The wavelength conversion afforded by an OEO use can be from any wavelength to any other.

We select some nodes to be 3R nodes according to the following algorithm.[2] First, we find the shortest path for each pair of nodes, and count the number of times a node is traversed by these paths. Nodes are sorted in descending order of this number. For each topology, the first $T$ nodes in this order are selected as 3R nodes.

We introduce a few definitions here. A 3R node is called an *OEO node* if it has at least one OEO converter available for use, i.e., if not all OEO converters are being used by ongoing connections. An *allocated OEO node* is an OEO node providing OEO converters to the connection. The transparent path between two arbitrary OEO nodes is called an *OEO segment*. Further, the transparent path between two allocated OEO

[1] We will call these 3R nodes henceforth.

[2] We emphasize that this dissertation's focus is not on regenerator placement. We merely present a reasonable method for selecting the 3R node locations in order to investigate the RWA algorithms' performance.

nodes is called an *allocated OEO segment*. In this definition, the intermediate nodes may have OEO converters, but they are not allocated to the path in question. A *consecutive OEO segment* on a path is the segment between two consecutive OEO nodes (whether they are allocated to the connection or not).

### 2.2.1 Physical Impairment Model

We adopt the physical layer model in [16]. Two kinds of physical impairments are considered: ASE noise and nonlinear impairments. The optical signal to noise ratio (OSNR) can be calculated as $OSNR = \frac{P_{TXch}}{P_{ASE}+P_{NLI}}$, where $P_{TXch}$ is the launched signal power per channel in Watts, $P_{ASE}$ and $P_{NLI}$ are the noise power from ASE and nonlinear impairments (NLIs), respectively, falling within the chosen OSNR noise bandwidth $B_n$.

$P_{ASE}$ can be computed as $P_{ASE} = N_s(G-1)Fh\nu B_n$, where $N_s$ is the number of spans on the path (with one amplifier per span); $G$ is the amplifier gain, which is assumed equal to the power loss of one span; $F$ is the amplifier noise figure; $h$ is Plank's constant; and $\nu$ is the center frequency of the center channel.

The power spectral density (PSD) of dual-polarization NLI noise in a single span, $G_{NLI}$, is given in [16] as:

$$G_{NLI} \simeq \frac{8}{27}\frac{\gamma^2 G_{Tx}^3 L_{eff}^2}{\pi\beta_2 L_{eff,a}}\text{asinh}(\frac{\pi^2}{2}\beta_2 L_{eff,a} R_s^2 N_{ch}^{2\frac{R_s}{\Delta f}})$$

where $\gamma$ is the fiber nonlinearity coefficient; $L_{eff}$ is the effective length in km, defined as $\frac{1-e^{-2\alpha L_s}}{2\alpha}$, $L_s$ is the span length in km, $\alpha$ is the fiber loss coefficient in 1/km, such that signal power is attenuated over a span as $e^{-2\alpha L_s}$; $L_{eff,a} = \frac{1}{2\alpha}$ is the asymptotic effective length. $\beta_2$ is the fiber dispersion (in ps$^2$/km). The WDM signal spectrum $G_{Tx}(f)$ is assumed to be rectangular, i. e., $G_{Tx}(f) = \frac{P_{TXch}}{R_s}$, where $R_s$ is the symbol rate. $N_{ch} = W$ is the number of channels (wavelengths), and $\Delta f$ is the channel spacing.

With the assumption that the NLI noise generated in any given span can be summed in power, i.e., incoherently [17], with the NLI noise generated in any other

span, we can get $P_{NLI} = G_{NLI}B_nN_s$. The interested reader is referred to [16] and [17] for further details.

For the DP-QPSK (Dual Polarization-Quadrature Phase Shift Keying, also referred to as Polarization Multiplexed (PM)-QPSK) modulation format used in this dissertation, the BER for an OEO segment is computed by

$$BER = \frac{1}{2}\text{erfc}\left(\sqrt{\frac{SNR}{2}}\right). \tag{2.1}$$

where $SNR = OSNR \times \frac{Bn}{Rs}$. So the BER is only a function of the number of spans (it is wavelength independent since the NLI values are for the worst case, i.e., all channels are assumed "on"), therefore can be precomputed and saved in a look-up table.

If a path has multiple allocated OEO segments, the end-to-end BER is calculated by assuming independent bit errors as:

$$BER = 1 - \prod_i (1 - BER_i), \tag{2.2}$$

where $BER_i$ is the BER for allocated OEO segment $i$.

Although here the BER of a transparent segment is only a function of the number of spans, our algorithms can deal with more complex QoT models (e.g., the BER of each transparent segment is also dependent on the wavelength assigned to the lightpath and the QoT of existing connections is affected by new connections), as we did in [18] and [19].

### 2.2.2 Traffic Model

Bidirectional connection requests (each requires a wavelength per direction) between a pair of nodes $(s, d)$ randomly arrive to and depart from the network. The same specified BER is required for all connections. A RWA algorithm returns a path and one or more wavelengths and OEO allocations for a connection. A connection can be blocked because the RWA algorithm cannot find a path with either: (a) a wavelength on each allocated OEO segment of the path (*path blocking*), or (b) end-to-end BER that satisfies the BER requirement (*QoT blocking*).

## 2.3 RWA Algorithms

The general flowchart for all algorithms (except algorithm Auxiliary Graph (AG)) is shown in Fig. 2.1. Suppose a connection request between source $s$ and destination $d$ with a specified BER requirement arrives. An ordered path set $P'$ (sorted by increasing order of path length) is pre-computed offline for each $s$-$d$ pair. (For simplicity, we omit the subscript $s$-$d$ from all variables.) These are the paths from which every algorithm draws its candidate paths; they may be computed in a variety of ways.

Given the set $P'$, a candidate ordered set of paths $P \subseteq P'$ is selected by the algorithm according to its own criteria, which will be detailed hereafter. For each path $p \in P$, the algorithm checks $p$ according to its own satisfactory performance criteria (specified in 2.3.1 below). If $p$ is deemed not satisfactory by the algorithm, the next path is checked, and so on, until all paths in $P$ are tried. If a satisfactory path is found by the algorithm, the path and the associated wavelength(s) are passed to the *QoT checker*. The QoT checker computes the end-to-end BER of the incoming connection with this proposed path and wavelength(s). If the BER is adequate, the incoming connection is set up; otherwise it is blocked. The various algorithms differ in: (a) the computation of the candidate path set $P$, and (b) the selection of the path and wavelength(s) to be passed to the QoT checker.

### 2.3.1 Selection of Candidate Path Set

We use the following methods for selecting the candidate path set $P$ in the various RWA algorithms.

- Plain: Here, the first (shortest) $K$ paths in $P'$ are selected to be included in $P$.
- Seg: The BER requirement in the network imposes an upper limit on the length of a transparent path, (or equivalently, on the number of spans), often called the *transmission reach*. Let the maximum number of spans allowed be $L$. In this method, all paths with more than $L$ spans between any pair of consecutive 3R nodes on the path are discarded. The remaining paths are sorted by increasing

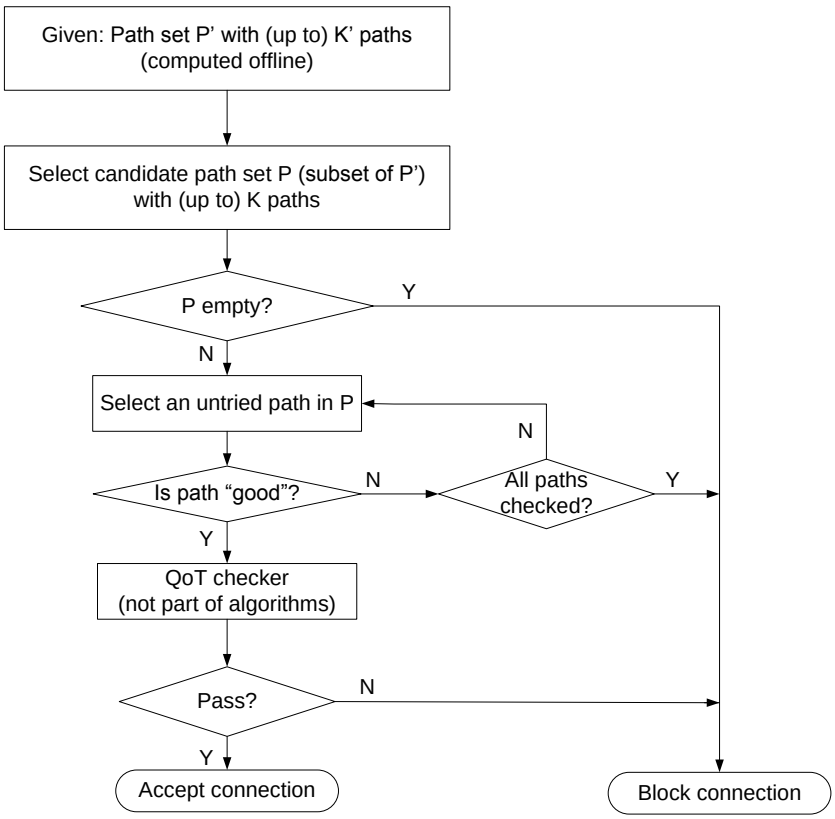


Figure 2.1: General flowchart for RWA algorithms.

length, and the first $K$ of these form $P$. Note that the limit on the number of spans and the path set $P$ can be computed offline.

- Min: This method is used by the algorithm in [15]. Here, the first path in $P$ is the shortest path (i.e., first path in $P'$); the other paths are sorted by increasing value of $(1+S)\times D$, where $S$ is the number of shared links with the previously selected paths, and $D$ is the path length. Once again, $P$ can be computed offline.

- Online: Discard the paths in which any consecutive OEO segment has no free wavelength and/or the segment has more than $L$ spans. Then sort the remaining paths by increasing length. Note that this is an online method because it considers the availability of OEO converters at 3R nodes and wavelengths of links (see definitions of OEO node and consecutive OEO segment in Section 2.2).

- RAA: This method is used by the Regenerator Availability Advertisement (RAA) algorithm in [11]. $P'$ consists of all paths that have either the same number of hops as the shortest path or one more hop than the shortest path. An available transparent lightpath is searched within $P'$. If no transparent lightpath is available, the path characterized by the maximum number of available regenerators is selected. Note that this is also an online method because it considers the availability of wavelengths on links.

For Plain, Seg, Min and Online methods, $P'$ consists of (up to) $K'$ paths (where $K'$ is a parameter) for each $s$-$d$ pair. In this dissertation, it is assumed that these are the $K'$ shortest paths (based on actual link lengths) computed using Yen's algorithm [20] (sorted by increasing length). Note that there may not exist $K'$ paths between $s$ and $d$, which is why we say "up to $K'$" paths above.

### 2.3.2 Routing and Wavelength Assignment Algorithms

*QoT-Guaranteed algorithm (QoT-G)*

This is a non-QoT-aware algorithm that completely ignores physical impairments in selecting the path, and is used as a reference algorithm. The candidate path set is formed using the Plain method. Given a candidate path $p_i \in P$, OEO allocation and wavelength assignment on $p_i$ are done as follows. Starting from node $s$, the longest wavelength-continuous OEO segment that is possible on $p_i$ is selected (nodes $s$ and $d$ are assumed to be dummy OEO nodes). If there is more than one wavelength available on the segment, then the lowest index available wavelength is chosen (First-Fit WA). Suppose the segment terminates at node $k$. If $k = d$, then the algorithm terminates; otherwise, another longest wavelength-continuous OEO segment starting from node $k$ is found and the FF wavelength is assigned, and so on. If there is a consecutive OEO segment on $p_i$ that does not have any available wavelength, then path $p_i$ is considered to have failed the test, and the next path from $P$ is tested, and so on, until all paths in $P$ have been tested. The path that passes the test is sent to the QoT-checker. If the BER requirement is satisfied, the connection is set up with

this path; otherwise it is blocked. The time complexity of QoTG is $O(KNW)$, where $N$ is the number of nodes in the network, and $W$ is the number of wavelengths per fiber.

The next three algorithms are popular algorithms from the literature which we have found to perform well. We have implemented these algorithms, and present performance results comparing these algorithms with our proposed algorithm later in the chapter. These algorithms are reviewed here for completeness and reader convenience.

*Regenerator Availability Advertisement (RAA) [11]*

The candidate path set is formed by using the RAA method above. If the path selected is not a transparent one, then source $s$ designates regenerator nodes in order to partition the path into the minimum number of transparent segments, each with acceptable QoT. We change the algorithm in [11] by passing the selected path and wavelength(s) to the QoT checker that uses Equation (2.2); if the end-to-end BER requirement is not satisfied, the connection is blocked. The time complexity of RAA is $O(ZWN)$, where $Z$ is the number of paths in $P'$.

*Auxiliary Graph (AG) [13]*

The $P'$ and $P$ sets are not used for this algorithm. For each connection $s, d$, construct an auxiliary graph composed of $s$, $d$ and the regenerator nodes. Edges are placed between nodes in the graph if there is a path between them that does not use any regenerators and satisfies the BER requirement. The cost of this edge is assigned as the number of hops on the minimum-hop path between them. Then, find a shortest path from $s$ to $d$ on this auxiliary graph. For finding the wavelength-continuous path of each logical link, index the wavelengths available in the original network. Randomly choose an available wavelength layer (the edges that do not have the selected wavelength available are not considered) and find the minimum-hop feasible path in that layer. If a solution is found at that layer, stop. Else, repeat the procedure with the next indexed wavelength. Similar to the previous one, we also

change the algorithm in [13] by passing the selected path and wavelength(s) to the QoT checker. The time complexity of AG is $O(WN^2T^2)$, where $T$ is the number of 3R nodes.

*Minimum Coincidence and Distance according to Q-factor with Regenerator allocation (MINCODQREG) [15]*

The candidate path set is formed by using the Min method above. Consider a candidate path $p_i \in P$. Starting from node $s$, find the first node on the path, say $k$, at which the BER from $s$ to $k$ on the first available wavelength on the subpath $(s, k)$ (computed by Equation (2.1) using the current network state) exceeds the BER requirement. Then, the algorithm finds the previous (upstream) OEO node (which has not allocated OEO converters to this connection yet), say $k'$, and allocates an OEO at $k'$. Now, check if the cumulative BER (see Equation (2.2)) on the sub-path $(s, k')$ and the sub-path $(k', k)$ satisfies the requirement. If not, go to the previous upstream OEO node $k''$ and allocate an OEO at $k''$ instead of $k'$, and check if the cumulative BER on sub-path $(s, k'')$ and sub-path $(k'', k)$ satisfies the requirement. If the BER requirement is not satisfied for any upstream OEO node, then path $p_i$ fails, and the next candidate path in $P$ is taken up. Otherwise, the algorithm continues from the upstream node where an OEO is allocated. The algorithm terminates with OEO allocations and wavelength assignments for all the segments on the path of the connection. The time complexity of MINCODQREG is $O(KTNW)$.

We also implemented the algorithm proposed in [12]. This algorithm gave worse results than either RAA or AG in all cases tested, so we do not present it here. We next present our proposed intra-domain RWA algorithm.

*QoT-aware Dynamic Programming algorithm (DP)*

We form $P$ using each of Plain, Seg, Min and Online methods for selecting the candidate path set, and call the corresponding algorithm DP-Plain, DP-Seg, etc. For each $p \in P$, we obtain the wavelength and OEO node allocations satisfying the BER requirement using the minimum number of OEO nodes along $p$, if this is possible. If

so, the connection is accepted and established (since it will certainly pass the QoT checker); otherwise, this path fails, and the algorithm proceeds to assign wavelengths and OEOs for the next path in $P$, and so on. The critical part of the algorithm is in finding the wavelength(s) and minimum OEO allocations on path $p$. We develop a dynamic programming approach to achieve this, described next.

Let the OEO nodes on the path from $s$ to $d$ be numbered $1, 2, \ldots, a$. For convenience, let us define $s = 0$, $d = a + 1$, and these are assumed to be dummy OEO nodes. Now, define $B(i, j, k)$ as the minimum obtainable BER on the path from node $i$ to node $j$ with exactly $k$ OEO converters allocated on the path. Further, define $B'(i, j, m, k)$ as the minimum obtainable BER on the path from $i$ to $j$ using $k$ OEO converters, with node $m > i$ being the first converter node (i.e., lowest index converter node). Then, using Equation (2.2) we can write a recursive function as follows:

$$1 - B'(i, j, m, k) = [1 - B(i, m, 0)] \cdot [1 - B(m, j, k - 1)], \tag{2.3}$$

where $i + 1 \leq m \leq j - k, k = 1, 2, \ldots, j - i - 1$, and

$$B(i, j, k) = \min_{m} B'(i, j, m, k). \tag{2.4}$$

if two $m$ indices give the same value of $B(i, j, k)$, select the one with more currently available OEO converters.

The base of the recursion is $B(i, j, 0),\ 0 \leq i < j \leq a+1$, which is simply the BER on the transparent path from $i$ to $j$, obtained using Equation (2.1). When computing $B(i, j, 0)$, if there is no available wavelength on the subpath $i$-$j$, we set its value as infinity. We use the first fit wavelength if more than one wavelength is available, and keep track of which OEO converters are allocated to obtain $B(i, j, k)$. The final $k$ of $B(s, d, k)$ for the connection is chosen as the smallest one (i.e., minimum number of OEOs) which makes the connection's BER satisfactory.

The time complexity of DP-Plain, DP-Seg and DP-Min is $O(KT^4)$. The time complexity of DP-Online is $O(KT^4 + K'NW)$ (since the $K$ candidate paths are found online).

## 2.4 Simulation Results

Connections are assumed to arrive to the network according to a Poisson process. The sources and destinations are uniformly drawn from the network. Each connection is assumed to have a BER requirement of $10^{-3}$. For the assumed physical parameters and for a BER of $10^{-3}$, the maximum number of allowed spans ($L$) on a path without OEO regeneration is 34. We assume $K' = 40$, i.e., up to 40 paths (not necessarily disjoint) are computed offline for each node pair. For each data point in the graphs, we simulated several instances of between 10,000 and 100,000 connection arrivals, and obtained 95% confidence intervals. Table 2.1 shows the physical parameters that were used in the simulation. We present results for two network topologies, the European Optical Network (EON) and USANET, shown in Figs. 2.2 and 2.3, respectively. For EON, when $T = 5$, the 3R nodes are nodes 9, 11, 13, 14 and 19; when $T = 15$, the 3R nodes are nodes 3-5, 7, 9, 11-16, and 18-21. For USANET, when $T = 3$, the 3R nodes are nodes 9, 12, 16; when $T = 15$, the 3R nodes are nodes 6-18, 20 and 22. Except when noted otherwise, there are 10 OEO converters at each 3R node, and $K = 2$ alternate paths are used for DP and MINCODQREG algorithms.

### 2.4.1 Performance Comparison of Algorithms

Figs. 2.4 - 2.6 show the blocking probability versus the network Erlang load for the various algorithms and various parameters. The loads were selected so that blocking probabilities fall in the $10^{-4}$ to $10^{-1}$ range. As expected, QoT-G performs much worse than the QoT-aware algorithms. Interestingly, the blocking for QoT-G stays essentially flat. This can be explained as follows. Recall that QoT-G selects the path and wavelength(s) considering only wavelength availability and not QoT. When the selected path is passed to the QoT checker, there is a high probability that the BER requirement is not satisfied, and hence the connection is blocked. When the load increases, a wavelength-continuous path from $s$ to $d$ becomes harder to find, and therefore, OEO converters are allocated to the connection for doing wavelength conversion. Since these OEO nodes also perform 3R regeneration, the probability

Table 2.1: Physical Parameters

| **Description** | **Value** |
|---|---|
| **Bit rate** | 100 Gbps |
| **Symbol rate** ($R_s$) | 32GBaud |
| **Modulation Scheme** | DP-QPSK (PM-QPSK) |
| **Launched power per channel** ($P_{TXch}^{dB}$) | 0 dBm |
| **WDM grid spacing** ($\Delta$) | 50 GHz |
| **Fiber loss** ($\alpha$) | 0.02533 1/km |
| **Nonlinear coefficient** ($\gamma$) | 1.3 (W km)$^{-1}$ |
| **Chromatic dispersion** ($\beta_2$) | 21.2852 ps$^2$/km |
| **Noise factor** ($F_{dB}$) | 5 dB |
| **OSNR bandwidth** ($B_n$) | 12.48 GHz (0.1nm) |
| **Number of wavelengths per fiber** ($W$) | 80 |
| **Center frequency of the center channel**($\nu$) | 193THz |
| **Span Length** ($L_s$) | 100 km |

that the selected path will be rejected by the QoT checker does not increase.

In general, DP-Online performs the best. As can be seen, DP-Online outperforms the other algorithms by up to 2 orders of magnitude, particularly at lower loads. This points out that both candidate path selection and OEO allocation are important for performance.

Another interesting observation is that DP-Min performs much better than DP-Seg for the 15 3R-nodes case (Fig. 2.5); this is the opposite of what happens with fewer 3R-nodes (Fig. 2.4). What is happening here is that when there are more 3R nodes, a candidate path is more likely to be selected by Seg because it is easier to find

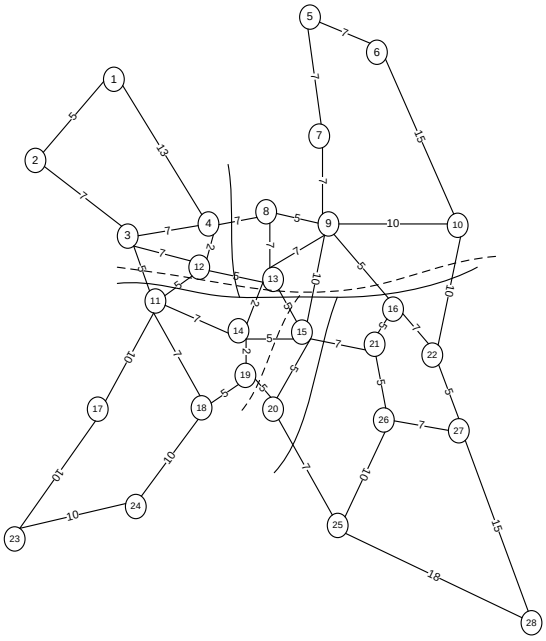

Figure 2.2: 28-node EON. The number on each link corresponds to the number of spans.

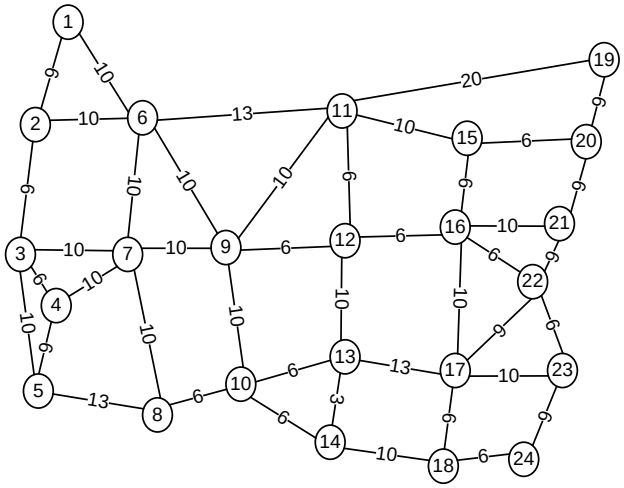

Figure 2.3: 24-node USANET. The number on each link corresponds to the number of spans.

a path where each segment between two consecutive 3R nodes is less than $L$ spans. Many of these paths end up not having an available wavelength, thereby causing large path blocking. This does not happen in the case with few 3R nodes because many of these paths are not likely to be selected as candidates in the first place because a segment between two consecutive 3R nodes on the path has length greater than $L$

spans (due to fewer 3R nodes).

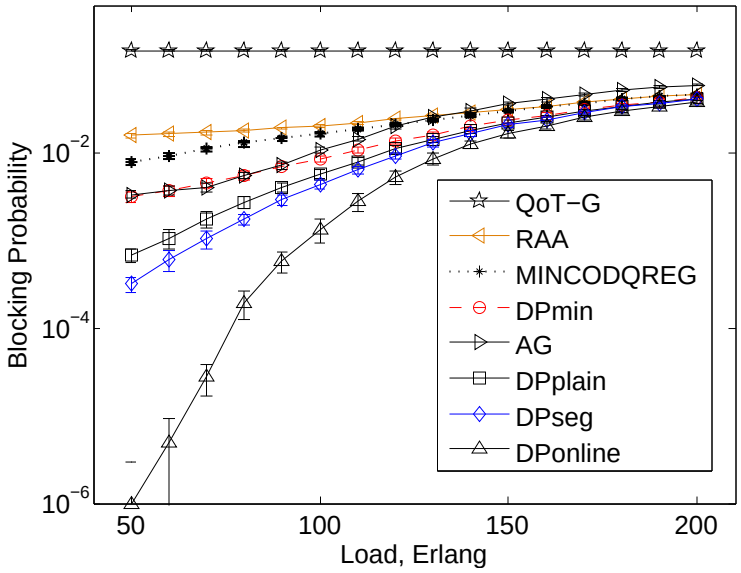


Figure 2.4: Blocking vs. Load for the EON (single domain case), 5 3R nodes. The curves for AG and DP-Min overlap at lower loads.

### 2.4.2 Blocking vs. Number of OEO Converters

The blocking probability is plotted as a function of the number of OEO converters per 3R node in Fig. 2.7 for EON; the results for USANET follow a similar trend. The performance improvement for DP-Online is especially sharp, pointing to its excellent ability to wisely allocate OEO converters. For instance, the blocking probability achieved by DP-Min with 20 OEO converters per 3R node can be achieved by DP-Online with only 15 OEO converters per 3R node, while the blocking probability achieved by DP-Seg with 30 OEO converters per 3R node can be achieved by DP-Online with less than 20 OEO converters per 3R node.

### 2.4.3 Blocking vs. Number of Alternate Paths

We next show in Figs. 2.8 - 2.9 how the number of alternate paths $K$ affects the performance. It is remarkable that while the other algorithms show improved performance as $K$ increases until the performance plateaus, DP-Online is able to

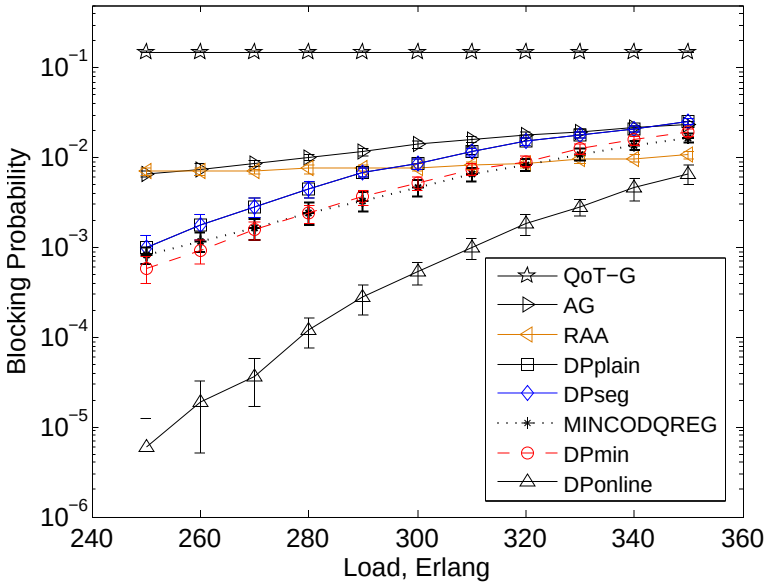


Figure 2.5: Blocking vs. Load for the EON (single domain case), 15 3R nodes. The curves for DP-Plain and DP-Seg overlap. The curves for MINCODQREG and DP-Min overlap.

achieve almost the same performance even with $K = 1$ (with more than one order of magnitude better performance than other algorithms with $K = 1$). The performance of DP-Seg and DP-Online is eventually the same; the primary difference lies in their level of complexity.

## 2.5 Conclusions

In this chapter, we investigated the QoT-aware routing and wavelength assignment problem in single domain translucent optical networks. We proposed an effective polynomial-time heuristic based on dynamic programming, and simulation results showed that this algorithm can allocate OEO converters to connections judiciously, and significantly improves the blocking performance over current methods in the literature. For example, in a 28-node EON network, our DP algorithm performs as much as 2 orders of magnitude better than other algorithms, particularly at lower loads, since the Online method can find a candidate path with enough wavelength and OEO converters to setup the new connection with high probability; and for a

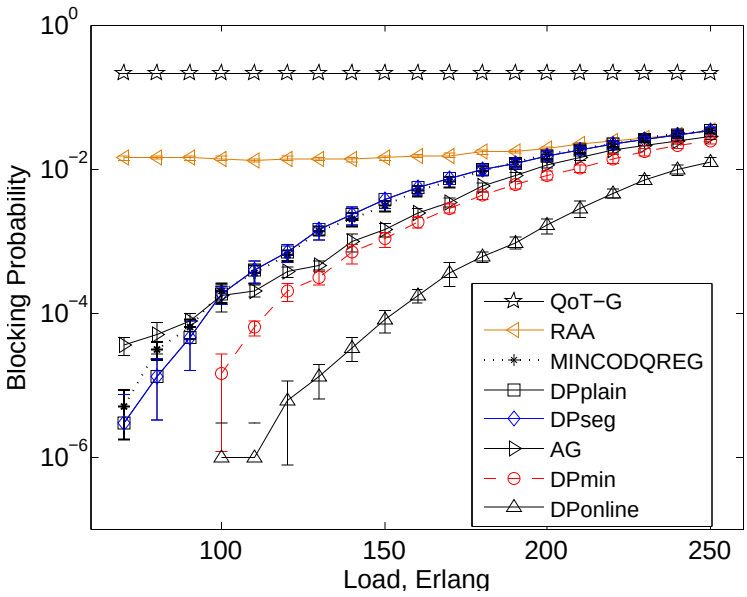


Figure 2.6: Blocking vs. Load for the USANET (single domain case), 15 3R nodes. The curves for MINCODQREG, DP-Plain and DP-Seg overlap.

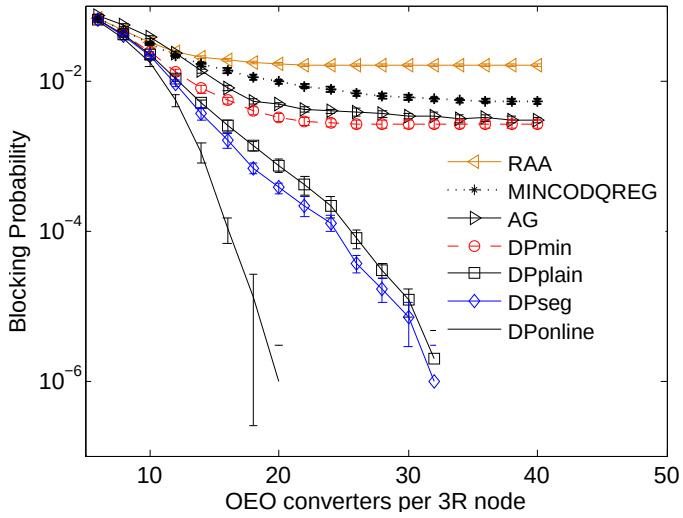


Figure 2.7: Blocking vs. number of OEO converters per 3R node for the EON, 5 3R nodes; load = 150 Erlangs.

specific candidate path, the dynamic programming gives the best OEO converters allocation considering both wavelength availability and BER value.

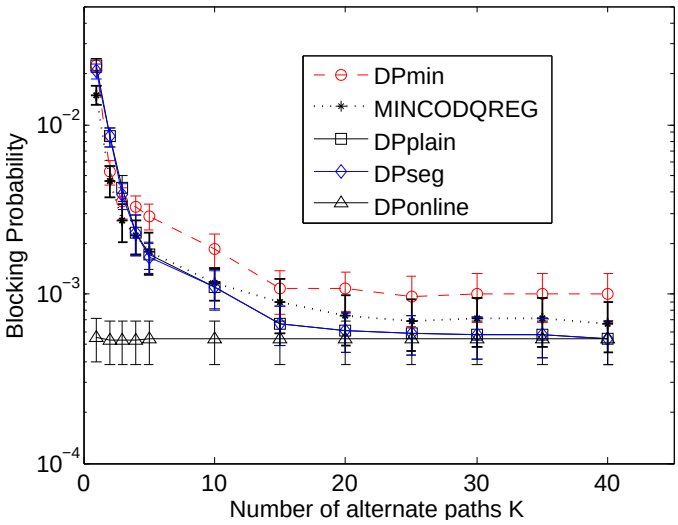


Figure 2.8: Blocking vs. number of alternate paths $K$ in the EON, load = 300, 15 3R nodes. The curves for DP-Plain and DP-Seg overlap.

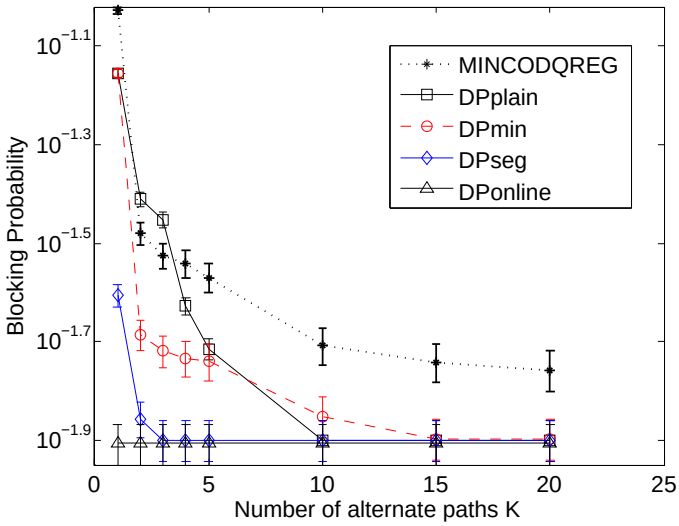


Figure 2.9: Blocking vs. number of alternate paths $K$ in the USANET, load = 50, 3 3R nodes.

# Chapter 3 Inter-domain QoT-aware RWA

The previous chapter focused on a single-domain network. This chapter investigates the impairment-aware RWA and OEO allocation problem in multi-domain networks. Recall that multiple domains may exist due to diverse technologies, protocols, granularities, and carriers. The main implication of multiple domains for our purpose is the limited information sharing between domains. Our main goal is to investigate the impact of information sharing on the network's performance.

## 3.1 Related Work

Several researchers have also studied inter-domain routing recently. The authors of [21] implement, deploy, and experimentally validate three different path computation algorithms: the per-domain, the PCE-based BRPC, and their PCE-based EBRPC (Enhanced BRPC) approach to efficiently address the wavelength continuity constraint. In [1], the authors provide a novel and economical way to disseminate information while performing inter-domain lightpath provisioning. Two novel virtual topology update triggering policies between PCEs with the full-mesh abstraction scheme are proposed in [22]. In [23], the authors propose two solutions based on novel PCE communication protocol messages for PCE-based multi-domain path computation. The authors of [2] propose a hybrid path computation procedure based on the H-PCE architecture and BRPC. However, none of these papers consider physical layer impairments. Among the works that consider impairments, a PCE-based OSNR (optical signal to noise ratio)-aware dynamic restoration in GMPLS (generalized multi-protocol label switching)-enabled multi-domain translucent WSON (wavelength switched optical networks) is proposed in [24], but it does not

specify a method to obtain a predetermined domain sequence that is required by the BRPC procedure, nor the QoT-aware information to be sent among domains. The authors of [25] present a lab-trial of multi-domain path computation using a H-PCE when domain topologies are aggregated as dynamic virtual meshes. In [26], the problem of interdomain dynamic wavelength routing is studied; the end-to-end lightpaths can be set up not only across multiple routing domains but also through optical and regeneration layers. The authors of [27] develop a physical-layer impairment model that encompasses both linear and nonlinear impairments. An information exchange (among different domains) model is also proposed, but no algorithm to find paths for inter-domain connections is given.

### 3.2 Network Model and Definitions

The network includes multiple domains, and there are two kinds of nodes in each domain: interior nodes and border nodes (gateways). Domains are connected together through links between gateways. Interior nodes are directly or indirectly connected to gateways in its corresponding domain. In each domain, there is a PCE with the capability to calculate paths within the domain. Each PCE is assumed to have full information (physical layer-related and wavelength-related) about the links within its domain as well as the inter-domain links terminating at its gateways. Some nodes in the network are 3R nodes. The notations *OEO node*, *allocated OEO node*, *OEO segment* and *consecutive OEO segment* defined in Section 2.2 will be used in chapter.

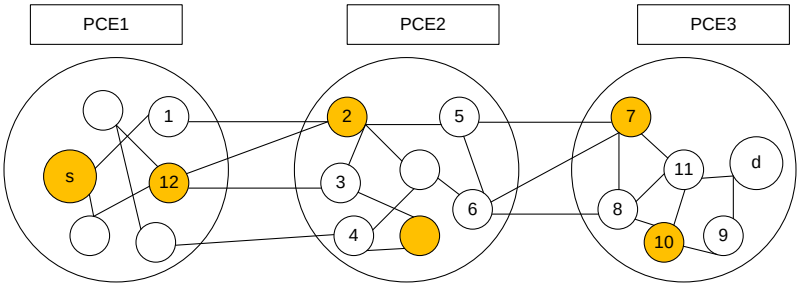


Figure 3.1: A multi-domain optical network. The shaded nodes are 3R nodes.

The same physical impairment model in Section 2.2.1 and traffic model in Section

2.2.2 is adopted for the inter-domain case. The only difference is that in Chapter 2 the source $s$ and destination $d$ of a connection are in the same domain, which is not the case in this chapter.

## 3.3 RWA Algorithms for Inter-Domain Connections

In this section, we consider the RWA for a connection whose source and destination are in different domains, and thus the lightpath assigned to it would traverse multiple domains. Our proposed algorithm is based on the Backward Recursive Path Computation (BRPC) framework, which we summarize below.

### 3.3.1 BRPC Framework

The BRPC framework allows a constrained path to be computed from a source $s$ to a destination $d$ in a multi-domain network, given a predetermined sequence of domains. As the name implies, the path computation actually proceeds from the destination to the source. In BRPC terminology, the border nodes that are connected to the next domain (i.e., towards the source) in the given domain sequence are called *entry boundary nodes (ENBs)*. Similarly, border nodes in the next domain that are connected to the current domain are called *exit boundary nodes (EXBs)* of the next domain. Given the domain sequence, the PCE in the destination domain sends to the next domain information about the path (e.g., path length) from each of its ENBs to the destination.

We illustrate the procedure with an example using Fig. 3.1. Assume we want to find a path from $s$ to $d$, and the predetermined domain sequence is 1-2-3. For domain 3, its ENBs are node 7 and node 8. Let the path found with node 7 be 7-11-$d$. (PCE3 also finds a path with node 8.) Then these paths from the ENBs to the destination (called Virtual Path Tree) are sent to domain 2. The PCE in domain 2 takes the two paths 7-$d$ and 8-$d$ as two links 7-$d$ and 8-$d$. The ENBs in domain 2 are nodes $2, 3, 4$. Suppose the path found with node 2 is 2-5-7-$d$. Similarly paths from nodes 3 and 4 are also found. Finally, when the source domain is reached, a path from $s$ to $d$ is

found. Suppose it is $s$-1-2-$d$. Then the entire path in this case is $s$-1-2-5-7-11-$d$.

### 3.3.2 Domain Sequence Selection

The BRPC procedure assumes a given domain sequence and leaves the selection of such a sequence to the network planner. Here, we propose the following approach, which depends on the current network state, to find the domain sequence for each new connection. We follow the six steps outlined below:

i) $J$ shortest paths (again using Yen's algorithm) are precomputed for each pair of nodes within the same domain, and from a node in one domain to each of the border nodes of adjacent domains (e.g., in Fig. 3.1, from node 2 to node 7). (Note that, except for possibly one end node, all nodes on a path at this point lie within a single domain.)

ii) For each pair of nodes, find a shortest path (shortest in distance) without any domain loop, but with the distance between any two consecutive 3R nodes no greater than the reach $L$ (recall $L$ is the upper limit on number of spans on transparent segment due to physical impairments). Call the domain sequence of this shortest path the *preferred domain sequence*.

iii) For each pair of domains, $M$ domain sequences are precomputed as follows. A domain graph is created such that each domain is represented by a single logical node, and there is a logical link connecting two logical nodes if there is at least one link with end nodes belonging to these two domains. The weight of a logical link is set to be the reciprocal of the number of physical links between the domains represented by the logical nodes. (This is done so that domain-pairs that have many links between them are favored in the selection of the domain sequence.) Then, for each domain-pair, $M$ shortest paths in the logical domain graph are found based on these link weights.

iv) Consider a connection request with source $s$ and destination $d$. Recall that $J$ shortest paths have been precomputed between every node in a domain and every border node in adjacent domains. We say that a domain $D_b$ with border node $b$ is *reachable* from the source $s$ (respectively, destination $d$) if at least one of the $J$ paths from $s$ (respectively, $d$) to $b$ satisfies the two conditions: (a) every segment between

consecutive OEO nodes on the path has no more than $L$ spans, and the segment from $b$ to its nearest OEO node (on path from $s$ (or $d$) to $b$) has no more than $L - L'$ spans, where $L'$ is a parameter called the *Reach-margin*, for considering the distance from the border node to a potential OEO node, and (b) each of these segments has at least one wavelength available. The set of reachable domains is computed by the source PCE and destination PCE respectively, and this information computed by the source PCE is sent to the destination PCE.

v) Of the $M$ candidate domain sequences between the source domain $D_s$ and the destination domain $D_d$, a candidate domain sequence is discarded if the source or destination cannot reach its corresponding adjacent domain in the virtual domain topology. For example, suppose $D_s$-1-2-3-$D_d$ is a candidate sequence; it will be retained if $d$ can reach domain 3 and $s$ can reach domain 1, otherwise the domain sequence will be discarded.

vi) If the preferred domain sequence still remains after the last step, this sequence is assigned to the connection; otherwise, the domain sequence (among $M$) that includes the most number of 3R nodes for domain pair $D_s$ and $D_d$ is assigned.[1]

### 3.3.3 RWA Algorithm per Domain PCE

We first present an algorithm (DPID), it is a variant version of our single domain algorithm DP-Online, which is performed by the PCE at each domain of the domain sequence to find a path from each of its ENBs to the destination (from source to destination for the source PCE). Each PCE (except for the destination PCE) has several candidate paths to the destination from the ENBs of the previous domain. These paths are considered as logical links from these ENBs to the destination by the current domain. The current domain PCE does an "intra-domain" routing to find a path from each of the domain's ENBs to the destination. (Note that PCE also has the information about inter-domain links terminating at its domain's border nodes.) For example, in Fig. 3.1, consider the node pair $s$-$d$ with domain sequence 1-2-3; the

[1]Note that this might not give the minimum number of domains. We did try the sequence with minimum number of domains, but our simulation results are better with the current sequence.

destination domain PCE3 finds intradomain paths from node 7 to $d$, and node 8 to $d$ (one path per ENB). These paths and some information about them (to be specified in the next section) are signaled to PCE2; PCE2 assumes it has logical links 7-$d$ and 8-$d$ and it uses the DPID algorithm to find the "intra-domain" paths from nodes $2, 3, 4$ to $d$. Finally, PCE1 finds a path from $s$ to $d$ in domain 1 with logical links 2-$d$, 3-$d$, and 4-$d$ (if the corresponding paths are possible). The algorithm has two steps.

*Candidate path selection*

The candidate path for DPID is found as follows. Recall again that there are $J$ precomputed paths for each pair of nodes within a single domain, and from a node to all border nodes in other adjacent domains. This part is similar to the Online method with $K = 1$.

From an ENB of the current domain (or the source node) to $d$ through each of the previous domain's ENBs, any path (assuming the lengths and free wavelengths of the logical links are known), in which any consecutive OEO segment has no free wavelength and/or if the segment length greater than $L$ spans is discarded (and $L - L'$ spans constraint for the OEO segment from the next domain's EXBs to the first OEO node (on the path from ENB to d)). The inter-domain links from this ENB to the next domain's EXBs are also considered; e.g., in Fig. 3.1, if ENB node 2 is under consideration, the wavelength availability and length of the inter-domain link 1-2 and 12-2 are also taken into consideration, and node 2 serves as a wavelength converter and regenerator if necessary and possible. The shortest of the remaining paths is selected; thus we get at most one qualified path through each of the previous domain's ENBs. The final candidate path is the shortest of these. For example, in Fig. 3.1, PCE2 receives two paths, one is 7-$d$ and another is 8-$d$ from PCE3. PCE2 checks the $J$ paths for 2-7 and 2-8, and selects one path each for 2-7-$d$ and 2-8-$d$; the final path 2-$d$ is the shorter one of the two.

*Wavelength and OEO allocation*

This part of DPID is almost the same as DP. Let the chosen path from an ENB, say $x$, to the destination be $p_x$. Assume the first allocated OEO node on the virtual link from the previous domain's ENB to the destination be node $y$ ($y = d$ if the current domain is the destination domain or if there is no allocated OEO node on the virtual link). The same procedure for calculating the BER and allocating OEOs as the DP algorithm is used for the subpath $x$-$y$. Let the OEO nodes on the path from $x$ to $y$ be numbered $1, 2, \ldots, a$, with $x = 0$, $y = a+1$ as dummy OEO nodes. Equations (2.3) and (2.4) are used to find the values of $B(i, j, k)$ and $B'(i, j, m, k)$ with various $i, j, k, m$. The difference between DP and DPID is that, for getting $B(0, a+1, k)$ from $B'(0, a+1, m, k)$, $m$ is selected as the smallest index with $B'(0, a+1, m, k)$ less than or equal to the BER requirement.

### 3.3.4 QoT-aware BRPC

We now present an algorithm for finding an end-to-end path from $s$ to $d$ with three versions that utilize different types of information signaled by the previous domain's PCE about the paths from that domain's ENBs to the destination.

*BRPC-DPID*

As we describe the algorithm, we use the illustrative example shown in Fig. 3.1. We are given a domain sequence (e.g., 1-2-3 in Fig. 3.1) for $s$-$d$. First, the destination PCE uses the DPID algorithm to find a path from each of the ENBs to the destination as described above (e.g., a path from 7 to $d$ by DPID). After that, wavelengths are assigned to every OEO segment except for the first segment. (Assume the path found with node 7 is 7-11-10-9-$d$, and node 10 is the allocated OEO for this path, assign a wavelength to segment 10-$d$; the first segment is 7-10.)

Let $x$ denote an ENB, $y$ denote the end node of first segment; the number of OEOs allocated to the path from $x$ to $y$ is selected as the smallest $k$ with the two properties: (i) $B(0, a+1, k) \leq$ BER requirement, and (ii) the length of the first segment plus the

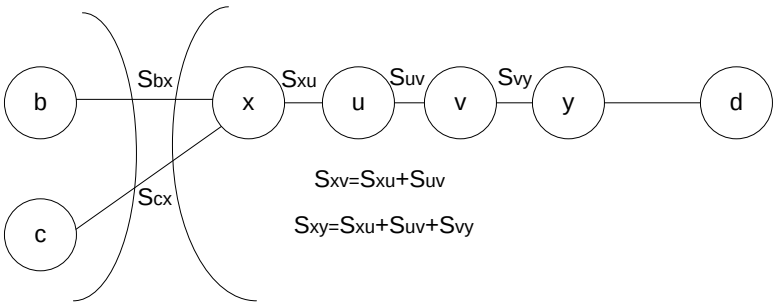


Figure 3.2: Example sub-path used to explain the BRPC-DPID algorithm.

length of the shortest inter-domain link with ENB $x$ (to the EXBs in next domain) is no greater than $L - L'$ spans.

For example, in Fig. 3.2, let $S_{ij}$ denote the length of segment $i$-$j$ on the path. Suppose $S_{bx} < S_{cx}$; and suppose for $k = 1$, OEO node $v$ is the allocated OEO node, thus the first segment is $x$-$v$; for $k = 2$, OEO node $u$ and $v$ are allocated, and the first segment is $x$-$u$. The values of $B(0, a + 1, 0)$, $B(0, a + 1, 1)$ and $B(0, a + 1, 2)$, corresponding to $k = 0, 1, 2$, are checked for property (i) above. For condition (ii), the distances $S_{bx} + S_{xy}$, $S_{bx} + S_{xv}$, and $S_{bx} + S_{xu}$ are checked for $k = 0, 1, 2$, respectively.

Then these paths' information is sent to the next domain of the predetermined domain sequence, and the next domain's PCE takes these paths as links with $d$ as an end node (e.g., 7-$d$ and 8-$d$). For each of its ENBs (nodes 2, 3, 4), the algorithm finds the candidate path from that ENB to $d$, and then uses DPID with the subpath from that ENB to the first allocated OEO node on the received path from the previous domain (it is part of the candidate path). In the above example, if the path from node 7 is path 7-11-10-9-$d$, and node 10 is the allocated OEO, and the candidate path for node 2 includes node 7, then PCE2 executes DPID with subpath from node 2 to node 10 (note that the subpath from node 7 to node 10 is not known to PCE2, it is just a logical link). This procedure is repeated until the source domain is reached; then the source PCE finds the final path from $s$ to $d$. The source PCE chooses the OEO allocation with the minimum $k$ which makes $B(0, a + 1, k)$ no larger than the BER requirement.

In BRPC-DPID, the following information about the path from an ENB $x$ is

signaled by the domain's PCE to the next domain's PCE:

$S_{xd}$ The total path length from the ENB $x$ to the destination (used to find the candidate path in DPID)

$I_x$ Binary value to show the current availability of OEOs at ENB $x$

The following are used by DPID to find the BER:

$S'_{xd}$ The first-segment length on the path from $x$ to $d$ (see above for definition of first segment)

$W_x$ The available wavelengths on the first segment.

$b_x$ The BER of the subpath from the first allocated OEO node on the current found path to the destination (used by next domain to check the path's BER)

To illustrate these definitions, consider Fig. 3.1 again. Assume that the path found with node 7 is 7-11-10-9-$d$, and node 10 is the allocated OEO node for this path; then the first segment is 7-10, and the length from 7 to $d$ ($S_{7d}$), the length from 7 to 10 ($S'_{7d}$), the available wavelengths on segment 7-10 ($W_7$), the BER of subpath 10-$d$ ($b_7$), and the OEO availability of node 7 ($I_7$) are sent to PCE2.

*BRPC-DPID-noBER*

This algorithm is the same as BRPC-DPID except that the $b_x$ information is not explicitly signaled to the next domain. Instead, $b_x$ is simply assumed to be the BER values for distance $S_{xd} - \lceil \frac{S_{xd}}{L-L'} \rceil (L - L')$ (recall that based on our physical layer impairment model, BER is a function of spans) by the next domain's PCE.

*BRPC-DPID-noBER-noLength*

This is the same as BRPC-DPID-noBER, except that $S'_{xd}$ is not sent to the next domain. In the absence of this information, the next domain's PCE simply assumes $S'_{xd}$ to be a fixed value, say $H$ spans, for all $x$. If $H > S_{xd}$, the PCEP assumes $S'_{xd} = S_{xd}$.

### 3.3.5 Full-Info

This is a reference algorithm that assumes that the whole network is a single domain (i.e., no restriction on information availability) for all of the inter-domain connections and runs the DP-Online algorithm for path computation (with $K = 1$).

## 3.4 Simulation Results

Connections are assumed to arrive to the network according to a Poisson process. The source and destination are uniformly picked from different domains. Each connection is assumed to have a BER requirement of $10^{-3}$. For each data point in the graphs, we simulated several instances between 10,000 and 100,000 connection arrivals, and obtained 95% confidence intervals. The physical parameters are in Table 2.1.

For 3R node selection, the same method in Section 2.2 is used here, except that if some domain has no 3R node after this selection, the node with maximum count number in that domain is selected as a 3R node. The $L$ is set to 34, and $J = 40$.

To study the performance of inter-domain RWA algorithms, we present results for two network topologies, the European Optical Network (EON) (Fig. 2.2) and a larger 9-domain synthetically-generated network (Fig. 3.3). The number of candidate domain sequences $M = 5$. The Reach-margin $L'$ is set to 5. There are $T = 10$ 3R nodes in the EON (nodes 7, 9, 11-16, 19 and 21). For the 9-domain network, there are $T = 20$ 3R nodes (nodes are shown in Fig. 3.3). There are 10 OEO converters at each 3R node.

Results showing blocking probability versus the total network load in Erlangs are presented in Figs. 3.4 - 3.6. For BRPC-DPID-noBER-noLength, the parameter $H$ is selected to minimize the average blocking probability in the range $1 \leq H \leq L$; for EON, $H = 30$ spans, for the 9-domain topology, $H = 23$ spans.

There is a significant difference between the performance of BRPC without first segment length information (BRPC-DPID-noBER-noLength), and the one that uses this information (BRPC-DPID-noBER and BRPC-DPID) that suggests that it is

necessary to signal this information to the next domain in order to achieve good performance. Also, providing the BER information is not so important until the network becomes large. There is also a significant difference between BRPC-DPID and Full-Info indicating that other information (e.g., more than one logical path with corresponding information sent to the next domain's PCE) may be needed as well in order to achieve good performance. Perhaps the domain sequence selection method can be improved, such as by using alternative sequences per connection.

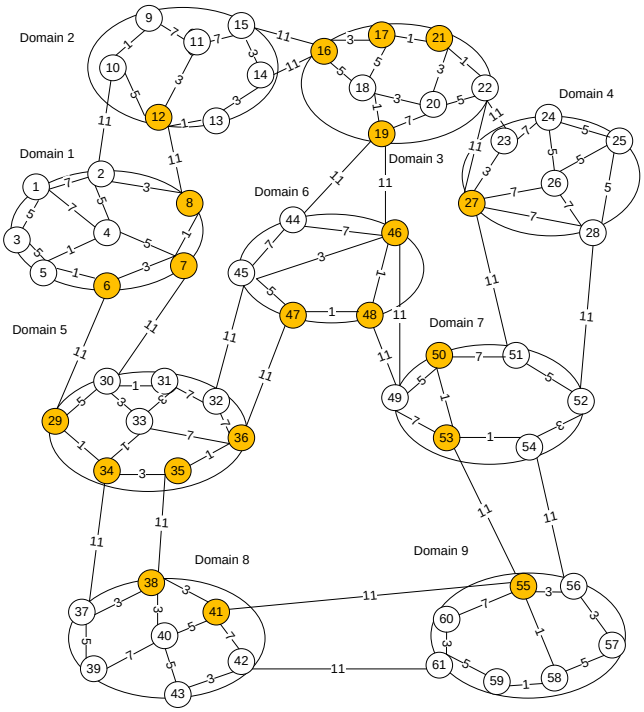


Figure 3.3: 9-domain and EON. The number on each link corresponds to the number of spans. The shaded nodes are 3R nodes.

## 3.5 Conclusion

In this chapter, we proposed effective QoT-aware BRPC algorithms for RWA in multidomain optical networks. It is shown by simulation that information about BER is not very significant to be distributed among domains for path calculation. However, the information about the length of the first segment in the previous domain is an important piece of information, it can improve the blocking probability by up to 70%,

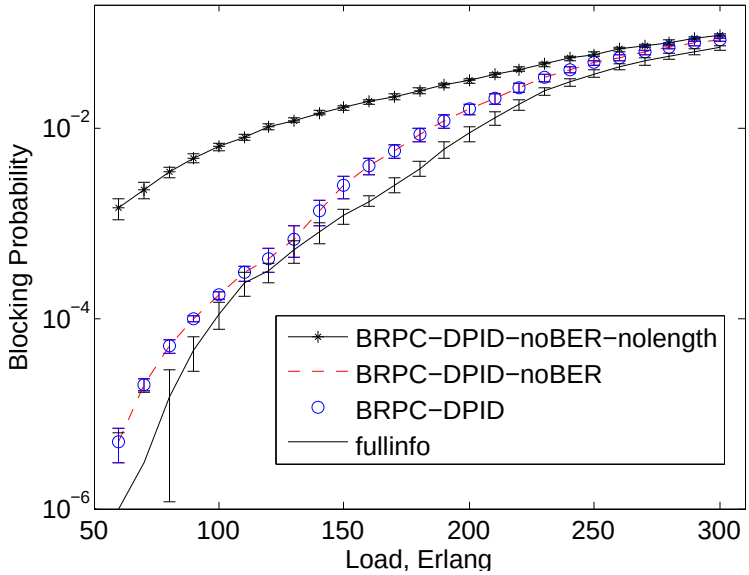


Figure 3.4: Blocking vs. load in EON; 3 domains. The curves for BRPC-DPID-noBER and BRPC-DPID overlap.

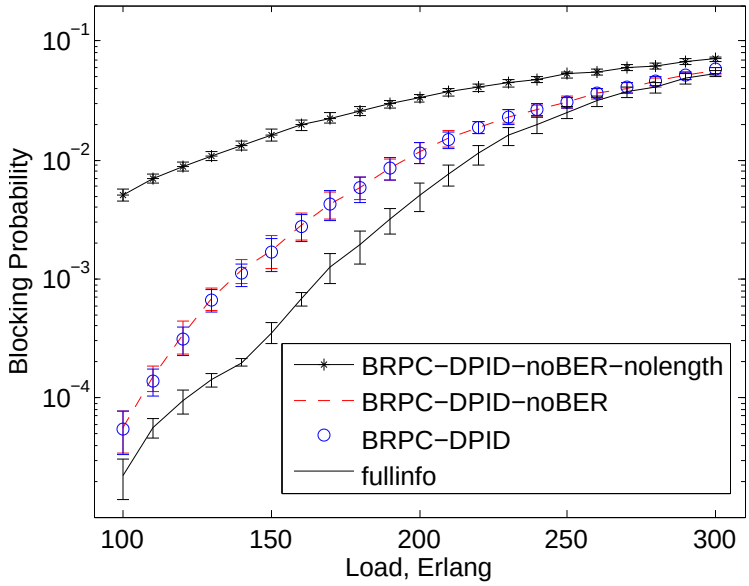


Figure 3.5: Blocking vs. load in EON; 4 domains. The curves for BRPC-DPID-noBER and BRPC-DPID overlap.

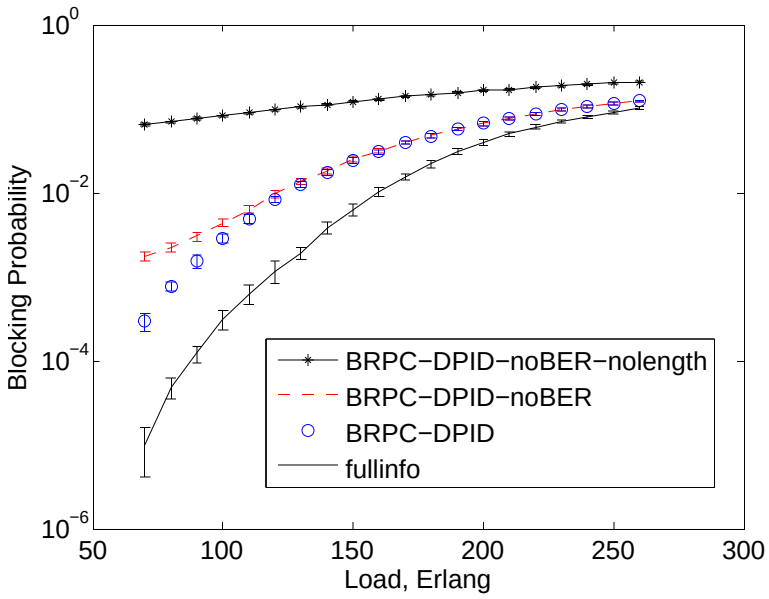


Figure 3.6: Blocking vs. load in 9-domain. The curves for BRPC-DPID-noBER and BRPC-DPID overlap.

since it affects whether an OEO converter should be allocated as a regenerator.

# Chapter 4 QoT-aware GRWA for MLR optical networks

In this chapter, we consider QoT-aware Grooming, Routing, and Wavelength Assignment (GRWA) of connections in a mixed-line-rate (MLR) translucent optical network. Cross-layer heuristics based on Logical Graph and Shortest Path are proposed to effectively groom and route dynamic multi-bit-rate connections and allocate the Optical-Electrical-Optical (OEO) converters in sparsely located regenerators.

## 4.1 Related Work

Most of the work in MLR deals with static traffic, i.e., all the demands are known a priori. The authors of [28–30] and [31] consider QoT-aware routing with the objective to minimize the cost of transponders. Various Integer Linear Programming (ILP) formulations and effective heuristics are proposed. The authors of [32] design a QoT-aware cost-effective transparent MLR network that provides dedicated protection at the lightpath level. ILP and heuristics for an energy-efficient MLR optical network are proposed in [33] and [34]. In [35], the authors study reliable and cost-effective QoT-aware routing. An IA routing and wavelength assignment (IA-RWA) algorithm called IA-KS-EDP was proposed in [36]; it considers the effects of several impairments and uses edge disjoint paths to satisfy static traffic demands.

Some research on dynamic traffic has been done recently. In [37], the authors present a QoT (in terms of BER) model considering Cross-phase Modulation (XPM). In addition, novel dynamic lightpath provisioning in several MLR scenarios is investigated. The problem of IA-RWA in MLR Wavelength-Switched Optical Networks (WSONs) with two Path Computation Element (PCE) architectures is addressed in [38], and a novel PCE protocol extension is introduced. However, these two papers

consider transparent networks without regenerators. The authors of [39] propose heuristics for dynamic connection RWA in MLR optical networks, but QoT is not considered. A recent paper that considers grooming and IA-RWA for dynamic traffic is [40]; however, the network model used in [40] is different from what is used in our work.

## 4.2 Network Model

The network is modeled as a graph $G(V, E)$, where $V$ is the set of nodes in the network, $N = |V|$, and $E$ is the set of links. Each link $e \in E$ consists of two fibers with $W$ wavelengths each, oriented in opposite directions. Bidirectional connection requests with 10G, 40G, or 100G bandwidth requirement between a pair of nodes $(s, d)$ randomly arrive to and depart from the network [1]. The objective is to assign a route and wavelength(s) and allocate OEO regenerators as needed to minimize blocking.

### 4.2.1 MLR Model

We assume that the line rates in the network are 10G, 40G, or 100G with different modulation methods. Each wavelength on any link can be modulated at any one of these line rates with the corresponding modulation scheme, as assumed in [31] and [37], as long as the corresponding transponder is available.

A transponder is used to initiate and terminate lightpaths. It is assumed to function at a specific line rate, e.g., a 40G transponder can only be used for launching a 40G lightpath and not a 10G or 100G lightpath. Each node in the network has a limited number of transponders for each line rate. However, we assume that a transponder at a node can be shared across all links at the node (share-per-node model).

[1] The focus of our work is on RWA for MLR networks. As such, we assume that bandwidth requirements of sub-wavelength connections are aggregated so that only 10G, 40G, or 100G requests are made to the network.

### 4.2.2 3R Model

A 3R node uses one of a limited number of OEO converters at the node to regenerate an optical signal. Like transponders, OEO converters are also line-rate-specific. For each line rate, there is a set of 3R nodes in the network. The set of nodes for one line rate may be different from the set for another rate, and a single node may be a 3R node for more than one line rate.

### 4.2.3 QoT Model

We assume that a connection's QoT requirement can be met as long as there is no segment that is longer than the transmission reach (TR) (as in [31, 33, 35]). For each line rate, there is a specific TR that ensures that the QoT of a connection at that line rate is satisfactory. If the length of a transparent segment between two allocated OEOs is not greater than the corresponding TR, the QoT of the segment is acceptable; otherwise, it cannot be a subpath for a connection.

### 4.2.4 Grooming Model

We assume that grooming can be done only at the end nodes of a connection, and not at intermediate nodes. For example, two 10G connections between the same source and destination may be groomed onto a 40G lightpath between those nodes, but a connection that does not have the same source and destination may not be groomed onto this lightpath. This simplifies network design, because it does not require the 3R nodes to perform grooming in addition to regeneration [2].

### 4.2.5 Splitting Model

Similar to the grooming model, the end nodes of a connection can split (at source) and combine (at destination) multiple paths, which are used to satisfy that connec-

[2]It may be possible to improve the performance with multi-hop grooming, as in [41], but we do not consider that in this work. Note that the performance improvement is not guaranteed because of the extra transponders that would be used for grooming at intermediate nodes.

tion's bandwidth demand. For example, a 100G connection may be split and satisfied using two 40G and two 10G lightpaths between the same source and destination. Whether a connection is assigned a single path or multiple paths depends on the algorithm policy and the network state (e.g., available network resources) when the connection arrives.

### 4.2.6 Performance Metrics

Since the bit rate (bandwidth) requirements of connections are different, instead of the usual connection blocking ratio, two metrics related to bit rate of connections are used. Let $B_i$ denote the bandwidth requirement of connection $i$, and $t_i$ denote the duration of the connection (i.e., the time from setup to termination of the connection). Further, let $J$ be the set of connections that arrive to the network, and $I$ be the set of blocked connections ($I \subset J$). We define:

1. Bandwidth blocking ratio (BW Blocking)

BW Blocking=$\frac{\sum_{i \in I} B_i}{\sum_{j \in J} B_j}$

2. Throughput blocking ratio (TH Blocking)

TH Blocking=$\frac{\sum_{i \in I} B_i t_i}{\sum_{j \in J} B_j t_j}$.

A connection can be blocked due to any of three reasons: (a) there are not enough transponders for the connection, (b) lack of wavelength, or (c) the algorithm cannot find a path with every segment shorter than the TR. Calls are typically blocked for a combination of reasons. Although multiple paths may be used for a connection, a connection is accepted into the network only if its bandwidth requirement can be fully satisfied. Connections whose bandwidth demands can only be partially satisfied are blocked. The objective is to select paths and effectively allocate the OEO converters to the connections so that the reach limit is met and the blocking probability is minimized.

## 4.3 Algorithms

We now present our GRWA algorithms. Our main algorithm is called LG as the algorithm is based on constructing a logical graph. We also present an algorithm called SP that is based on shortest physical length paths, and a couple of other variants for benchmarking purposes. Suppose a new connection request (with bandwidth 10G, 40G, or 100G) arrives between source $s$ and destination $d$.

Since the existing (i.e., already established) lightpaths between $s$ and $d$ may have some residual capacity available, the first step in all of the algorithms is to groom as much of the bandwidth demand of the new connection into those lightpaths. Note that grooming onto an existing lightpath does not need any new resources (transponders, OEOs, wavelengths) to be allocated. The algorithms may differ in which lightpaths are selected for grooming, if many are available. If the grooming step can completely satisfy the bandwidth demand of the new connection, the algorithm terminates.

After the grooming step, the remaining requested bandwidth can be any multiple of 10 Gbps, up to and including 100 Gbps. There may exist many potential combinations of different newly created paths of different line-rates for satisfying the remaining bandwidth. All the possible combinations for each value of remaining bandwidth are shown in Fig. 4.1.

### 4.3.1 Logical Graph (LG)

Our algorithm considers the availability of transponders, OEOs, and wavelengths as well as the TR when providing path(s) to a connection. Before describing the algorithm, some notation is needed. The number of currently available transponders with line rate $r$ at node $n$ is denoted as $T_r(n)$; the number of transponders allocated to a path $p$ is $t_r^p(n)$; the number of currently available number of OEOs is $O_r(n)$; the number of OEOs allocated to a path $p$ is $o_r^p(n)$.

Grooming Step: Recall that only existing paths with same source and destination are considered. If a lightpaths residual capacity is greater than the requested bandwidth of the new connection, we simply set it equal to the requested bandwidth. Then,

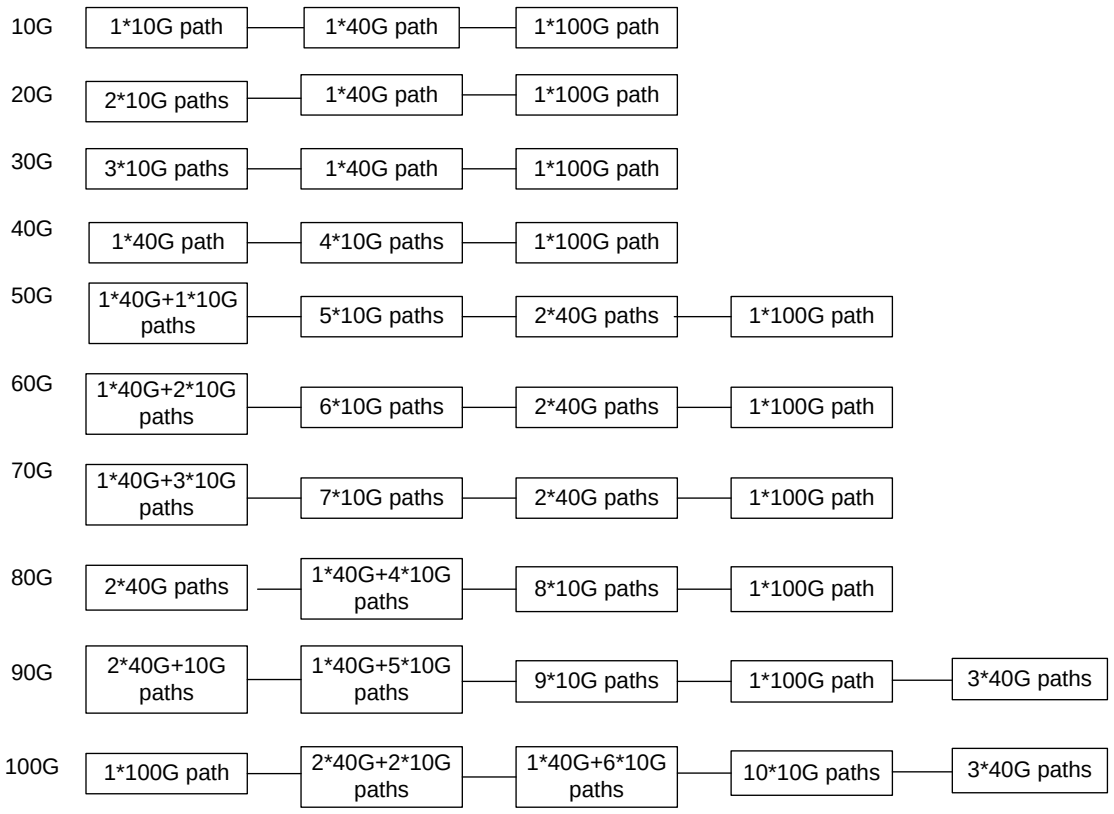


Figure 4.1: Path line-rate combinations for different remaining bandwidth requests after grooming.

we assign a cost to each existing lightpath as follows: $\max\{\frac{1}{T_r(s)}, \frac{1}{T_r d}, \max_n \frac{1}{O_r(n)}\}$, where $n$ is any allocated OEO node on the existing path, and $r$ is the line rate with the existing path. Existing paths are sorted in decreasing order of residual capacity, and the paths with the same residual capacity are sorted in increasing order of this cost. The idea behind assigning costs in this manner is to ensure that a path and line-rate with many available transponders is chosen for the connection, thereby leaving more resources for future connections. By following the sorted order of paths, as much of the new connection's demand as possible is satisfied using existing paths. The time complexity for the grooming step can be shown to be $O(Hq + H \log H)$ , where $H$ denotes the maximum number of existing lightpaths in the network; and $q$ denotes the number of 3R nodes in the network.

Remaining Bandwidth Step: For the remaining bandwidth, one or more logical graphs will be created sequentially if possible  one logical graph $G'_r(V', E')$ for each

required path with line rate $r$ (if the corresponding transponders at the source and destination are available). For example, for the combination 2*40G+2*10G paths for 100G remaining bandwidth, two logical graphs with $r = 40$ and two logical graphs with $r = 10$ will be created sequentially if both the source and destination have at least two 40G transponders and two 10G transponders.

We next explain how a logical graph for a particular rate $r$ is constructed. $V'$ includes the OEO nodes at line rate $r$ as well as the source $s$ and destination $d$ of the connection. A logical link $e'_{x,y}$ exists between two logical nodes $x$ and $y$ if there exists at least one path in the physical graph $G$ whose length is no more than the TR for r and the path has at least one wavelength available. The logical link $e'_{x,y}$ is represented by two directed edges, one from $x$ to $y$, with cost set as $\frac{1}{O_r(y)}$ (if $y = s$ or $y = d$, the cost is set to zero), and the other from $y$ to $x$, with cost set as $\frac{1}{O_r(x)}$ (if $x = s$ or $x = d$, the cost is set to zero).

The physical path for a logical link $e'_{x,y}$ is selected as follows: $K'$ (an algorithm parameter) shortest paths are pre-computed [20] between $x$ and $y$, and the path with most available wavelengths is selected; if there are many such paths, then the one with minimum number of hops is selected.

After the logical graph is constructed, a logical path from $s$ to $d$ with minimum cost is found by Dijkstras shortest path algorithm. An OEO is allocated at each node along the logical path, and the concatenation of the physical links forms the physical lightpath for the request. The First-Fit (FF) wavelength is assigned to each allocated OEO segment. The time complexity to find a new candidate path can be shown to be $O(K'WNq^2 + q^3)$, where $W$ denotes the number of wavelengths per fiber and $N$ denotes the number of nodes in the network.

We illustrate the logical graph construction with the example in Fig. 4.2. Suppose the source and destination are nodes 0 and 5, respectively, in the original (physical) graph, shown in Fig. 4.2(a), and let nodes 2 and 3 be the OEO nodes. Suppose the logical links obtained after wavelength availability and reach are checked are as shown in Fig. 4.2 (b). Suppose the currently available number of OEOs at node 3 is 5, and at node 2 is 4; then the costs of the directed logical edges to node 3 and 2 are set to

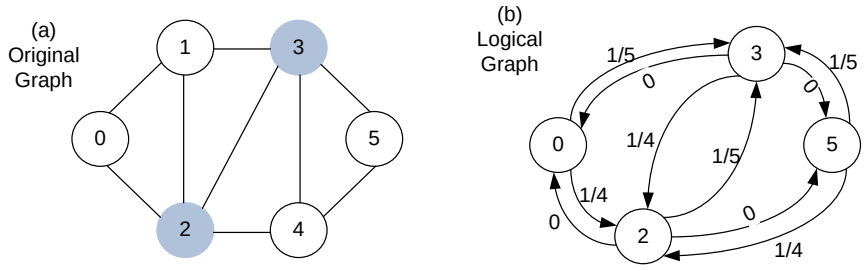


Figure 4.2: Example showing (a) a physical topology and (b) the corresponding logical topology.

$\frac{1}{5}$ and $\frac{1}{4}$, respectively, and the costs of directed logical edges to node 0 and 5 are set as 0.

Running Dijkstras shortest path algorithm produces the logical path 0-3-5 with cost $\frac{1}{5}$. Then, this path is allocated to the connection, and node 3 is the allocated OEO node. The FF wavelengths on OEO segments 0-3 and 3-5 are assigned.

Now, recall that the remaining bandwidth is satisfied using one of the possible combinations shown in Fig. 4.1. The particular combination to satisfy the remaining bandwidth is selected as follows. A cost $C$ is assigned for each combination $c$. For a combination $c$ with path set $P_c$, and for each allocated OEO node $n$, let

$o_r^c(n) = \sum_{p \in P_c} o_r^p(n)$

$t_r^c(s) = \sum_{p \in P_c} t_r^p(s)$

and

$t_r^c(d) = \sum_{p \in P_c} t_r^p(d)$

Then define

$C_c = \max_{r \in R}\{\max_n \frac{o_r^c(n)}{O_r(n)}, \frac{t_r^c(s)}{T_r(s)}, \frac{t_r^c(d)}{T_r(d)}\}$

where set $R$ includes the line rates that are involved in the combination (e.g., $R = \{10, 40\}$ for the combination 2*40G+2*10G). The selected combination is the one with minimum cost. Roughly speaking, this cost function picks a combination so that the number of allocated transponders and OEOs is as small as possible (relative to the number deployed at the nodes). The complexity of the entire LG algorithm is $O(K'WNq^2 + q^3 + Hq + H \log H)$ .

### 4.3.2 Shortest Path (SP)

This algorithm gives preference to paths with shorter physical length.

Grooming Step: Existing paths are sorted in decreasing order of residual capacity (if residual capacity is greater than bandwidth requirement of the new connection, set residual capacity as the bandwidth requirement), and the paths with same residual capacity are sorted in increasing order of their lengths. This order is used to satisfy as much of the bandwidth demand as possible for the new connection. The time complexity for the grooming step is $O(H \log H)$.

Remaining Bandwidth Step: For each possible combination for the remaining bandwidth, new lightpaths of this combination are found one by one. When finding each new path, the algorithm first selects a path and allocates OEOs, and then assigns a wavelength to each allocated OEO segment. In the path selection and OEO allocation step, the algorithm first uses the $K'$ shortest pre-computed paths as candidate paths (same path set used by the LG algorithm for finding paths for logical links), belonging to $P_{s,d}$ for node pair $s$-$d$. Given a candidate path $p_i \in P_{s,d}$ , OEO allocation on $P_{s,d}$ is done as follows. Starting from node $s$, find the furthest OEO node $x$ with the property that: if node $x'$ is the next OEO node after $x$, there is at least one available wavelength on OEO segment $s$-$x$ and the length of $s$-$x$ is not greater than the TR for the corresponding rate with the path, but no available wavelength can be found for the segment $s$-$x'$ or the length of $s$-$x'$ is longer than TR. This means that node $x$ needs to serve as a wavelength converter or regenerator, i.e., node $x$ will be an allocated OEO for this connection. If $x = d$, then path $p_i$ is considered to have passed the test; otherwise, repeat the above procedure from node $x$ and so on. (All the wavelengths available on each allocated OEO segment will be candidates for the next wavelength assignment step.) If there is a consecutive OEO segment on $p_i$ which does not have any available wavelength or its length is longer than the TR, then path $p_i$ is considered to have failed the test, and the next path from $P_{s,d}$ is tested, and so on.

The first $K$ paths that pass the test are retained, and the shortest of these (in

terms of physical distance) is selected for the new path; if lengths are tied, the one with minimum number of allocated OEOs is selected; if there is still a tie, the path with the least number of hops is selected.

Wavelength assignment is done as follows by noting that OEOs also provide wavelength conversion. For each wavelength, find the number of longest continuous allocated OEO segments that it can be assigned to; then sort the wavelengths by increasing order of this number. Wavelengths are assigned according to this order, i.e., if the currently considered wavelength is available on some OEO segments, assign it to these segments, and then consider the remaining segments, and so on, until all segments are assigned wavelengths. The reason behind this method is to preserve continuous wavelengths for future connections, which might otherwise need OEOs to be used as wavelengths converters, and OEOs may not be available. The total time complexity to find a single lightpath is $O(K'NW)$.

A cost is assigned to each combination for the remaining bandwidth. If a combination includes $M$ paths, denote the length of $p_m$ as $l_m$, $1 \leq m \leq M$ . Then the cost of the combination is defined as $\max_{1 \leq m \leq M} l_m$ . The remaining bandwidth is satisfied by the combination with minimum cost. The time complexity of the entire SP algorithm is $O(K'NW + H \log H)$.

### 4.3.3 Logical Graph-single path (LG-single path)

This algorithm is used as a reference to study the performance effect of connection splitting (a connection's bandwidth demand using multiple paths, e.g., 100G as 2*40G + 2*10G). It is identical to LG, except that only one path (either an existing path or a newly established one) is used for the connection. The time complexity of LG-single path is the same as that of LG, i.e., $O(K'WNq^2 + q^3 + Hq + H \log H)$.

*QoT Guaranteed (QoT-G)*

This algorithm is the same as the SP algorithm above except that the TR limit is ignored when finding a new path. The path(s) that are selected are then tested to see if all OEO segments are shorter than TR; if not, the connection is blocked. The time

Table 4.1: 3R node placement and number of transponders

| Network | 3R nodes | | | Number of transponders per node | | |
|---|---|---|---|---|---|---|
| | 10G | 40G | 100G | 10G | 40G | 100G |
| EON | 5,19 | 10,13 | 9,10,12,1719,25 | 9 | 15 | 9 |
| USANET | 9 | 9 | 7,12,21 | 10 | 17 | 10 |

complexity of QoT-G is the same as that of SP algorithm, i.e., $O(K'NW + H \log H)$.

### 4.4 Simulation Results

Connections are assumed to arrive to the network according to a Poisson process, and require an exponential service time with unit mean. The source and destination of the connection are randomly picked. The bandwidth requirement of the connection is 10G, 40G, or 100G with probability 25%, 50%, and 25%, respectively. For each data point in the graphs, we simulated several instances between 10,000 and 100,000 connection arrivals, and obtained 95

We present results for the European Optical Network (EON) and USA network (USANET) (Figs. 4.3 and 4.4) topologies. The 3R nodes are selected according to the Greedy algorithm presented in [42]; the algorithm is applied to each line rate separately. The 3R node placement in EON and USANET are shown in Table 4.1. The number of transponders per line rate at each node is found according to [43], which considers the expected load of the network (i.e., the number of connections in the network) and the probabilities of different line rate connections. The number of transponders with each line rate for EON and USANET are shown in Table 4.1. The TR values used in this work are from [33]: they are 1750 km, 1800 km and 900 km, respectively. Note that the TR for 40G is actually higher than for 10G because a different modulation method is assumed [33]. We assume that $K' = 40$, i.e., up to 40 shortest paths are computed offline for each node pair. In addition, $K = 3$ alternate paths are used by the algorithms. Each fiber is assumed to have 32 wavelengths.

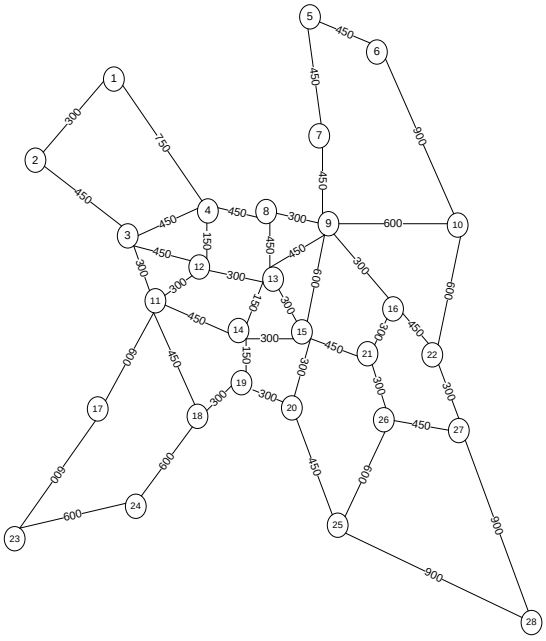


Figure 4.3: 28-node EON. The number on each link corresponds to the length in km.

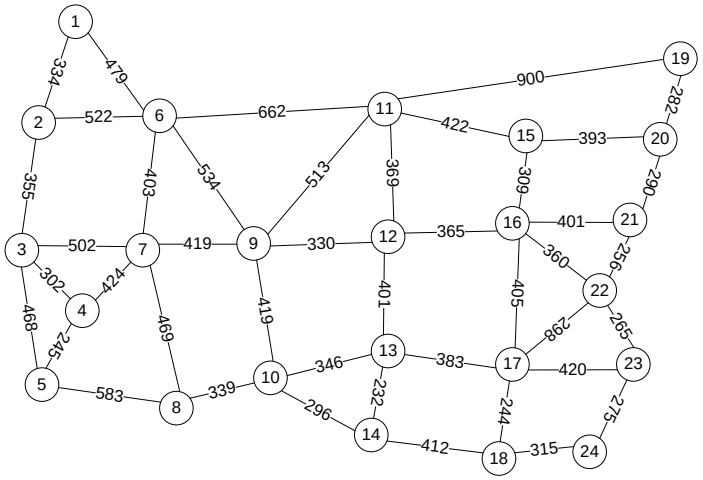


Figure 4.4: 24-node USA network (USANET). The number on each link corresponds to the length in km.

### 4.4.1 Performance Comparison of Algorithms

Figs. 4.5 - 4.12 show the BW Blocking and TH Blocking versus the network Erlang load for the various algorithms with 10 OEO converters and 30 OEO converters per 3R node in EON, and with 16 OEO converters and 34 OEO converters per 3R node in USANET. The loads were selected so that blocking probabilities fall in the $10^(-4)$ to $10^(-1)$ range. As can be seen, QoT-G, which ignores the TR (and therefore

physical impairments) during RWA, performs much worse than the other algorithms that are QoT-aware. Interestingly, the blocking ratio stays essentially flat. This can be explained as follows. Recall that QoT-G allocates OEO converters to paths considering only wavelength availability and not the TR. When the selected path is tested to see if every OEO segment is shorter than TR, there is a high probability that the test fails, and hence the connection is blocked. When the load increases, a wavelength-continuous path from source to destination becomes harder to find, and therefore, OEO converters are allocated to the connection for doing wavelength conversion. Since these OEO nodes also perform 3R regeneration, the probability that the selected path will be rejected by the test does not increase.

Further, LG clearly outperforms the other algorithms. The significant difference between LG and LG-single path shows that the network performance can be greatly improved by multi-path provisioning (path splitting), particularly at lower loads. Interestingly, LG-single path outperforms SP when the number of OEOs is larger, despite the fact the SP allows connection splitting. We explain this a little later. Both BW Blocking and TH Blocking have similar trends, indicating that these results are not dependent on connection holding times, which are not assumed to be known when the connection is set up.

For the EON network, two more simulations are done with different numbers of OEO converters at different 3R nodes. Specifically, in the first simulation, for 10Gbps and 40Gbps, the first 3R node has 10 OEO converters, and the second has 6 OEO converters; for 100Gbps, of the six 3R nodes, the first three have 10 OEO converters each, and the other three have 6 OEO converters each. In the second simulation, for 10Gbps and 40Gbps, one 3R node has 30 OEO converters, and the other has 20 OEO converters; for 100Gbps, the first three 3R nodes have 30 OEO converters each, and the other three have 20 OEO converters each. Figs. 4.13 - 4.16 shows the results of BW Blocking and TH Blocking versus the network Erlang load for the various algorithms. These results further confirm that the performance improvement of our algorithm is not sensitive to parameter changes.

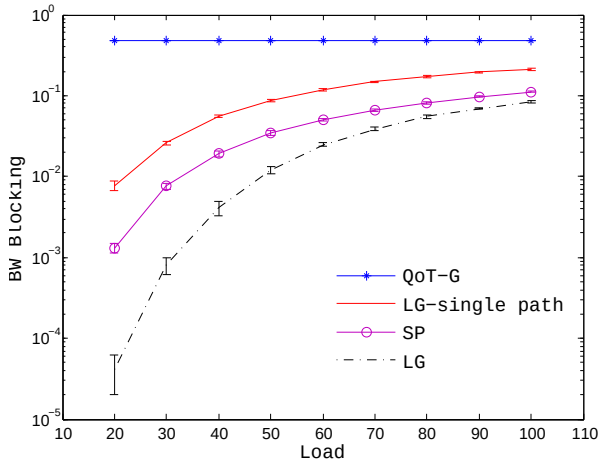


Figure 4.5: BW Blocking vs. Erlang load; 10 OEO converters per 3R node in EON.

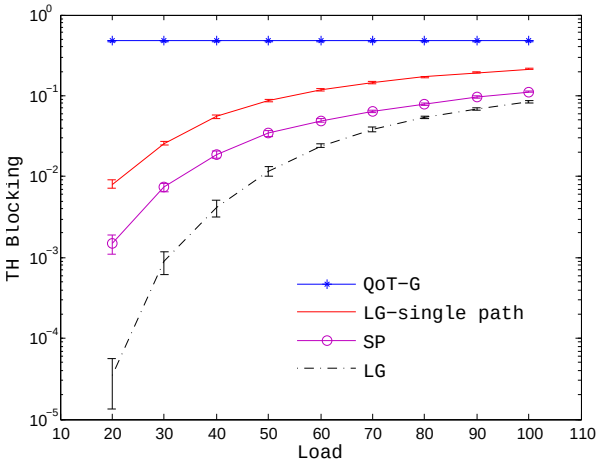


Figure 4.6: TH Blocking vs. Erlang load; 10 OEO converters per 3R node in EON.

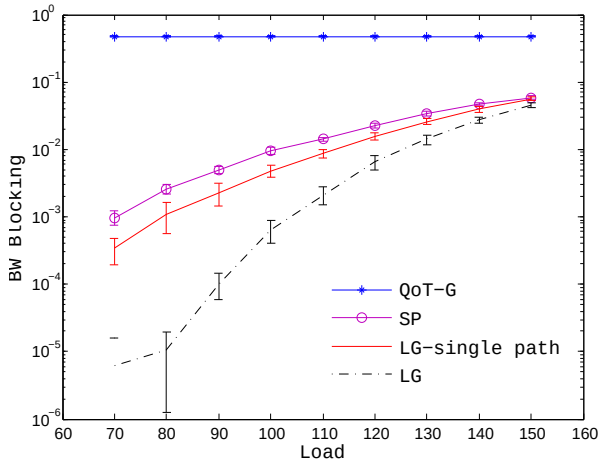


Figure 4.7: BW Blocking vs. Erlang load; 30 OEO converters per 3R node in EON.

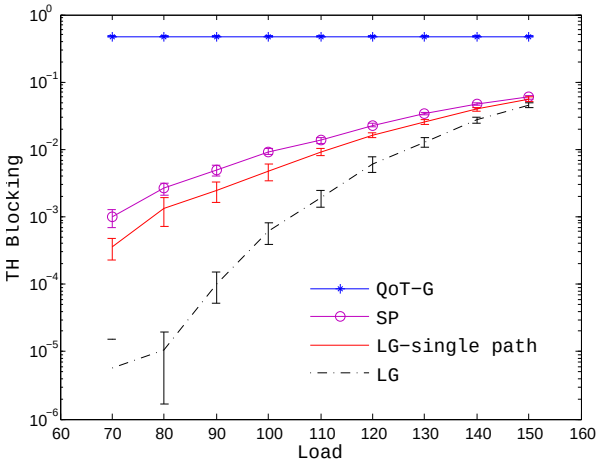


Figure 4.8: TH Blocking vs. Erlang load; 30 OEO converters per 3R node in EON.

### 4.4.2 Blocking vs. Number of OEO Converters

The blocking ratios are plotted as a function of the number of OEO converters per 3R node for EON in Figs. 4.17 - 4.18 and for USANET in Fig. 4.19 - 4.20. Once again, the superior performance of LG is obvious. As we can see, there is a significant decrease in blocking as the number of converters increases for both LG and LG-single path, pointing to the ability of these algorithms to wisely allocate OEO converters.

An interesting observation is that when the number of OEO converters is small,

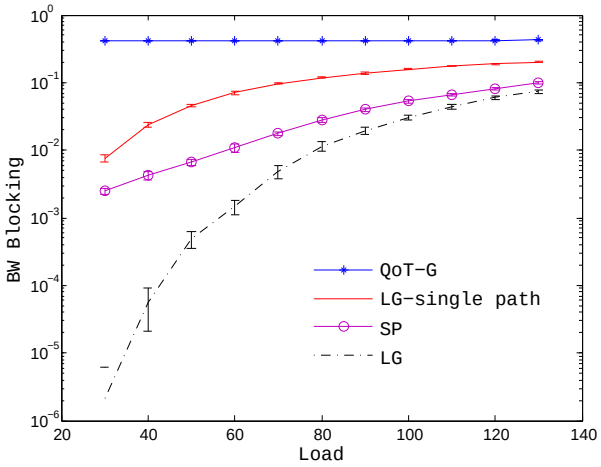


Figure 4.9: BW Blocking vs. Erlang load; 16 OEO converters per 3R node in US-ANET.

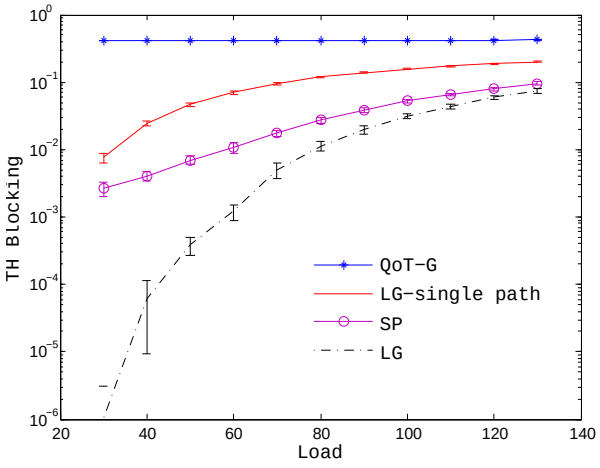


Figure 4.10: TH Blocking vs. Erlang load; 16 OEO converters per 3R node in US-ANET.

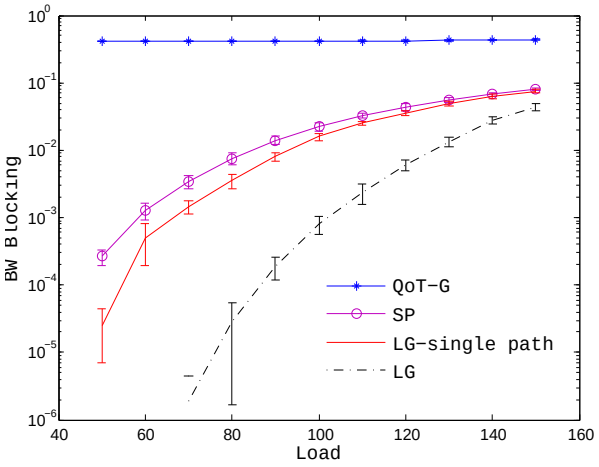


Figure 4.11: BW Blocking vs. Erlang load; 34 OEO converters per 3R node in US-ANET.

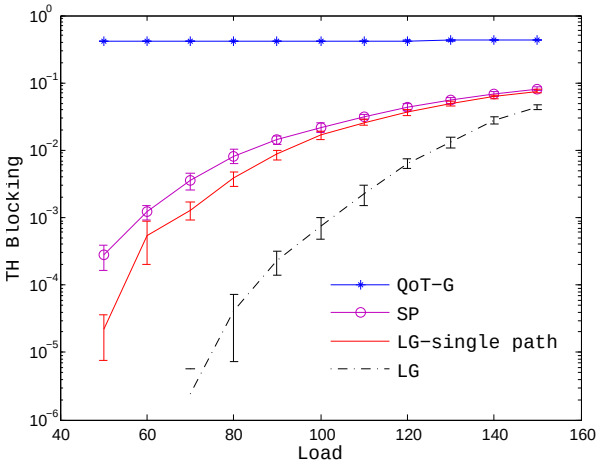


Figure 4.12: TH Blocking vs. Erlang load; 34 OEO converters per 3R node in US-ANET.

the performance of LG-single path is worse than SPs; but LG-single path outperforms SP despite no connection splitting, when the number of OEO converters is large. SP prefers shorter length paths, but these paths end up using more OEOs as wavelength converters; in other words, longer paths that need fewer OEO nodes may not be selected by SP. But for LG-single path, the OEO nodes are used when they are

needed as wavelength converters or regenerators, thus they are used more efficiently. On the other hand, when the number of OEOs is small, the single path restriction dominates and SP performs better.

## 4.5 Conclusion

In this chapter, we investigated the QoT-aware grooming, routing and wavelength assignment problem in mixed line rate translucent optical networks. We proposed an effective heuristic called LG based on a logical graph, and another heuristic called SP based on shortest paths. Simulation results show that the LG heuristic is able to effectively allocate network resources and reduce blocking, compared to other heuristics. For example, in 24-node USANET network with 16 OEO converters per 3R node, the blocking probability with LG algorithm can be up to 2 orders of magnitude better than that with SP algorithm, which can be explained as that the LG method considers the availability of transponders and OEO converters in the network, which are precious resources for accommodating connections. Further, connection splitting is shown to yield significant performance benefits. For example, in the same 24-node USANET network with 16 OEO converters per 3R node, the blocking probability with LG algorithm can be up to 3 orders of magnitude better than that with LG-single path algorithm. The reason is that for connections with high bit rate requirement, such as 100Gbps, it is very likely that it cannot be satisfied by only one lightpath due the lack of transponder, and/or OEO converters with 100Gbps.

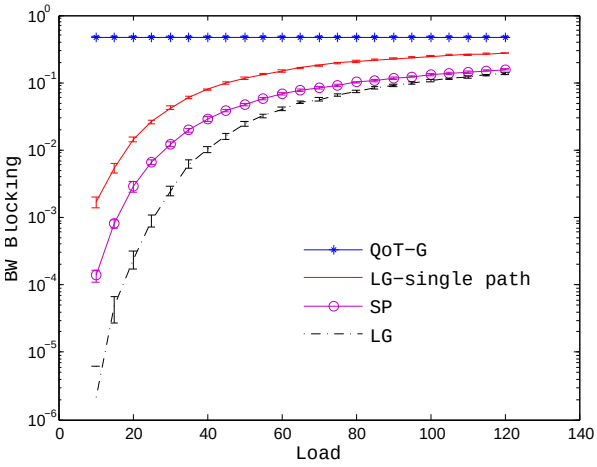


Figure 4.13: BW Blocking vs. Erlang load; 10/6 OEO converters per 3R node in EON.

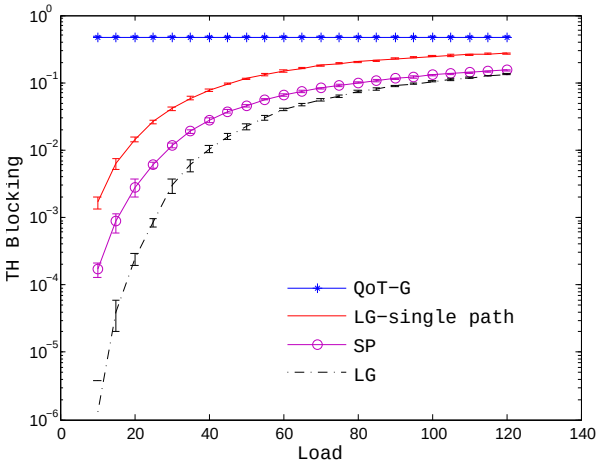


Figure 4.14: TH Blocking vs. Erlang load; 10/6 OEO converters per 3R node in EON.

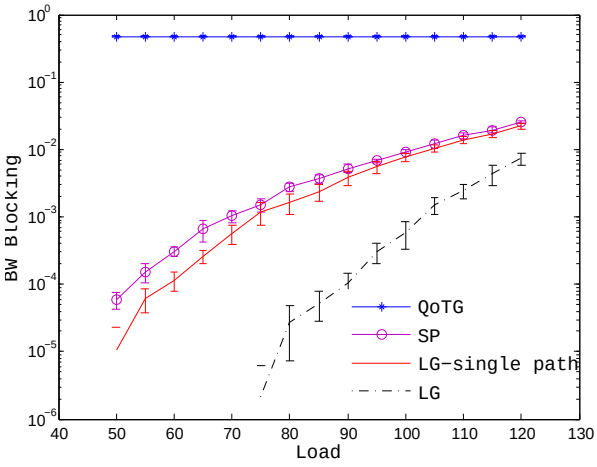


Figure 4.15: BW Blocking vs. Erlang load; 30/20 OEO converters per 3R node in EON.

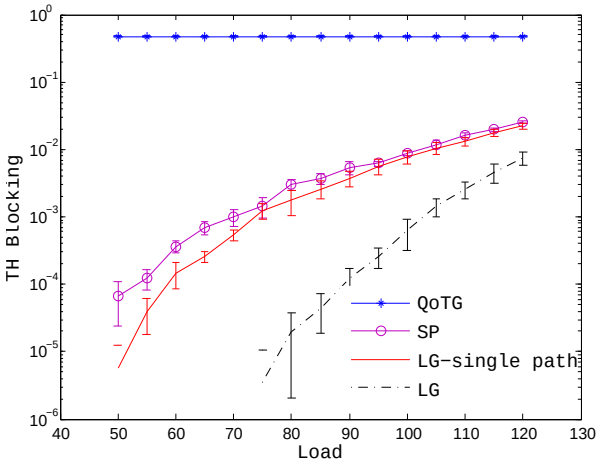


Figure 4.16: TH Blocking vs. Erlang load; 30/20 OEO converters per 3R node in EON.

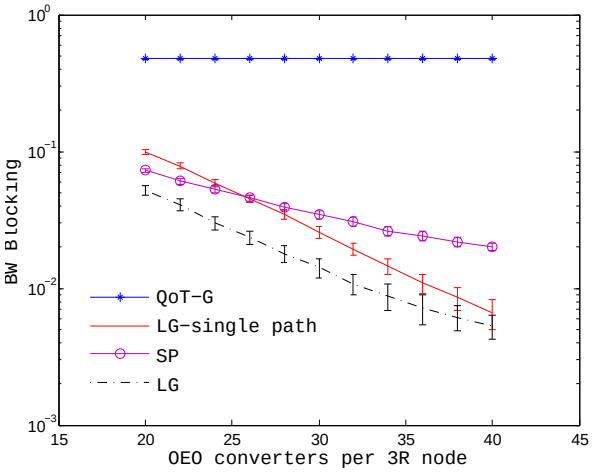


Figure 4.17: BW Blocking vs. OEO converters per 3R node in EON; load=130 Erlangs.

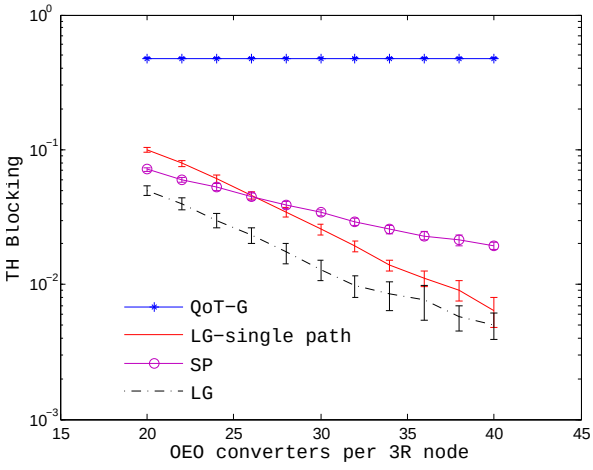


Figure 4.18: TH Blocking vs. OEO converters per 3R node in EON; load=130 Erlangs.

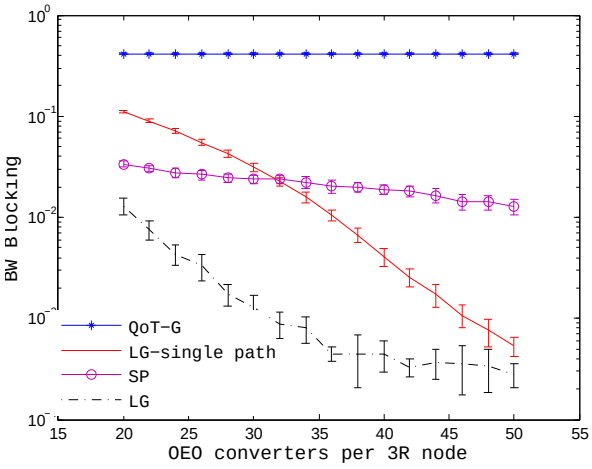


Figure 4.19: BW Blocking vs. OEO converters per 3R node in USANET; load=100 Erlangs

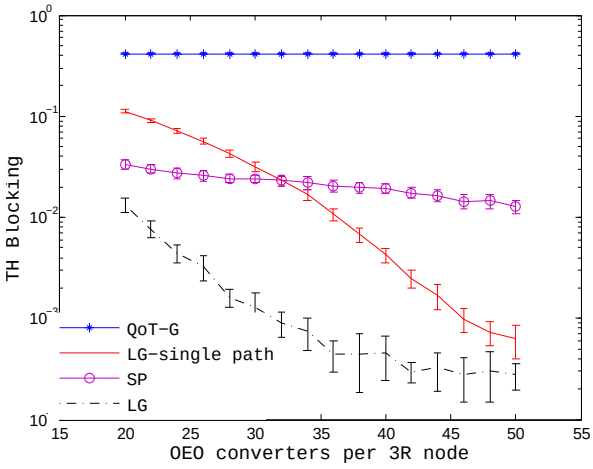


Figure 4.20: BW Blocking vs. OEO converters per 3R node in USANET; load=100 Erlangs.

# Chapter 5 Virtual Topology Mapping in Elastic Optical Networks

In this chapter, we consider the problem of mapping virtual topologies in elastic optical networks based on optical orthogonal frequency division multiplexing (OOFDM). In this problem, a virtual topology request includes a set of virtual nodes, the amount of computation requirements at the virtual nodes (e.g., number of virtual machines (VMs) needed), and the bandwidth requirements between the virtual nodes.

## 5.1 Model and Problem Statement

### 5.1.1 Virtual Optical Network Problems

We first provide a classification of virtualization problems. These problems are applicable to WDM- as well as OOFDM-based optical networks. In general, these problems can be classified into Slice Provisioning problems or Virtual Network (VN) Mapping problems. In Slice Provisioning, each request requires a slice of the entire physical network including (sub)wavelengths on fibers, ports of optical devices, and/or optical-electrical-optical (OEO) converters at regenerator nodes [3]. The objective can be maximizing the acceptance ratio or maximizing revenue (each VON request has to pay the price of the resources). This model can further be classified in two ways:

1. Slice Provisioning: specific model

The slice request includes specific (sub)wavelengths of each physical link, specific ports of each optical device (e.g., optical cross-connects (OXC)), and the number of OEO circuits in each regenerator.

2. Slice Provisioning: flexible model

The slice request includes the bit rate requirement on each physical link, the number

of ports at each optical device, and the reachability of each pair of nodes. The provider assigns (sub)wavelengths on each link, the ports on each node and the OEO converters on each regenerator node to the request.

In VN Mapping, each request is a virtual network topology including virtual nodes and/or virtual links. The provider assigns physical nodes to virtual nodes, and allocates (sub)wavelengths on each link to the virtual links. In both versions, the request may also include Bit Error Rate (BER) or survivability requirements.

1. VN mapping: pipe model

The VN request includes a topology consisting of virtual nodes and virtual links, each virtual node has a set of candidate physical nodes that it could be assigned to (based, for example, on proximity) and possibly a computing resources requirement [44]. Virtual links have a bit-rate requirement.

2. VN mapping: hose model ([45])

The VN request consists of virtual nodes with computing resources requirement, and the aggregate incoming/outgoing traffic from/to the other virtual nodes.

We consider the VN mapping using the pipe model in this chapter.

### 5.1.2 OOFDM

OOFDM is a technology providing flexible subcarrier assignments and more efficient bandwidth utilization. The optical spectrum of each fiber (e.g., C-band) is divided into subcarriers, which are orthogonal to each other, and a guardband consisting of multiple subcarriers is placed between two adjacent subcarrier bands assigned to different connections. Guardbands are used for avoiding interference, and their width is in general a function of the maximum number of filters on the path and the filter characteristics (such as filter bandwidth and order) [46].

Different modulation levels can be adopted by different subcarriers, and a connection can be assigned multiple subcarriers depending on its bit rate requirement. However, all the subcarriers assigned to a single lightpath use the same modulation level. The highest modulation level of a path depends on the length of that path due to physical layer impairments [6]. Regenerators in the network can extend the reach

of a lightpath.

The subcarriers assigned to a connection may be contiguous or non-contiguous. Contiguous assignment can take advantage of overlap between adjacent subcarriers due to their orthogonality, but is obviously more restrictive because of the contiguity restriction. Non-contiguous assignment is more flexible but may increase total guardband overhead. There may be subcarrier converters [47] in the network; at a subcarrier converter, a whole band of subcarriers assigned to a connection on the incoming link can be converted to another band of subcarriers on the outgoing link.

### 5.1.3 Network Model and Notation

The physical network includes a set of physical nodes, each with $h$ virtual machines (VMs), and a set of fibers, each with multiple subcarriers. Each subcarrier is $C$ GHz. Guardband $G$ is a fixed integer number of subcarriers. The shortest path $p_{s,d}$ (based on distance) for each pair of nodes $(s, d)$ is precomputed, and depending on its length each path has a highest modulation level that can be used.

Virtual topology (VT) request $i$ includes a set of virtual nodes and a set of virtual links.[1] For virtual link $k^i$, there is a bit rate requirement $\Lambda_k^i$. Virtual node $j^i$ has a candidate set $(N_j^i)$ of physical nodes to map to, and a VM requirement $m_j^i$. Determined by the candidate nodes, virtual link $k^i$ has a candidate path set $P_k^i$. Path $p \in P_k^i$ has a subcarrier requirement $b_k(p)$, which is obtained from its highest modulation level and $\Lambda_k^i$.

### 5.1.4 Problem Statement

We consider the VN mapping problem using the pipe model. Within this context, there are several variants based on whether traffic can be split among multiple paths or not, whether the subcarrier bands should be contiguous or not, etc. We assume that the network is all-optical (i.e., no regenerators), a single path is used for each virtual link, and subcarriers for each virtual link are contiguous.

[1] We use the letter $i$ for VT index, $j$ for virtual node index, $k$ for virtual link index, $n$ for physical node index, $p$ for physical path index.

Consider a VT request. For each of its virtual nodes, a physical node that has sufficient VMs available must be assigned from the set of candidate physical nodes. At the same time, a physical path $p$ should be assigned to each virtual link, and a band of contiguous subcarriers on each physical link of the path should be allocated to the virtual link to satisfy the virtual link's bit rate requirement. We allow different virtual nodes of a request to be mapped to the same physical node in case they have common candidate physical nodes; in this case, there is no need to map the virtual link between these virtual nodes (and no subcarriers are allocated).

For the static traffic case, a set of VT requests is given, and the objective is to minimize the maximum used subcarrier index on any link. For the dynamic traffic case, the number of subcarriers per link is fixed and VT requests arrive and depart in a random manner. The objective is to minimize the *request blocking* ratio. All virtual links are assumed to be bidirectional and use the same path and subcarriers for both directions. Since the bit rate (bandwidth) requirements of each VT could be different, in addition to the request blocking ratio, we consider *bandwidth blocking* ratio, defined as: Bandwidth blocking = $(\sum_{i' \in I'} B_{i'})/(\sum_{i \in I} B_i)$, where $B_i$ denote the aggregate bit rate requirement of request $i$ (the sum of the bit rate requirements over all virtual links in request $i$).

### 5.2 Algorithms

In this section we introduce our algorithms for VT mapping. We first present an ILP formulation for static requests that can be used to solve small problem instances. We then present two heuristics for static requests, and later adapt them to dynamic requests. Recall that for static traffic we are given a set of VT requests which never depart, and VT requests arrive and depart in a random manner for dynamic traffic. Each VT request has bit-rate requirements on its virtual links, VM requirements at the virtual nodes, and there is a constraint on the set of physical nodes a virtual node can be mapped to.

### 5.2.1 ILP Formulation

Input parameters used in the ILP formulation are listed below: $S(p)$ denotes source of path $p$; $D(p)$ denotes destination of path $p$; $\gamma_{p,l} = 1$ if path $p$ uses link $l$; $S(k^i)$ denotes the source virtual node for virtual link $k$ of request $i$; $D(k^i)$ denotes the destination virtual node for virtual link $k$ of request $i$; $q$ denotes a dummy path with $S(q) = D(q)$.

$$\text{Objective: Minimize } \max_s sf_s$$

Variables:

a)

$$f_s = \begin{cases} 1, & \text{if subcarrier index } s \text{ is used on some physical link} \\ 0, & \text{otherwise} \end{cases}$$

b)

$$x_{ijn} = \begin{cases} 1, & \text{if virtual node } j^i \text{ uses physical node } n \\ 0, & \text{otherwise} \end{cases}$$

c)

$$y_{ikp} = \begin{cases} 1, & \text{if virtual link } k^i \text{ uses path } p \\ 0, & \text{otherwise} \end{cases}$$

d)

$$z_{ikpc} = \begin{cases} 1, & \text{if virtual link } k^i \text{ uses path } p \\ & \text{and the starting subcarrier index is } c \\ 0, & \text{otherwise} \end{cases}$$

Constraints:

a) Each virtual node is assigned to one physical node.

$$\sum_{n \in N_j^i} x_{ijn} = 1 \text{ for all } i, j$$

b) Each virtual link is assigned to one physical path.

$$\sum_{p \in P_k^i} y_{ikp} = 1 \text{ for all } i, k$$

c) Each physical node's VM capacity cannot be exceeded.

$$\sum_{i,j}(x_{ijn} \cdot m_j^i) \leq h, \text{ for all } n$$

d) If the source and destination of a virtual link are assigned to the same physical node, the virtual link is assigned to dummy path $q$ (which uses no subcarriers).

$$y_{ikq} = [\sum_{n \in N^i_{S(k^i)}} (x_{iS(k^i)n} \cdot n) = \sum_{n \in N^i_{D(k^i)}} (x_{iD(k^i)n} \cdot n)]$$

(Note that $n$ is *not* a decision variable, and so the constraint is linear.)

e) If virtual link $k$ is assigned to physical path $p$ ($p \neq q$), the source and destination of the two must match, i.e.,

if $y_{ikp} = 1$, then either $x_{iS(k^i)S(p)} = 1$, $x_{iD(k^i)D(p)} = 1$ or $x_{iS(k^i)D(p)} = 1$, $x_{iD(k^i)S(p)} = 1$.

f) If virtual link $k$ uses path $p$, then it must be assigned subcarriers on that path, i.e.,

$$\sum_c z_{ikpc} = y_{ikp}$$

g) All assigned subcarriers for non-dummy paths are marked as used, i.e.,

$c_{ikpc} = 1$ ($p \neq q$), the corresponding $f_s = 1$

$$z_{ikpc} \leq f_s \text{ for } c \leq s < c + b_k(p) + G$$

h) Each subcarrier on a physical link can be used by at most one virtual link.

$$\sum_{i,k,p,c \leq s < c+b_k(p)+G} z_{ikpc}\gamma_{p,l} \leq 1 \text{ for all } l, s.$$

### 5.2.2 Static Requests

Before describing the algorithms, we present three functions (that are used by the heuristics) that check if certain VT assignments can be made.

i) *TrivialRequestCheck()*: This function checks whether any VT can be mapped to a single physical node with no influence on other virtual node mappings in other VTs (i.e., the candidate node sets of the other virtual nodes won't be affected by

**Algorithm 1** TrivialRequestCheck

```
for VT i = 1, 2, ..., I do
  if there is a physical node n that all j^i can be mapped to then
    let W_n = Σ_{j^i} m^i_j
    for all other VTs i' do
      for all virtual nodes j'^{i'} do
        if j' can be mapped to n then
          W_n = W_n + m_{j'^{i'}}
        end if
      end for
    end for
    if W_n ≤ h then
      Map the whole VT i to n
    end if
  end if
end for
```

this mapping). In this case, it is best to assign the whole VT to that physical node (since it will not use any subcarrier). The pseudo-code of the algorithm is shown as Algorithm1.

ii) *CheckNode()*: If a virtual node has only one candidate physical node (taking into account the number of currently available VMs at physical nodes), then we assign it to that physical node. Since each time a virtual node mapping may affect candidate nodes for other virtual nodes (due to the VM limit), this procedure is repeated for at most $I \cdot N_l$ times (where $I$ is the number of VT requests and $N_l$ is the maximum number of virtual nodes in a VT). In addition, if a virtual link's two terminal virtual nodes are mapped to the same physical node, we mark the virtual link as an assigned virtual link (a dummy physical path).

iii) *CandidateCheck()*: A candidate physical node $n \in N_j^i$ for virtual node $j^i$ will be considered for node mapping if it can satisfy the following condition: after mapping

node $j^i$ to $n$, all other unmapped virtual nodes (belonging to the same or other VTs) still have at least one potential candidate physical node by considering the number of free VMs on each physical node.

The following two algorithms are proposed.

*First Fit (FF)*

This is a simple greedy algorithm. VTs are considered one by one (from lowest index) and unmapped virtual nodes of each VT are mapped one by one. For each virtual node $j^i$, the first fit physical node (the one with smallest index) is selected from the candidate set, as long as the physical node has enough available VMs to satisfy the virtual node's VM requirement $m_j^i$. Each time a virtual node is mapped, the function CheckNode() is called. After all the virtual nodes are mapped, subcarriers are allocated to unassigned virtual links. Since the node mapping is already done, each virtual link's path (say $p$) is fixed (recall that the shortest path is used for each pair of physical nodes), and the number of subcarriers $b_k(p)$ is also known. Then, the first available band of $b_k(p)$ subcarriers is allocated to virtual link $k^i$. The pseudo-code of the algorithm is shown as Algorithm 2.

**Algorithm 2** First Fit

```
TrivialRequestCheck() and CheckNode()
for VT i = 1, 2, ..., I do
  for each unmapped virtual node j^i do
    CandidateCheck()
    Map it to the first qualified candidate node
    CheckNode()
  end for
  for for each unassigned virtual link k^i do
    Assign it to the first available subcarrier band of the path p
  end for
end for
```

*Link List (LL)*

The idea behind this algorithm is to map the VTs one by one in decreasing order of their VM and bit-rate requirements because these require the most resources. Within each VT, virtual links are mapped one by one, starting from the "most-constrained" virtual link.

We will use the following notations in the algorithm. For VT $i$, denote the sum of the VM requirements of unmapped virtual nodes as $M_i$; the sum of the bit rate requirements of unassigned virtual links as $B_i$. Further, let the number of used VMs on physical node $n$ be $c_n$, and denote the two ends of a generic virtual link as $t_1$ and $t_2$.

A VT list is created first. For each VT, a virtual link list is created based on the relative weight of a virtual link $k^i$'s bit rate requirement $\Lambda_k^i$. When considering the current virtual link in the list, the candidate nodes of virtual node $t_1$ and $t_2$ are checked by the function CandidateCheck() if they are not mapped yet. Suppose the virtual link $k$ is mapped to a path $p$ ending with candidate nodes (or mapped physical nodes) $n_1$ and $n_2$ for virtual nodes $t_1$ and $t_2$ respectively. Let the resulting maximum subcarrier index on any link be $s_n$ after first-fit subcarrier assignment. Assign a cost to the path as $\max(c_{n_1} + m_{t_1}^i, c_{n_2} + m_{t_2}^i, s_n)$ (if either $t_1$ or $t_2$ are already mapped, set the corresponding cost to 0). Finally, virtual link $k^i$ is mapped to the candidate path with minimum cost, and $t_1$, $t_2$ are mapped to the corresponding end nodes of the selected path. The pseudo-code of the algorithm is shown as Algorithm 3.

### 5.2.3 Dynamic Requests

For dynamic traffic, since VTs arrive (and depart) one by one, VTs are mapped in the order they arrive. No remapping of currently mapped VTs is done. The same heuristics for static traffic are adapted by removing the TrivialRequestCheck() function. Further, the CheckNode() and CandidateCheck() functions consider only the virtual nodes in the current VT.

**Algorithm 3** Link List

TrivialRequestCheck() and CheckNode()

**for** VT $i = 1, 2, \ldots, I$ **do**

Find $M_i$, $B_i$, and assign VT $i$ a cost $\max(\frac{M_i}{\sum_i M_i}, \frac{B_i}{\sum_i B_i})$

**end for**

Create $LIST$ in decreasing order of the cost

**for** each VT $i$ in $LIST$ **do**

**for** unassigned virtual link $k^i$ **do**

Assign it a cost $\frac{\Lambda_k^i}{B_i}$

**end for**

Create virtual link $LIST(i)$ in decreasing order of the cost

**for** each virtual link $k^i$ in $LIST(i)$ **do**

1. CandidateCheck() for $t_1$ and $t_2$
2. Assign a cost to each candidate path
3. Assign link $k^i$ to the path with minimum cost
4. Map $t_1$ and $t_2$

CheckNode()

**end for**

**end for**

### 5.3 Simulation Results

We present results for two network topologies, a small 6-node network and the larger Deutsche Telekom (DT) network, shown in Fig. 5.1.

We use 6 modulation levels for the subcarriers: BPSK, QPSK, 8QAM, 16QAM, 32AQM, 64QAM, and adopt the half distance law used in [48] for the optical reach. According to that, BPSK, QPSK, 8QAM, 16QAM, 32QAM, 64QAM can be used for paths up to 3000 km, 1500 km, 750 km, 375 km, 187.5 km, and 93.75 km, respectively. With each subcarrier being 5 GHz, the data rate for BPSK is 2.5 Gbps per subcarrier [48], and the data rates for other modulation schemes increase by factors of 2, 4, 8, 16, and 32. We assume that each physical node has 100 VMs (as modern-day

servers allow tens of VMs per host [44]) and there are 800 subcarriers on each link (as C-band is 4000 GHz). In addition, the guardband is assumed to be $G = 2$ subcarriers.

VT requests are generated as follows. Each VT in the small network is a complete graph with 3 or 4 virtual nodes (selected randomly). In the DT network, each VT has between 3 and 10 virtual nodes, and a virtual link exists between a pair of nodes with probability 0.5 (we discard any topologies that are not connected). Each virtual node has between 1 and 3 physical node candidates (candidate nodes are all adjacent to each other), and requires a random number of VMs between 1 and 4. Each virtual link requires a bit-rate that is uniformly distributed over the range $0 - 2.5L$ Gbps, where $L$ is a data-rate load parameter.

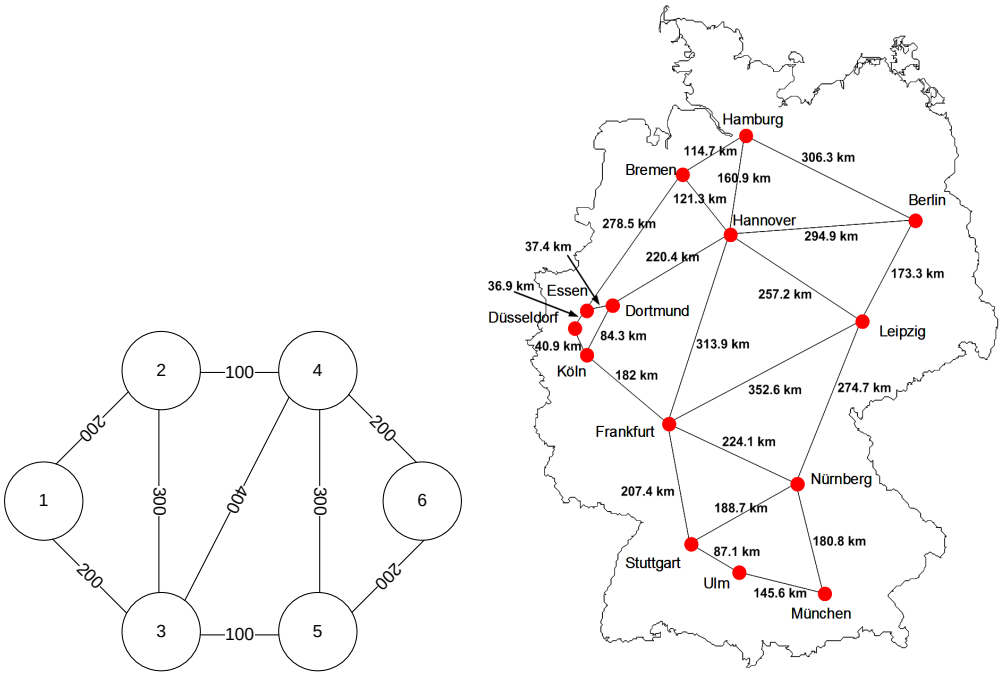


(a) 6-node network (b) DT

Figure 5.1: 6-node network and 14-node DT. The number on each link corresponds to the number of distance in km.

### 5.3.1 Static Requests

We first present results for the static traffic case. Due to the high complexity of the ILP, we are only able to obtain results for the small network. Sample results for

20 VT requests for various load values are shown in Table 5.1.

Table 5.1: Number of Subcarriers for ILP

| **20 VTs** | **First Fit** | **Link List** | **ILP** |
|---|---|---|---|
| **L=5** | 63 | 47 | 41 |
| **L=10** | 79 | 54 | 44 |
| **L=15** | 95 | 62 | 51 |
| **L=20** | 112 | 68 | 58 |
| **L=25** | 128 | 73 | 64 |
| **L=30** | 143 | 87 | 71 |
| **L=35** | 159 | 92 | 78 |
| **L=40** | 176 | 102 | 86 |

From these results, we observe that the LL algorithm performs much better than FF, suggesting that the simple greedy algorithm can be vastly improved upon with a clever heuristic. The LL results are quite close to those achieved by the ILP (no more than 25% in the cases considered), though there is some room for improvement. For the DT network, results for the two heuristics are presented in Table 5.2. These results confirm our earlier observations.

### 5.3.2 Dynamic Case

For dynamic traffic, VT requests are assumed to arrive to the network according to a Poisson process. For each data point in the graphs, we simulated 10,000 to 100,000 VT request arrivals. Each request has a holding time of 1 unit. The VT request arrival rate per unit time is variable, but intends to produce blocking rates between around $10^{-4}$ and $10^{-1}$. Figs. 5.2 and 5.3 show the request blocking and bandwidth blocking versus the virtual link bit rate load $L$ for the two algorithms with arrival rates of 20 and 30. The results show that for both performance metrics, LL is much better than FF.

Table 5.2: Number of Subcarriers for Static Traffic

| **20 VTs** | **First Fit** | **Link List** | **30 VTs** | **First Fit** | **Link List** |
|---|---|---|---|---|---|
| **L=5** | 167 | 143 | **L=5** | 194 | 162 |
| **L=10** | 213 | 172 | **L=10** | 244 | 214 |
| **L=15** | 254 | 208 | **L=15** | 293 | 240 |
| **L=20** | 291 | 239 | **L=20** | 341 | 280 |
| **L=25** | 334 | 275 | **L=25** | 392 | 324 |
| **L=30** | 379 | 313 | **L=30** | 439 | 360 |
| **L=35** | 420 | 326 | **L=35** | 492 | 405 |
| **L=40** | 468 | 375 | **L=40** | 543 | 432 |
| **L=45** | 513 | 390 | **L=45** | 594 | 505 |
| **L=50** | 557 | 454 | **L=50** | 646 | 523 |
| **L=55** | 602 | 485 | **L=55** | 699 | 571 |
| **L=60** | 652 | 489 | **L=60** | 755 | 608 |

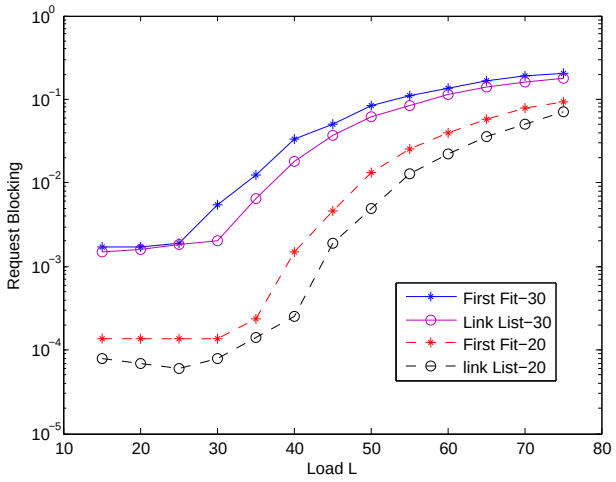


Figure 5.2: Request Blocking vs. Load L for arrival rates 20 and 30.

## 5.4 Conclusions

In this chapter, we investigated the virtual network mapping and subcarrier allocation problem for both static and dynamic traffic in elastic optical networks. We proposed two heuristics based on list scheduling, and simulation results showed the

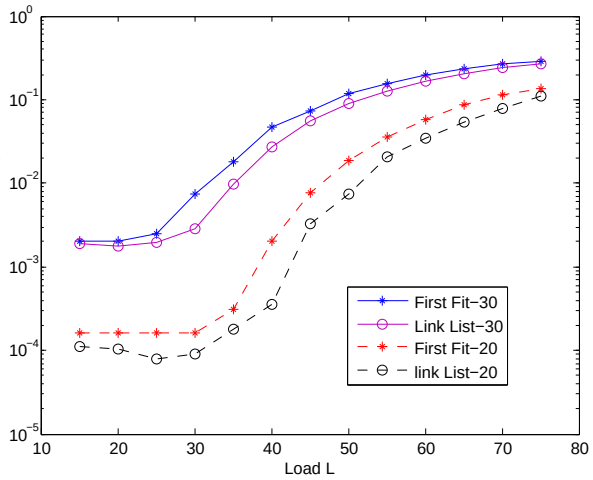


Figure 5.3: Bandwidth Blocking vs. Load L for arrival rates 20 and 30.

virtual link list scheduling approach achieves better performance than a simple first fit approach.

# Chapter 6 Analytical Performance Modeling

Our previous work has focused on designing new algorithms that outperform currently available methods. These algorithms are heuristic in nature, due to the complexity of the problems. In order to develop deeper insight into the impact of impairments and regeneration, we now turn our attention to analytical modeling. In this chapter, we develop analytical models to calculate the call blocking probability for three typical regeneration node allocation policies. The first policy allocates regeneration nodes when the lightpath needs either regeneration or wavelength conversion; while the other two allocation policies allocate regenerators only for one of the two reasons. The analytical models strike a balance between computational complexity and prediction accuracy. They are able to predict even surprising and counter-intuitive performance trends.

## 6.1 Related Work

Analytical performance modeling of optical networks without PLIs (i.e., considering only wavelength continuity) has been the subject of study for about two decades, and many models exist, e.g., [49–55]. However, modeling of translucent optical networks considering PLIs is much scarcer in the literature since the problem becomes much more difficult. Recently, some papers have addressed PLI-aware blocking probability analysis. In [56], an analytical method is presented to evaluate blocking probability accounting for PLIs; fixed routing and random wavelength assignment are used. The authors of [57] improve that work by using first-fit and first fit with ordering wavelength assignment methods. However, these papers consider transparent networks without 3R regenerators.

## 6.2 Contributions

To the best of our knowledge, this is the first work that presents complete analytical models for translucent optical networks considering the TR and limited regeneration resources. The models take into account realistic algorithms for wavelength conversion and regenerator allocation. The introduction of regenerator allocation to the problem of Routing and Wavelength Assignment (RWA) brings about new and significant challenges in modeling. Our rigorously derived models strike a balance between complexity and accuracy, as demonstrated through extensive simulation results. The input to the models is the optical network topology with a limited number of OEO converters at selected 3R nodes (which can be used as wavelength converters and/or regenerators when necessary), and the number of wavelengths per fiber. Connections arrive to and depart from the network according to a stochastic process. The output of the analytical performance models is the blocking probability of a connection request.

## 6.3 Network and Traffic Model

The network is modeled as a set of nodes and links, where each link consists of two fibers, one in each direction, with $W$ wavelengths each.

There are two kinds of nodes in the network: *transparent nodes* which do not have regenerators, and *regeneration (3R)* nodes, and the locations of these nodes are given. Each 3R node has a given limited number of OEO converters (called just OEOs for brevity, henceforth) for each outgoing link, which can be used for signal regeneration and/or wavelength conversion; these OEOs are shared by any connections using that outgoing link.[1] An OEO that is allocated to a connection cannot be used by another connection until the first connection is released. If an OEO is allocated to a connection, it can also provide wavelength conversion through retransmission on any desired output wavelength. We assume that a connection's

[1]This is the so-called share-per-link model. The alternative, share-per-node, is left for future work.

QoT requirement can be met as long as there is no OEO segment (subpath between regeneration points) longer than the TR on the connection's path.

Unidirectional connection requests (of full wavelength capacity) arrive to and depart from the network according to a Poisson process.[2] A connection can be blocked due to either of two reasons: (a) the RWA algorithm cannot find an available wavelength on an OEO segment of the path (*Wavelength blocking*), or (b) the TR constraint cannot be satisfied (*QoT blocking*) because of unavailability of OEOs.

We assume static fixed routing and random wavelength assignment, in which one of the available wavelengths on a path is randomly chosen to set up the connection. We recognize the importance of considering alternate paths and better wavelength assignment methods such as First Fit, and techniques to model these methods already exist [53, 57]. However, since our focus is on accounting for PLIs and limited regeneration in this work, we make these assumptions in order to keep the analysis (relatively) simple.

We assume the following realistic path selection algorithm. One candidate path is precomputed for each pair of nodes as follows. A logical graph is created for each source-destination pair. The logical nodes include all the 3R nodes and the source and destination nodes. A logical link exists between two logical nodes if the shortest path between those nodes in the original network is not longer than the TR. The cost of each logical link is set as the distance of its corresponding shortest path. The candidate path for the source-destination pair is chosen as the shortest path in the logical graph (if more than one shortest path has the same cost, choose the one with the least number of logical links).

### 6.4 Analytical Models

The models for the three resource allocation policies are presented in this section. These models are based on the analytical model for transparent networks (without physical layer impairment consideration) originally presented in [58]. As will be seen,

[2]This is by far the most common traffic model in the optical networking literature.

significant extensions to this model are necessary to accurately compute the performance of translucent networks.

### 6.4.1 Assumptions

The main model assumptions (for analytical tractability) are the following:

- The offered load to a 3R node (i.e., the rate at which regenerators are requested from a 3R node, for either regeneration or wavelength conversion or both) is independent of the offered loads to other 3R nodes.
- Wavelength usages on adjacent links are assumed to be correlated (as in [58]), except when the two links are separated by an OEO converter that is allocated to the connection. Accordingly, we call this model the "two-link model". The simpler assumption of wavelength usage independence on links (leading to the "independence model") will be shown later to be too inaccurate in certain cases.

These are reasonable simplifying assumptions that will be shown later in the paper to have minimal impact on the accuracy of the model.

### 6.4.2 Notation

Some basic notation used in the models is presented in Table 6.1.

### 6.4.3 Reduced Load Approximation

Since our analyses are link-based, and loads are offered to paths rather than links, we adopt the well-known iterative reduced load approximation technique [55, 59] as follows. First, we calculate the initial blocking probability on a connection's path $p$ with the offered load value $\rho_p^{(0)}$ with the assumption that $b_n^l = 0$ for all $n, l$. Then, for every iteration $i$, we calculate the new blocking values with the adjusted values of the offered load as $\rho_p^{(i)} = \rho_p^0(1 - B_p^{(i-1)})$, where $B_p$ is the blocking probability on path $p$. This process is repeated until $\frac{B_N^{(i)} - B_N^{(i-1)}}{B_N^{(i-1)}} \leq 1\%$ after a few iterations. In the next few sections, we develop the models and describe the blocking probability computation for a generic iteration.

### 6.4.4 OEO Allocation Policy I: Reach and Wavelength (RW)

First, we develop the analytical model for what we call the *Reach and Wavelength* OEO allocation policy. This most general policy allocates OEO nodes when either the signals need regeneration or the wavelengths need to be converted (or both). The algorithm can be explained in a straightforward manner. Starting at the source, proceed along the connection's path as far as possible, i.e., until either a continuous wavelength is not available or the TR is exceeded. Allocate an OEO at the furthest possible node to the connection so these constraints are met. Note that it is possible that all OEOs are being used at the furthest 3R node, so the algorithm may have to backtrack to the previous 3R node. After an OEO is allocated at a 3R node, the constraints are reset, and the algorithm starts afresh from that node; the algorithm terminates when the destination node is reached or the call is blocked. As simple as this algorithm may appear to be, modeling its performance is not easy. The main challenge comes from the fact that OEOs are allocated only when necessary (i.e., not allocated just because they are available at a node) and OEOs may not be available at a 3R node when needed, thus causing the backtrack mentioned above. This makes it necessary to evaluate the probabilities of a large set of (not always independent) events. The following example illustrates some of the possible steps of the algorithm.

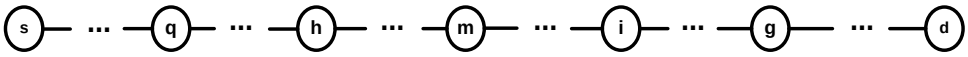


Figure 6.1: An example showing OEO allocation.

Let us look at the example path in Fig. 6.1 which shows the source and destination nodes of a connection and some 3R nodes on the path. Consider the 3R node $i$; suppose the next 3R node with available OEOs is node $g$; if $D(p_{s,g}) \leq \Omega$, $E_{s,i} = 1$, and $E_{s,g} = 0$, then node $i$ is allocated to convert wavelength. If $D(p_{s,g}) > \Omega$, $D(p_{s,i}) \leq \Omega$, $D(p_{i,g}) \leq \Omega$, and $E_{s,i} = 1$, then node $i$ is allocated to regenerate the signal. Similarly, suppose the previously allocated 3R node is node $h$; if $D(p_{h,g}) \leq \Omega$, $E_{h,i} = 1$, and $E_{h,g} = 0$, then node $i$ is allocated to convert wavelength. If $D(p_{h,g}) > \Omega$, $D(p_{h,i}) \leq \Omega$, $D(p_{i,g}) \leq \Omega$, and $E_{h,i} = 1$, then node $i$ is allocated to regenerate the signal. The

reason for the condition $D(p_{i,g}) \leq \Omega$ is that the call will be blocked due to bad QoT when $D(p_{i,g}) > \Omega$; in this case, there is no load on OEO $i$. (In other words, when $D(p_{i,g}) > \Omega$, there is no need to allocate OEO $i$ to the call, since the call will be blocked.)

*Single-hop path*

For a connection $(s, d)$, if its candidate path $p_{s,d}$ has only one link $l_{s,d}$, the blocking probability $B_{s,d}$ can be found by the Erlang B formula with the offered load $\rho_{l_{s,d}}$ and total capacity $W$. Since $\mu = 1$, $\rho_{l_{s,d}} = \lambda_{l_{s,d}}$, and

$$\rho_l = \sum_{p: l \in p} \lambda_p. \tag{6.1}$$

$$B_{s,d} = F_0(s, d) = \frac{\frac{\rho_l^W}{W!}}{\sum_{i=0}^{W} \frac{\rho_l^i}{i!}}. \tag{6.2}$$

*Two-link model*

Since, by assumption, wavelength dependencies are only limited to adjacent links of a path, let us consider a generic two-hop path *a-b-c*. Some additional notation is defined in Table 6.2. Then, we have [58]:

$$\mathcal{P}_1(h|i, j, k) = \frac{\binom{W}{k}\binom{W-k}{i}\binom{i}{h}\binom{W-i-k}{j-h}}{\binom{W}{k}\binom{W-k}{i}\binom{W-k}{j}} = \frac{\binom{i}{h}\binom{W-i-k}{j-h}}{\binom{W-k}{j}}. \tag{6.3}$$

for $\min(i, j) \geq h \geq \max(0, i + j + k - W)$. Further, from the notation in Table 6.2, we have

$$F_k(u, v) = \sum_{e=k}^{W} T^m(k, e), \tag{6.4}$$

where $m \geq 2$ is the number of hops on $p_{u,v}$. If $m = 1$, $F_k(u, v)$ can be found by the Erlang B formula as

$$F_k(u, v) = \frac{\frac{\rho_{l_{u,v}}^{W-k}}{(W-k)!}}{\sum_{i=0}^{W} \frac{\rho_{l_{u,v}}^i}{i!}}. \tag{6.5}$$

$T^m(k,e)$ is computed in the following sections for $m > 1$.

The set of connections traversing a two-link subpath (where the middle node may be a 3R node) is partitioned into five subsets, whose cardinalities are $\mathcal{C}_e$, $\mathcal{C}_f$, $\mathcal{C}_c$, $\mathcal{C}_r$ and $\mathcal{C}_w$. Note that $\mathcal{C}_r$ and $\mathcal{C}_w$-type calls [3], respectively, are allocated OEOs to regenerate signals and convert wavelengths. However, once allocated, these calls also avail of the other function, namely, convert wavelengths and clean up impairments, respectively. There is no reason to assume otherwise.

The reason we differentiate between $\mathcal{C}_w$-type calls and $\mathcal{C}_r$-type is the following. If the OEO is allocated to convert wavelengths, then the assigned wavelengths on the two links adjacent to the 3R node are necessarily different. But if the OEO node is allocated to regenerate the signal, the assigned wavelengths on the two links may or may not be different since the wavelengths on the two segments are randomly picked from the available wavelengths. This important distinction will be relevant to the calculation of $\mathcal{P}_4(k|i,j)$ later.

For the two links $a$-$b$ and $b$-$c$, we have

$$\rho_e = \sum_{p:a\text{-}b\in p, b\text{-}c\notin p} \lambda_p, \tag{6.6}$$

$$\rho_f = \sum_{p:a\text{-}b\notin p, b\text{-}c\in p} \lambda_p, \tag{6.7}$$

$$\rho_c = \sum_{p:a\text{-}b\in p, b\text{-}c\in p} \lambda_p - \rho_r - \rho_w. \tag{6.8}$$

Due to the assumption that connections arrive at each path according to a Poisson process, and the connections' holding times are exponentially distributed, we can model the state of connections on a two-link path as a five-dimensional Markov chain (along the lines of [58]). The steady state probability for state $(\mathcal{C}_e, \mathcal{C}_f, \mathcal{C}_c, \mathcal{C}_r, \mathcal{C}_w)$ is:

$$\boldsymbol{\pi}(\mathcal{C}_e, \mathcal{C}_f, \mathcal{C}_c, \mathcal{C}_r, \mathcal{C}_w) = \frac{\frac{\rho_e^{\mathcal{C}_e}}{\mathcal{C}_e!}\frac{\rho_f^{\mathcal{C}_f}}{\mathcal{C}_f!}\frac{\rho_c^{\mathcal{C}_c}}{\mathcal{C}_c!}\frac{\rho_r^{\mathcal{C}_r}}{\mathcal{C}_r!}\frac{\rho_w^{\mathcal{C}_w}}{\mathcal{C}_w!}}{\Delta} \tag{6.9}$$

[3] By an abuse of notation, we use the cardinality to also mean the type of call.

where the normalization factor $\Delta$ can be calculated as

$$\Delta = \sum_{h=0}^{\min(R,W)} \sum_{g=0}^{\min(R-h,W-h)} \sum_{k=0}^{W-h-g} \sum_{i=0}^{W-k-h-g} \sum_{j=0}^{W-k-h-g} \frac{\rho_e^i}{i!} \frac{\rho_f^j}{j!} \frac{\rho_c^k}{k!} \frac{\rho_r^h}{h!} \frac{\rho_w^g}{g!} \tag{6.10}$$

with constraints $0 \leq \mathcal{C}_r + \mathcal{C}_w \leq R$, $0 \leq \mathcal{C}_r + \mathcal{C}_c + \mathcal{C}_e + \mathcal{C}_w \leq W$ and $0 \leq \mathcal{C}_r + \mathcal{C}_c + \mathcal{C}_f + \mathcal{C}_w \leq W$.

*The Distributions of $\rho_r$ and $\rho_w$*

We still need $\rho_r$ and $\rho_w$ to compute the above equation. If the middle node $b$ is a transparent node, then $\rho_r = \rho_w = 0$. If node $b$ is a 3R node, the values are obtained as follows. We will first find $\hat{x}_n^l(p)$ and $\bar{x}_n^l(p)$ (where $n = b$) for the paths that include links $a$-$b$ and $b$-$c$ ($l$ is link $b$-$c$); denote these paths as set $P$. Then

$$\rho_r = \sum_{p \in P} \bar{x}_n^l(p), \tag{6.11}$$

$$\rho_w = \sum_{p \in P} \hat{x}_n^l(p). \tag{6.12}$$

The challenge in computing these loads is in part due to the several events (beyond the two-link path) that need to be considered, as suggested by the example in Fig. 6.1.

We introduce some additional notation in Table 6.3. In the table, $u$, $v$, and $t$ are 3R nodes on a path. Node $u$ is closer to the source, node $t$ is closer to the destination, and node $v$ is between $u$ and $t$. Also, the phrase "there is no blocking from source to node $v$" means that OEOs can be allocated so that the constraints of wavelength continuity and TR can be satisfied on the path from source to $v$.

$\hat{x}_i$ and $\bar{x}_i$ for an arbitrary 3R node $i$ on path $p$ are computed as follows. Consider the example in Fig. 6.1. We have,

$$\hat{x}_i^l(p) = \sum_{\substack{s \leq h \leq i-1 \\ D(p_{h,i}) \leq \Omega}} \sum_{\substack{i+1 \leq g \leq d \\ D(p_{h,g}) \leq \Omega}} X(h,i,g)\lambda_p \tag{6.13}$$

where the previous allocated 3R node is node $h$; this can be any 3R node between source $s$ and 3R node $i-1$, with the condition that the distance from $h$ to $i$ is not longer than TR. The next 3R node $g$ with free OEOs can be any node from 3R node $i+1$ to destination $d$, with the condition that the distance from $h$ to $g$ is not longer than TR.

On the other hand,

$$\bar{x}_i^l(p) = \sum_{\substack{s \le h \le i-1 \\ D(p_{h,i}) \le \Omega}} \sum_{\substack{i+1 \le g \le d, \\ D(p_{h,g}) > \Omega \\ D(p_{i,g}) \le \Omega}} Z(h,i,g)\lambda_p \tag{6.14}$$

*The Distributions of $\mathcal{P}_2$, $\mathcal{P}_3$ and $\mathcal{P}_4$*

We can obtain these probabilities (Equations (6.15), (6.16), (6.17)) from the steady-state probabilities of the Markov chain. The probability $P(\alpha, K, \mathcal{C}_r, \mathcal{C}_w, \mathcal{C}_c, \mathcal{C}_e, \mathcal{C}_f)$ in Equation (6.17) is defined as the joint probability of the following events: there are $W-\mathcal{C}_c-\mathcal{C}_e-\mathcal{C}_w$ available wavelengths on the first link, $W-\mathcal{C}_c-\mathcal{C}_f-\mathcal{C}_w$ on the second link, $K$ available (common) wavelengths on both links, and when $\mathcal{C}_r$ wavelengths are randomly chosen from the available wavelengths on each of the two links, $\alpha$ (of the $\mathcal{C}_r$) are identical on both links, its calculation is in Appendix A.

$$\begin{aligned}\mathcal{P}_2(i) &= P(\mathcal{C}_c + \mathcal{C}_e + \mathcal{C}_r + \mathcal{C}_w = W - i) \\ &= \sum_{\mathcal{C}_r=0}^{\min(R,W-i)} \sum_{\mathcal{C}_w=0}^{\min(R-\mathcal{C}_r, W-i-\mathcal{C}_r)} \sum_{\mathcal{C}_c=0}^{W-i-\mathcal{C}_r-\mathcal{C}_w} \sum_{\mathcal{C}_f=0}^{W-\mathcal{C}_r-\mathcal{C}_c-\mathcal{C}_w} \boldsymbol{\pi}(W-i-\mathcal{C}_c-\mathcal{C}_r-\mathcal{C}_w, \mathcal{C}_f, \mathcal{C}_c, \mathcal{C}_r, \mathcal{C}_w).\end{aligned} \tag{6.15}$$

$$\begin{aligned}\mathcal{P}_3(j|i) &= P(\mathcal{C}_f + \mathcal{C}_c + \mathcal{C}_r + \mathcal{C}_w = W - j \mid \mathcal{C}_e + \mathcal{C}_c + \mathcal{C}_r + \mathcal{C}_w = W - i) \\ &= \frac{\sum_{\mathcal{C}_r=0}^{up1} \sum_{\mathcal{C}_w=0}^{up2} \sum_{\mathcal{C}_c=0}^{up3} \boldsymbol{\pi}(W-i-\mathcal{C}_c-\mathcal{C}_r-\mathcal{C}_w, W-j-\mathcal{C}_c-\mathcal{C}_r-\mathcal{C}_w, \mathcal{C}_c, \mathcal{C}_r, \mathcal{C}_w)}{\sum_{\mathcal{C}_r=0}^{\min(R,W-i)} \sum_{\mathcal{C}_w=0}^{up4} \sum_{\mathcal{C}_c=0}^{W-i-\mathcal{C}_r-\mathcal{C}_w} \sum_{\mathcal{C}_f=0}^{W-\mathcal{C}_r-\mathcal{C}_w-\mathcal{C}_c} \boldsymbol{\pi}(W-i-\mathcal{C}_c-\mathcal{C}_r-\mathcal{C}_w, \mathcal{C}_f, \mathcal{C}_c, \mathcal{C}_r, \mathcal{C}_w)},\end{aligned} \tag{6.16}$$

where $up1 = \min(R, W-i, W-j)$, $up2 = \min(R-\mathcal{C}_r, W-i-\mathcal{C}_r, W-j-\mathcal{C}_r)$, $up3 = \min(W-i-\mathcal{C}_r-\mathcal{C}_w, W-j-\mathcal{C}_r-\mathcal{C}_w)$, $up4 = \min(R-\mathcal{C}_r, W-i-\mathcal{C}_r)$.

$$\mathcal{P}_4(k|i,j) = P(\mathcal{C}_c + \alpha = k | \mathcal{C}_e + \mathcal{C}_c + \mathcal{C}_r + \mathcal{C}_w = W - i, \mathcal{C}_f + \mathcal{C}_c + \mathcal{C}_r + \mathcal{C}_w = W - j)$$
$$= \frac{\sum_{\alpha=0}^{up3} \sum_{\mathcal{C}_w=0}^{up4} \sum_{\mathcal{C}_e=low1}^{up5} \sum_{K=\alpha}^{up6} P(\alpha, K, W - i - \mathcal{C}_e - \mathcal{C}_w - k + \alpha, \mathcal{C}_w, k - \alpha, \mathcal{C}_e, i - j + \mathcal{C}_e)}{\sum_{\mathcal{C}_r=0}^{\min(R,W-i,W-j)} \sum_{\mathcal{C}_w=0}^{up1} \sum_{\mathcal{C}_c=0}^{up2} \boldsymbol{\pi}(W - i - \mathcal{C}_c - \mathcal{C}_r - \mathcal{C}_w, W - j - \mathcal{C}_c - \mathcal{C}_r - \mathcal{C}_w, \mathcal{C}_c, \mathcal{C}_r, \mathcal{C}_w)}, \tag{6.17}$$

where $up1 = \min(R - \mathcal{C}_r, W - i - \mathcal{C}_r, W - j - \mathcal{C}_r)$, $up2 = \min(W - i - \mathcal{C}_r - \mathcal{C}_w, W - j - \mathcal{C}_r - \mathcal{C}_w)$, $up3 = \min(R, k)$, $up4 = W - i - k - \mathcal{C}_w$, $up5 = \min(R - \alpha, W - i - k + \alpha, W - j - k + \alpha)$, $up6 = \min(W - \mathcal{C}_e - \mathcal{C}_w - k + \alpha, W - \mathcal{C}_f - \mathcal{C}_w - k + \alpha)$, $low1 = \max(0, j - i, W - i - k + \alpha - R - \mathcal{C}_w)$; the upper and lower bounds of $\mathcal{C}_e$ are found with $\alpha \leq \mathcal{C}_r \leq R$.

*Blocking on a Path Without 3R Nodes*

The blocking probabilities on paths without any 3R nodes can be calculated by $B_p = F_0(s,d) = \sum_{e=0}^{W} T^m(0,e)$, where $m$ is the number of hops on the path.

The values of $T^m(h,e)$ can be calculated recursively from $T^{m-1}(f,j)$ as follows by assuming the subpath with $m-1$ hops as a link, and the last hop of the path as the second link.

$$T^m(h,e) = \sum_{f=h}^{W} \sum_{j=f}^{W} \sum_{k=0}^{\min(W-e,W-j)} \mathcal{P}_1(h|f,e,k)\mathcal{P}_4(k|j,e)\mathcal{P}_3(e|j)T^{m-1}(f,j). \tag{6.18}$$

The starting point of the recursion, $T^1(h,e) = 0$ when $h \neq e$, and is equal to the probability of having $e$ free wavelengths on a link, $\mathcal{P}_2(e)$, when $h = e$.

*Blocking on a Path With 3R Nodes*

For a path $p$ from source $s$ to destination $d$, we will first find its acceptance probability $A_p$ as follows; then $B_p = 1 - A_p$.

An example path from $s$ to $d$ with several 3R nodes is shown in Fig. 6.2, the 3R nodes on the paths are numbered as $1, 2, 3, ...$, and suppose node $h$ is the last 3R node

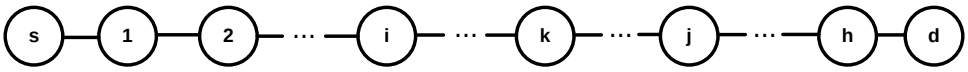


Figure 6.2: An example showing a path with 3R nodes.

on the path. $i, k, j$ are three variable 3R nodes, their relative positions are shown in Fig. 6.2. We will use the notations $E_{u,v}, H_n$ and $G_{u,v}$, which are defined in Table 6.1.

We can get the $\rho_n^l$ from the $x_n^l(p)$ values, i.e., $\rho_n^l = \sum_{p:l\in p} x_n^l(p)$. Then $b_n^l$ can be calculated by the Erlang B formula, i.e.,

$$b_n^l = \frac{\frac{(\rho_n^l)^R}{R!}}{\sum_{r=0}^{R} \frac{(\rho_n^l)^r}{r!}}. \tag{6.19}$$

Based on the OEO availability at 3R node 1, we can calculate $A_p$ as:

$$\begin{aligned} A_p &= \Pr\{H_1 = 1, G_{s,d} = 1\} + \Pr\{H_1 = 0, G_{s,d} = 1\} + \Pr\{G_{s,d} = 1 \,|E_{s,1} = 1, H_1 = 1\} \\ &\quad + \Pr\{E_{s,1} = 1, H_1 = 1\} + \Pr\{G_{s,d} = 1 \,|E_{s,1} = 0, H_1 = 1\}\Pr\{E_{s,1} = 0, H_1 = 1\} \\ &\quad + \Pr\{H_1 = 0, G_{s,d} = 1\} \\ &= (1 - b_1^l)F(s,1)\Pr\{G_{s,d} = 1 \,|E_{s,1} = 1, H_1 = 1\} + b_1^l \Pr\{G_{s,d} = 1 \,|H_1 = 0\}. \end{aligned} \tag{6.20}$$

Note that $\Pr\{G_{s,d} = 1 \,|E_{s,1} = 0, H_1 = 1\} = 0$, since if there is no available wavelength from the source to the first 3R node on the path, the connection is blocked, i.e., $\Pr\{G_{s,d} = 1\} = 0$.

Then we move on to consider the OEO availability at 3R node 2, node 3, and so on until node $h$. Each time only one 3R node is under consideration. The idea is that if there is no blocking on the path, the current 3R node under consideration is node $j$, and the previously allocated 3R node (to the connection) is $i$, then we know there is no blocking from source $s$ to node $i$ (some 3R nodes could be allocated in between), and there should be no blocking from $i$ to $d$. It is possible that an OEO is allocated at node $j$ to make this true (if necessary and if there are available OEOs at node $j$).

Thus, we need two definitions. Let $M(i, j, d)$ denote the probability that there is no blocking from $i$ to $d$, given that there are available OEOs at node $j$, the previously

allocated 3R node is node $i$ (if there is no previously allocated 3R node, node $i$ is source node $s$), and there are available wavelengths on $p_{i,j}$. Let $M'(i,j,d,k)$ denote the probability that there is no blocking from $i$ to $d$, given that there are no available OEOs at node $j$, the previously allocated 3R node is node $i$ (if there is no previously allocated 3R node, node $i$ is source node $s$), and the previous 3R node with available OEOs, but not yet allocated is node $k$, there are available wavelengths on $p_{i,k}$. (Node $k$ is set as 0 if there is no such $k$, e.g., $j = i + 1$; in this case, there is no condition that there are available wavelengths on $p_{i,k}$.).

In order to compute $M(i,j,d)$ and $M'(i,j,d,k)$, we need to consider the availability of OEOs at node $j+1$. Also, the OEOs at node $j$ or node $k$, respectively, may be allocated to regenerate signal and/or convert the wavelengths to ensure there is no blocking from $i$ to destination $d$. When we reach $j = h$, the next 3R node is $d$, (i.e., $j + 1 = d$), and this procedure is finished. The details of the computation of $M(i,j,d)$ and $M'(i,j,d,k)$ are in Appendix B.

*Summary*

The procedure to find the network blocking probability for the RW policy is summarized in Algorithm 1.

### 6.4.5 OEO Allocation Policy II: Wavelength Only (WO)

We now consider a popular OEO allocation policy that does not consider physical layer impairments. According to this policy, OEOs are allocated only if wavelength conversion is needed. The WO policy allocates OEOs as follows. Starting at the source, proceed along the path until a continuous wavelength is not available. Allocate an OEO to perform wavelength conversion at the previous node, if available. If an OEO is not available at that node, backtrack to a previous node at which an OEO is available, and restart the process from that node. Continue until the destination is reached or the call is blocked. Note, however, that while the allocation policy does not consider the TR, a connection is assumed to be blocked if any OEO segment is longer than the TR. In other words, all admitted connections are guaranteed to satisfy the

**Algorithm 4** Blocking Computation for the RW Policy

Step 1: Precompute the values of $\mathcal{P}_1(h|i,j,k)$ (Equation (6.3)), which are independent with traffic loads.

Step 2: Consider each single link, the values of $\rho_{u,v}$, $F_k(u,v)$, $F(u,v)$ and $\hat{F}(u,v)$ will be used later when considering paths with multiple links.

**for** each link $l_{u,v}$ **do**

1. Calculate offered load $\rho_{u,v}$ (Equation (6.1))

2. Calculate the probability that the link has $k$ free wavelengths, $F_k(u,v)$ (Equation (6.5))

3. Calculate the probability that the link has at least one free wavelength, $F(u,v) = \sum_{k=1}^{W} F_k(u,v)$

4. Calculate the probability $\hat{F}_k(u,v)$ (defined in Table 6.3)

5. Calculate the blocking probability of single-hop path $p$ between nodes $u, v$, $B_p = F_0(u,v)$

**end for**

Step 3: Then we consider paths with more than one link. We need the steady state distribution of the five-dimensional Markov Chain, and the offered loads for the five types of connections, $\rho_e$, $\rho_f$, $\rho_c$, $\rho_w$, and $\rho_r$. In this step, the values of $\hat{x}_i^l(p)$ and $\bar{x}_i^l(p)$ are calculated, which will be used to get $\rho_w$ and $\rho_r$ in the next step.

**for** each path $p_{s,d}$ containing at least one 3R node **do**

**for** each 3R node $i$ on path $p_{s,d}$, starting from the one closest to $s$ and proceeding to the one closest to $d$ **do**

1. Calculate the values of $X(s,i,g)$ (Equation (6.45)), $X'(s,i,g)$ (Equation (6.46)), $Z(s,i,g)$ (Equation (6.49)), $Z'(s,i,g)$ (Equation (6.50)), $X(h,i,g)$ (Equation (6.47)), $X'(h,i,g)$ (Equation (6.48)), $Z(h,i,g)$ (Equation (6.51)) and $Z'(h,i,g)$ (Equation (6.52)) (In Appendix C) (The involved values of $b_n^l$, $F(u,v)$, $\hat{F}_k(u,v)$, $\bar{F}_k(u,v,t)$ and $F'_k(u,v,t)$ are those found in Steps 5 and 6 of the previous iteration; as explained in Section 6.4.3)

2. Calculate $\hat{x}_i^l(p)$ (Equation (6.13)) and $\bar{x}_i^l(p)$ (Equation (6.14)) (where $l$ is the corresponding outgoing link of 3R node $i$ on path $p$)

**end for**

**end for**



Step 4: Now we can calculate the offered loads of the five types of connections. Then we can get the steady state distribution of the Markov Chain. In turn, we

**Algorithm 3** Blocking Computation for the RW Policy (continued)

Step 5: In this step, we will calculate $T^m(h, e)$, which is used to find the blocking probabilities for paths without 3R nodes on them.

**for** each path $s, d$ ($m > 1$ hops) **do**

1. Calculate $T^m(h, e)$ (Equation (6.18))

2. Calculate $F_k(s, d)$ (Equation (6.4)), $\hat{F}_k(u, v)$ (defined in Table 6.3), $\bar{F}_k(u, v, t)$ (Equation (6.43)) and $F'_k(u, v, t)$ (Equation (6.44). (Note that these values will be used in Step 3 of the next iteration.)

**end for**

Step 6:

**for** each path $s, d$ ($m > 1$ hops) without any 3R nodes on it **do**

Calculate the blocking probability $B_p = F_0(s, d)$

**end for**

Step 7: Now we will consider the paths with 3R nodes on them. In this step, we will calculate the offered loads to each 3R node's outgoing link $\rho_n^l$; and in turn, the probability that there are no available OEO converters at a 3R node $b_n^l$. Then we can get the acceptance probability of a path $A_p$ based on $M(i, j, d)$ and $M'(i, j, d, k)$.

**for** each path $s, d$ containing 3R nodes **do**

**for** each 3R node $n$ on the path **do**

1. Calculate the offered load to 3R node $n$ on outgoing link $l$; $\rho_n^l = \sum_{l \in p} \hat{x}_n^l(p) + \bar{x}_n^l(p)$

2. Calculate the probability that there are no OEOs available at the node $b_n^l$ (Equation (6.19)) (where $l$ is the corresponding outgoing link with node $n$ on the path) (Note that these values will be used in the next iteration.)

**end for**

1. Calculate the acceptance probability of the path $A_p$ (Equation (6.20)) depending on the OEO availability at the first 3R node on the path. This calculation is based on the values of $M(i, j, d)$ and $M'(i, j, d, k)$ (In Appendix B.)

2. Calculate the blocking probability $B_p = 1 - A_p$

**end for**

Step 8: Calculate the network blocking probability $B_N = \frac{\sum_{s,d} \lambda_{s,d} B_{s,d}}{\sum_{s,d} \lambda_{s,d}}$

QoT requirement. This allocation policy is called as QoT-guaranteed in the literature ([57]). Note that due to this QoT guarantee, the earlier models for transparent networks (that consider only wavelength continuity and ignore QoT) cannot be used. In this subsection, we develop the analytical model for the Wavelength Only OEO allocation policy. It turns out that the previous model can be simplified for this policy. We present the necessary modifications below.

*Single-hop path*

The blocking probabilities of paths including a single link are still found by equations (6.1) and (6.2).

*Two link model*

For this policy, a four dimensional Markov chain suffices (by discarding the $\mathcal{C}_r$ part from the previous 5-D Markov chain used in the Reach and Wavelength model). The equations for calculating $\rho_e$ and $\rho_f$ are still equations (6.6) and (6.7).

The equation to find $\rho_c$ is as follows.

$$\rho_c = \sum_{p:a\text{-}b\in p, b\text{-}c\in p} \lambda_p - \rho_w. \tag{6.21}$$

Then, the steady state probability for state $(\mathcal{C}_e, \mathcal{C}_f, \mathcal{C}_c, \mathcal{C}_w)$ and the normalization factor $\Delta$ are similar to equations (6.9) and (6.10) by removing the $\mathcal{C}_r$ part. (Note that this is a different Markov Chain from the one used for the RW policy, with $C_r$ being subsumed within other connection types.)

$$\boldsymbol{\pi}(\mathcal{C}_e, \mathcal{C}_f, \mathcal{C}_c, \mathcal{C}_w) = \frac{\frac{\rho_e^{\mathcal{C}_e}}{\mathcal{C}_e!}\frac{\rho_f^{\mathcal{C}_f}}{\mathcal{C}_f!}\frac{\rho_c^{\mathcal{C}_c}}{\mathcal{C}_c!}\frac{\rho_w^{\mathcal{C}_w}}{\mathcal{C}_w!}}{\Delta} \tag{6.22}$$

where the normalization factor $\Delta$ can be calculated as

$$\Delta = \sum_{h=0}^{\min(R,W)} \sum_{k=0}^{W-h} \sum_{i=0}^{W-k-h} \sum_{j=0}^{W-k-h} \frac{\rho_e^i}{i!}\frac{\rho_f^j}{j!}\frac{\rho_c^k}{k!}\frac{\rho_w^h}{h!} \tag{6.23}$$

with constraints $0 \leq \mathcal{C}_w \leq R$, $0 \leq \mathcal{C}_w + \mathcal{C}_c + \mathcal{C}_e \leq W$ and $0 \leq \mathcal{C}_w + \mathcal{C}_c + \mathcal{C}_f \leq W$.

In addition, only $\hat{x}_n^l(p)$, $X(u,v,t)$ and $X'(u,v,t)$ are needed for this policy when calculating the values of $\rho_w$. The equations of $X(u,v,t)$ and $X'(u,v,t)$ are the same as the ones in Appendix B, except that the values of all $Z$ and $Z'$ are assumed to be zero. Also,

$$x_n^l(p) = \hat{x}_n^l(p). \tag{6.24}$$

The equations to find $\mathcal{P}_2(i)$, $\mathcal{P}_3(j|i)$ are similar to Equations (6.15), (6.16) by removing $\mathcal{C}_r$. Equation (6.27) is used to find $\mathcal{P}_4(k|j,i)$.

$$\begin{aligned}\mathcal{P}_2(i) &= P(\mathcal{C}_c + \mathcal{C}_e + \mathcal{C}_w = W - i) \\ &= \sum_{\mathcal{C}_w=0}^{\min(R,W-i)} \sum_{\mathcal{C}_c=0}^{W-i-\mathcal{C}_w} \sum_{\mathcal{C}_f=0}^{W-\mathcal{C}_c-\mathcal{C}_w} \boldsymbol{\pi}(W-i-\mathcal{C}_c-\mathcal{C}_w, \mathcal{C}_f, \mathcal{C}_c, \mathcal{C}_w).\end{aligned} \tag{6.25}$$

$$\begin{aligned}\mathcal{P}_3(j|i) &= P(\mathcal{C}_f + \mathcal{C}_c + \mathcal{C}_w = W - j \mid \mathcal{C}_e + \mathcal{C}_c + \mathcal{C}_w = W - i) \\ &= \frac{\sum_{\mathcal{C}_w=0}^{up1} \sum_{\mathcal{C}_c=0}^{up2} \boldsymbol{\pi}(W-i-\mathcal{C}_c-\mathcal{C}_w, W-j-\mathcal{C}_c-\mathcal{C}_w, \mathcal{C}_c, \mathcal{C}_w)}{\sum_{\mathcal{C}_w=0}^{\min(R,W-i)} \sum_{\mathcal{C}_c=0}^{W-i-\mathcal{C}_w} \sum_{\mathcal{C}_f=0}^{W-\mathcal{C}_w-\mathcal{C}_c} \boldsymbol{\pi}(W-i-\mathcal{C}_c-\mathcal{C}_w, \mathcal{C}_f, \mathcal{C}_c, \mathcal{C}_w)},\end{aligned} \tag{6.26}$$

where $up1 = \min(R, W-i, W-j)$, $up2 = \min(W-i-\mathcal{C}_w, W-j-\mathcal{C}_w)$.

$$\begin{aligned}&\mathcal{P}_4(k|j,i) = P(\mathcal{C}_c = k | \mathcal{C}_e + \mathcal{C}_c + \mathcal{C}_w = W - i, \mathcal{C}_f + \mathcal{C}_c + \mathcal{C}_w = W - j) \\ &= \frac{\sum_{\mathcal{C}_w=0}^{\min(R,W-j-k,W-i-k)} \boldsymbol{\pi}(W-i-\mathcal{C}_w-k, W-j-\mathcal{C}_w-k, k, \mathcal{C}_w)}{\sum_{\mathcal{C}_w=0}^{\min(R,W-j,W-i)} \sum_{\mathcal{C}_c=0}^{min(W-\mathcal{C}_w-i,W-\mathcal{C}_w-j)} \boldsymbol{\pi}(W-i-\mathcal{C}_w-\mathcal{C}_c, W-j-\mathcal{C}_w-\mathcal{C}_c, \mathcal{C}_c, \mathcal{C}_w)}.\end{aligned} \tag{6.27}$$

For the paths that don't include a 3R node, their blocking probabilities can be calculated by $B_p = F_0(s,d) = \sum_{e=0}^{W} T^m(0,e)$, where $m$ is the number of hops with the path. The values of $T^m(h,e)$ can be calculated from (6.18).

*Blocking on a Path With 3R Nodes*

The probability that a 3R node has available OEOs is found by Equation (6.19). For each path, we first find its acceptance probability with the same method as for

Reach and Wavelength Model, except with different equations to find $M$ and $M'$ as follows.

$$M(i,j,d) = \begin{cases} (1-b_{j+1}^l)\frac{\hat{F}(i,j+1)}{F(i,j)}M(i,j+1,d) + (1-b_{j+1}^l)\frac{F'(i,j,j+1)}{F(i,j)} \\ M(j,j+1,d) + b_{j+1}^l M'(i,j+1,d,j), \\ \qquad\qquad \text{if } j \neq h, D(p_{i,j}) \leq \Omega \\ \frac{\hat{F}(i,d)}{F(i,j)} + \frac{F'(i,j,d)}{F(i,j)}, \qquad \text{if } j = h, D(p_{i,j}) \leq \Omega \\ 0. \qquad\qquad \text{otherwise} \end{cases} \tag{6.28}$$

$$M'(i,j,d,k) = \begin{cases} (1-b_{j+1}^l)\frac{\hat{F}(i,j+1)}{F(i,k)}M(i,j+1,d) + (1-b_{j+1}^l)\frac{F'(i,k,j+1)}{F(i,k)} \\ M(k,j+1,d) + b_{j+1}^l M'(i,j+1,d,k), \\ \qquad\qquad \text{if } k \neq 0, j \neq h, D(p_{i,k}) \leq \Omega \\ (1-b_{j+1}^l)\hat{F}(i,j+1)M(i,j+1,d) + b_{j+1}^l M'(i,j+1,d,k), \\ \qquad\qquad \text{if } k = 0, j \neq h \\ \frac{\hat{F}(i,d)}{F(i,k)} + \frac{F'(i,k,d)}{F(i,k)}, \qquad \text{if } k \neq 0, j = h, D(p_{i,k}) \leq \Omega \\ \hat{F}(i,d), \qquad\qquad \text{if } k = 0, j = h \\ 0. \qquad\qquad \text{otherwise} \end{cases} . \tag{6.29}$$

The constraint $D(p_{i,k}) \leq \Omega$ in the above two equations ensures that the denominator $F(i,k)$ is greater than zero. Compared with the Reach and Wavelength policy, the cases for $D(p_{i,j+1}) > \Omega$ and $D(p_{i,j+1}) > \Omega, D(p_{k,j+1}) \leq \Omega$ for $M$ and $M'$, respectively, are removed, since in the previous policy, the OEOs at node $i$ and $k$ (respectively) are allocated to regenerate the signal, but that is not the case in the current policy. The other difference is that $F(i,j+1)$ (or $F(i,d)$) are replaced by $\hat{F}(i,j+1)$ (or $\hat{F}(i,d)$), which is equal to $F(i,j+1)$ (or $F(i,d)$) when $D(p_{i,j+1}) \leq \Omega$ (or $D(p_{i,d}) \leq \Omega$), otherwise, these values are zero. These replacements are done since $M$ and $M'$ are the probabilities that there is no blocking from source to $j$, but when $D(p_{i,j+1}) > \Omega$ (or $D(p_{i,d}) > \Omega$), the cases with $F(i,j+1) > 0$ (or $F(i,d) > 0$) mean that OEOs at node $j$ (or at node $k$) won't be allocated (since there is no need to convert wavelengths, recall

that WO policy only allocates OEO converters to convert wavelengths), and therefore the call will be blocked due to bad QoT (since $D(p_{i,j+1}) > \Omega$ (or $D(p_{i,d}) > \Omega$), but no OEO converters are allocated to regenerate signal). Thus we use $\hat{F}(i, j+1)$ (or $\hat{F}(i, d)$) to force the values of $M$ and $M'$ to be zero in these cases. (Note that the cases that OEOs at node $j$ (or at node $k$) are allocated correspond to other cases of the equations, the ones with $F'(i, j, j+1)$ (or $F'(i, k, j+1)$)).

*Summary*

A summarized procedure for computing network blocking probability $B_N$ for the WO policy is given in Algorithm 5.

### 6.4.6 OEO Allocation Policy III: Reach Only (RO)

For completeness, we have also analyzed the Reach Only OEO allocation policy. According to this policy, OEOs are allocated only when the signals need regeneration. For connections with candidate paths no longer than TR, no OEOs will be allocated. For connections with candidate paths longer than TR, there is at least one 3R node on the path. The procedure to allocate OEOs to the path is as follows. The source allocates an OEO at the furthest possible node to the connection so the TR constraint is met. Similar to the other two policies, it is possible that all OEOs are being used at the furthest 3R node, so the algorithm may have to backtrack to the previous 3R node. After an OEO is allocated at a 3R node, the constraint is reset, and the algorithm starts afresh from that node; the algorithm terminates when the destination node is reached or the call is blocked. Consider the example shown in Fig. 6.3. (Only 3R nodes on the path are shown here.) Suppose the farthest 3R node within TR from node $s$ is node $c$; the policy first tries to allocate OEOs at node $c$ to the path; if there is no available OEO at node $c$, node $b$ is considered, and so on. Similarly, if the currently allocated 3R node is node $b$, and the farthest 3R node within TR from $b$ is node $e$, then the policy first tries to allocate node $e$ to the path; if it fails, then node $d$ is tried. (Note that in this case, node $c$ won't be considered, since the case that node $b$ is allocated means there is no available OEO at node $c$.) If node $e$ (or

**Algorithm 4** Blocking Computation for the WO Policy

Step 1: Precompute the values of $\mathcal{P}_1(h|i,j,k)$ (Equation (6.3)), which are independent with traffic loads.

Step 2: Consider each single link, the values of $\rho_{u,v}$, $F_k(u,v)$, $F(u,v)$ and $\hat{F}(u,v)$ will be used later when considering paths with multiple links.

**for** each link $l_{u,v}$ **do**

1. Calculate offered load $\rho_{u,v}$ (Equation (6.1))

2. Calculate the probability that the link has $k$ free wavelengths, $F_k(u,v)$ (Equation (6.5))

3. Calculate the probability that the link has at least one free wavelength, $F(u,v) = \sum_{k=1}^{W} F_k(u,v)$

4. Calculate the probability $\hat{F}_k(u,v)$ (defined in Table 6.3)

5. Calculate the blocking probability of single-hop path $p$ between nodes $u, v$, $B_p = F_0(u,v)$

**end for**

Step 3: Then we consider paths with more than one link. We need the steady state distribution of the four-dimensional Markov Chain, and the offered loads for the four types of connections, $\rho_e$, $\rho_f$, $\rho_c$ and $\rho_w$. In this step, the values of $\hat{x}_i^l(p)$ is calculated, which will be used to get $\rho_w$ in the next step.

**for** each path $p_{s,d}$ containing at least one 3R node **do**

**for** each 3R node $i$ on path $p_{s,d}$, starting from the one closest to $s$ and proceeding to the one closest to $d$ **do**

1. Calculate the values of $X(s,i,g)$ (Equation (6.45)), $X'(s,i,g)$ (Equation (6.46)), $X(h,i,g)$ (Equation (6.47)), $X'(h,i,g)$ (Equation (6.48)) (In Appendix C, with the assumption that the values of $Z(s,i,g)$, $Z'(s,i,g)$, $Z(h,i,g)$ and $Z'(h,i,g)$ in these equations are zero. Also, the involved values of $b_n^l$, $F(u,v)$, $\hat{F}_k(u,v)$, $\bar{F}_k(u,v,t)$ and $F'_k(u,v,t)$ are those found in Steps 5 and 6 of the previous iteration; as explained in Section 6.4.3)

2. Calculate $\hat{x}_i^l(p)$ (Equation (6.13)) (where $l$ is the corresponding outgoing link of 3R node $i$ on path $p$)

**end for**

**end for**



Step 4: Now we can calculate the offered loads of the five types of connections. Then we can get the steady state distribution of the Markov Chain. In turn, we

**Algorithm 3** Blocking Computation for the WO Policy (Continued)

Step 5: In this step, we will calculate $T^m(h, e)$, which is used to find the blocking probabilities for paths without 3R nodes on them.

**for** each path $s, d$ ($m > 1$ hops) **do**

1. Calculate $T^m(h, e)$ (Equation (6.18))
2. Calculate $F_k(s, d)$ (Equation (6.4)), $\hat{F}_k(u, v)$ (defined in Table 6.3), $\bar{F}_k(u, v, t)$ (Equation (6.43)) and $F'_k(u, v, t)$ (Equation (6.44). (Note that these values will be used in Step 3 of the next iteration.)

**end for**

Step 6:

**for** each path $s, d$ ($m > 1$ hops) without any 3R nodes on it **do**

Calculate the blocking probability $B_p = F_0(s, d)$

**end for**

Step 7: Now we will consider the paths with 3R nodes on them. In this step, we will calculate the offered loads to each 3R node's outgoing link $\rho_n^l$; and in turn, the probability that there are no available OEO converters at a 3R node $b_n^l$. Then we can get the acceptance probability of a path $A_p$ based on $M(i, j, d)$ and $M'(i, j, d, k)$.

**for** each path $s, d$ containing 3R nodes **do**

**for** each 3R node $n$ on the path **do**

1. Calculate the offered load to 3R node $n$ on outgoing link $l$; $\rho_n^l = \sum_{l \in p} \hat{x}_n^l(p)$
2. Calculate the probability that there are no OEOs available at the node $b_n^l$ (Equation (6.19)) (where $l$ is the corresponding outgoing link with node $n$ on the path) (Note that these values will be used in the next iteration.)

**end for**

1. Calculate the acceptance probability of the path $A_p$ (Equation (6.20)) depending on the OEO availability at the first 3R node on the path. This calculation is based on the values of $M(i, j, d)$ (Equation (6.28)) and $M'(i, j, d, k)$ (Equation (6.29))
2. Calculate the blocking probability $B_p = 1 - A_p$

**end for**

Step 8: Calculate $B_N = \frac{\sum_{s,d} \lambda_{s,d} B_{s,d}}{\sum_{s,d} \lambda_{s,d}}$

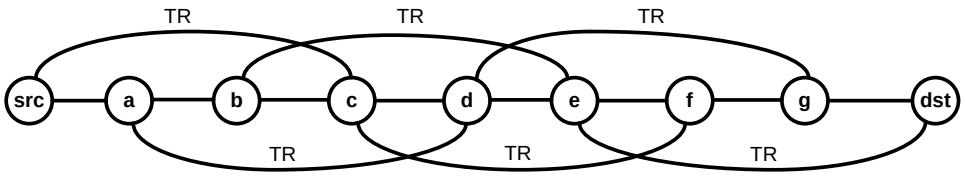


Figure 6.3: Example for the Reach Only policy.

$f$, $g$) is the currently allocated OEO node, then no more 3R nodes will be allocated to the path, since $D(P_{e,d}) \leq \Omega$. Note, however, that while the allocation policy does not consider the wavelength availability, a connection is assumed to be blocked if any OEO segment has no available wavelengths. The changes in the model essentially come from the fact that wavelength conversion needs are not checked when OEOs are allocated. (However, we remind the reader that if an OEO is allocated, it may be used to provide wavelength conversion.)

*Single-hop path*

The blocking probabilities of paths including a single link are still found by equations (6.1) and (6.2).

*Two link model*

A four dimensional Markov chain suffices for this policy (by discarding the $\mathcal{C}_w$ part from the previous 5-D Markov chain used in Reach and Wavelength model). Equations (6.6) and (6.7) are still used for calculating $\rho_e$ and $\rho_f$.

The equation to find $\rho_c$ is as follows.

$$\rho_c = \sum_{p:a\text{-}b\in p, b\text{-}c\in p} \lambda_p - \rho_r. \tag{6.30}$$

Then, the steady state probability for state $(\mathcal{C}_e, \mathcal{C}_f, \mathcal{C}_c, \mathcal{C}_r)$ and the normalization factor $\Delta$ are the similar to Equations (6.9) and (6.10) by removing $\mathcal{C}_w$. (Again, note that this is a different Markov Chain from the one used for the RW policy, with $C_w$ being subsumed within other connection types.)

$$\boldsymbol{\pi}(\mathcal{C}_e, \mathcal{C}_f, \mathcal{C}_c, \mathcal{C}_r) = \frac{\frac{\rho_e^{\mathcal{C}_e}}{\mathcal{C}_e!}\frac{\rho_f^{\mathcal{C}_f}}{\mathcal{C}_f!}\frac{\rho_c^{\mathcal{C}_c}}{\mathcal{C}_c!}\frac{\rho_r^{\mathcal{C}_r}}{\mathcal{C}_r!}}{\Delta} \tag{6.31}$$

where the normalization factor $\Delta$ can be calculated as

$$\Delta = \sum_{h=0}^{\min(R,W)} \sum_{k=0}^{W-h} \sum_{i=0}^{W-k-h} \sum_{j=0}^{W-k-h} \frac{\rho_e^i}{i!}\frac{\rho_f^j}{j!}\frac{\rho_c^k}{k!}\frac{\rho_r^h}{h!} \tag{6.32}$$

with constraints $0 \leq \mathcal{C}_r \leq R$, $0 \leq \mathcal{C}_r + \mathcal{C}_c + \mathcal{C}_e \leq W$ and $0 \leq \mathcal{C}_r + \mathcal{C}_c + \mathcal{C}_f \leq W$.

In order to calculate the values of $\rho_r$, only $\bar{x}_n^l(p)$, $Z(u,v,t)$ and $Z'(u,v,t)$ are used. The equations of $Z(u,v,t)$ and $Z'(u,v,t)$ are the same as the ones in Appendix B, except that the values of all $X$ and $X'$ are assumed to be zero. In addition, we have $x_n^l(p) = \bar{x}_n^l(p)$.

The quations to find $\mathcal{P}_2(i)$, $\mathcal{P}_3(j|i)$ and $\mathcal{P}_4(k|j,i)$ are similar to Equations (6.15)-(6.17) by removing $\mathcal{C}_w$ part.

$$\begin{aligned}\mathcal{P}_2(i) &= P(\mathcal{C}_c + \mathcal{C}_e + \mathcal{C}_r = W - i) \\ &= \sum_{\mathcal{C}_r=0}^{\min(R,W-i)} \sum_{\mathcal{C}_c=0}^{W-i-\mathcal{C}_r} \sum_{\mathcal{C}_f=0}^{W-\mathcal{C}_r-\mathcal{C}_c} \boldsymbol{\pi}(W-i-\mathcal{C}_c-\mathcal{C}_r, \mathcal{C}_f, \mathcal{C}_c, \mathcal{C}_r).\end{aligned} \tag{6.33}$$

$$\begin{aligned}\mathcal{P}_3(j|i) &= P(\mathcal{C}_f + \mathcal{C}_c + \mathcal{C}_r = W - j \mid \mathcal{C}_e + \mathcal{C}_c + \mathcal{C}_r) \\ &= \frac{\sum_{\mathcal{C}_r=0}^{up1} \sum_{\mathcal{C}_c=0}^{up2} \boldsymbol{\pi}(W-i-\mathcal{C}_c-\mathcal{C}_r, W-j-\mathcal{C}_c-\mathcal{C}_r, \mathcal{C}_c, \mathcal{C}_r)}{\sum_{\mathcal{C}_r=0}^{\min(R,W-i)} \sum_{\mathcal{C}_c=0}^{W-i-\mathcal{C}_r} \sum_{\mathcal{C}_f=0}^{W-\mathcal{C}_r-\mathcal{C}_c} \boldsymbol{\pi}(W-i-\mathcal{C}_c-\mathcal{C}_r, \mathcal{C}_f, \mathcal{C}_c, \mathcal{C}_r)},\end{aligned} \tag{6.34}$$

where $up1 = \min(R, W-i, W-j)$, $up2 = \min(W-i-\mathcal{C}_r, W-j-\mathcal{C}_r)$.

$$\begin{aligned}\mathcal{P}_4(k|j,i) &= P(\mathcal{C}_c + \alpha = k | \mathcal{C}_e + \mathcal{C}_c + \mathcal{C}_r = W - i, \mathcal{C}_f + \mathcal{C}_c + \mathcal{C}_r = W - j) \\ &= \sum_{\alpha=0}^{\min(R,k)} \sum_{\mathcal{C}_e=low1}^{W-i-k} \sum_{K=\alpha}^{up3} P(\alpha, K, W-i-\mathcal{C}_e-k+\alpha, k-\alpha, \mathcal{C}_e, i-j+\mathcal{C}_e),\end{aligned} \tag{6.35}$$

where $up3 = \min(W-\mathcal{C}_e-k+\alpha, W-\mathcal{C}_f-k+\alpha)$, $low1 = \max(0, j-i, W-i-k+\alpha-R)$; the upper and lower bounds of $\mathcal{C}_e$ are found with $\alpha \leq \mathcal{C}_r \leq R$.

The probability $P(\alpha, K, \mathcal{C}_r, \mathcal{C}_c, \mathcal{C}_e, \mathcal{C}_f)$ in equation (6.35) is defined as the probability that there are $W - \mathcal{C}_c - \mathcal{C}_e$ available wavelengths on the first link, $W - \mathcal{C}_c - \mathcal{C}_f$ available wavelengths on the second link, there are $K$ available wavelengths on the

both links, then randomly choose $\mathcal{C}_r$ wavelengths from the available wavelengths of each link, $\alpha$ wavelength pairs of $\mathcal{C}_r$ have the same wavelength of the two links, its calculation is in Appendix E.

For paths whose distances are shorter than the TR (note that no OEO will be allocated to them), their blocking probabilities can be calculated by $B_p = F_0(s,d) = \sum_{e=0}^{W} T^m(0,e)$, where $m$ is the number of hops with the path. The values of $T^m(h,e)$ are calculated by Equation (6.18).

*Blocking on a Path With Distance Longer than TR*

For paths longer than TR, at least one 3R node needs to be allocated to the path. Recall that the policy allocates the possible 3R node that is furthest from the previously allocated 3R node (to the path) (or from the source if no 3R node has been allocated to the path yet). The probability that a 3R node has available OEOs is found by Equation (6.19).

For a path $p$ from source $s$ to destination $d$, number the 3R nodes as $1, 2, 3, ..., r$, with $r$ 3R nodes on the path. Suppose $D(p_{s,h}) \leq \Omega$ while $D(p_{s,h+1}) > \Omega$. We can calculate the value of $A_p$ as,

$$
\begin{aligned}
&A_p \\
&= \sum_{g=1}^{h} \Pr\{G_{s,d} = 1, \text{and the first allocated 3R node is node } g\} \\
&= \sum_{g=1}^{h} \Pr\{G_{s,d} = 1, H_g = 1, \text{ but there is no available OEOs at nodes from } g+1 \text{ to node } h \\
&= \sum_{g=1}^{h} (1 - b_g^l) \prod_{i=g+1}^{h} b_i^l \Pr\{E_{s,g} = 1, G_{g,d} = 1 \mid \text{there is no available OEOs at nodes from } g+1 \\
&\text{to node } h\} \\
&= \sum_{g=1}^{h} (1 - b_g^l)(1 - B_{p_{s,g}}) \prod_{i=g+1}^{h} b_i^l \Pr\{G_{g,d} = 1 \mid \text{there is no available OEOs at nodes from } g+1 \\
&\text{to node } h\} \qquad (6.36)
\end{aligned}
$$

Denote $N(g,h,d)$ as $\Pr\{G_{g,d} = 1 \mid \text{there is no available OEOs at nodes from } g+$

1 to node $h\}$, then we can have

$$A_p = \sum_{g=1}^{h}(1 - b_g^l)(1 - B_{p_{s,g}}) \prod_{i=g+1}^{h} b_i^l N(g, h, d). \tag{6.37}$$

To calculate $N(g, h, d)$, we have two cases based on the length of path $P_{g,d}$, as below.

(a) $D(P_{g,d}) \leq \Omega$: There is no need to allocate any OEO converter to regenerate the signal, so

$$N(g, h, d) = 1 - B_{p_{g,d}}. \tag{6.38}$$

(b) $D(P_{g,d}) > \Omega$: Suppose the farthest node within TR from node $g$ is node $t$, i.e., $D(P_{g,t}) \leq \Omega$, and $D(P_{g,t+1}) > \Omega$. Then an OEO converter between node $h+1$ and $t$ must be allocated to regenerate the signal. Denoting this node as $e$, we have

$$N(g, h, d) = \sum_{e=h+1}^{t} (1 - b_e^l)(1 - B_{p_{g,e}}) \prod_{f=e+1}^{t} b_f^l N(e, t, d) \tag{6.39}$$

*Summary*

We summarize the steps to find the network blocking probability $B_N$ for the RO policy in Algorithm 6.

### 6.4.7 Independence Model

In order to demonstrate the necessity of considering link load correlation (as in the Two-link Mode described above) in certain cases, we also developed a model which is similar to the Two-link but assuming independence of wavelength usages on links (called the Independence Model).

The only difference between the Two-link Model and the Independence Model is the method used to find $F_k(u, v)$. For a single-hop path $p_{s,d}$, the $F_k(s, d)$ is still found by the Erlang B formula with capacity $W$ and offered load $\rho_{s,d}$ by Equation (6.5). We don't need the Markov Chain which is used in the Two-link Model to calculate $F_k(u, v)$ for a multi-hop path. $F_k(u, v)$ for a multi-hop path is obtained as follows.

**Algorithm 4** Blocking Computation for the RO Policy

Step 1: Precompute the values of $\mathcal{P}_1(h|i,j,k)$ (Equation (6.3)), which are independent with traffic loads.

Step 2: Consider each single link, the values of $\rho_{u,v}$, $F_k(u,v)$, $F(u,v)$ and $\hat{F}(u,v)$ will be used later when considering paths with multiple links.

**for** each link $l_{u,v}$ **do**

1. Calculate offered load $\rho_{u,v}$ (Equation (6.1))

2. Calculate the probability that the link has $k$ free wavelengths, $F_k(u,v)$ (Equation (6.5))

3. Calculate the probability that the link has at least one free wavelength, $F(u,v) = \sum_{k=1}^{W} F_k(u,v)$

4. Calculate the probability $\hat{F}_k(u,v)$ (defined in Table 6.3)

5. Calculate the blocking probability of single-hop path $p$ between nodes $u, v$, $B_p = F_0(u,v)$

**end for**

Step 3: Then we consider paths with more than one link. We need the steady state distribution of the four-dimensional Markov Chain, and the offered loads for the five types of connections, $\rho_e$, $\rho_f$, $\rho_c$, and $\rho_r$. In this step, the values of $\hat{x}_i^l(p)$ is calculated, which will be used to get $\rho_r$ in the next step.

**for** each path $p_{s,d}$ containing at least one 3R node **do**

**for** each 3R node $i$ on path $p_{s,d}$, starting from the one closest to $s$ and proceeding to the one closest to $d$ **do**

1. Calculate the values of $Z(s,i,g)$ (Equation (6.49)), $Z'(s,i,g)$ (Equation (6.50)), $Z(h,i,g)$ (Equation (6.51)) and $Z'(h,i,g)$ (Equation (6.52)) (In Appendix C, with the assumption that the values of $X(s,i,g)$, $X'(s,i,g)$, $X(h,i,g)$, $X'(h,i,g)$ in these equations are zero. Also, The values of $b_n^l$, $F(u,v)$, $\hat{F}_k(u,v)$, $\bar{F}_k(u,v,t)$ and $F'_k(u,v,t)$ are those found in the previous iteration; to be explained in Section 6.4.3)

2. Calculate $\bar{x}_i^l(p)$ (Equation (6.14)) (where $l$ is the corresponding outgoing link of 3R node $i$ on path $p$)

**end for**

**end for**



Step 4: Now we can calculate the offered loads of the five types of connections. Then we can get the steady state distribution of the Markov Chain. In turn, we

**Algorithm 3** Blocking Computation for the RO Policy (Continued)

Step 5: In this step, we will calculate $T^m(h, e)$, which is used to find the blocking probabilities for paths without 3R nodes on them.

**for** each path $s, d$ ($m > 1$ hops) **do**

1. Calculate $T^m(h, e)$ (Equation (6.18))
2. Calculate $F_k(s, d)$ (Equation (6.4)), $\hat{F}_k(u, v)$ (defined in Table 6.3), $\bar{F}_k(u, v, t)$ (Equation (6.43)) and $F'_k(u, v, t)$ (Equation (6.44). (Note that these values will be used in the next iteration.)

**end for**

Step 6:

**for** each path $s, d$ ($m > 1$ hops) with distance no longer than TR **do**

Calculate the blocking probability $B_p = F_0(s, d)$

**end for**

Step 7: Now we will consider the paths with 3R nodes on them. In this step, we will calculate the offered loads to each 3R node's outgoing link $\rho_n^l$; and in turn, the probability that there are no available OEO converters at a 3R node $b_n^l$. Then we can get the acceptance probability of a path $A_p$ based on $N(g, h, d)$.

**for** each path $s, d$ with distance longer than TR **do**

**for** each 3R node $n$ on the path **do**

1. Calculate the offered load to 3R node $n$ on outgoing link $l$; $\rho_n^l = \sum_{l \in p} \bar{x}_n^l(p)$
2. Calculate the probability that there are no OEOs available at the node $b_n^l$ (Equation (6.19)) (where $l$ is the corresponding outgoing link with node $n$ on the path) (Note that these values will be used in the next iteration.)

**end for**

1. Calculate the acceptance probability of the path $A_p$ (Equation (6.36)). This calculation is based on the values of $N(g, h, d)$ (Equations (6.38) and (6.39))
2. Calculate the blocking probability $B_p = 1 - A_p$

**end for**

Step 8: Calculate $B_N = \frac{\sum_{s,d} \lambda_{s,d} B_{s,d}}{\sum_{s,d} \lambda_{s,d}}$

Let $U(k|a,b)$ denote that in a two-link path, given that there are $a$ available wavelengths on the first link, $b$ available wavelengths on the second link, the probability that there are $k$ available wavelengths on the path, $U(k|a,b) = \frac{\binom{a}{k}\binom{W-a}{b-k}}{\binom{W}{b}}$.

For a two-hop path $s$-$i$-$d$, $F_k(s,d) = \sum_{a=k}^{W}\sum_{b=k}^{W} U(k|a,b)F_a(s,i)F_b(i,d)$. For a path $p_{s,d}$ with $m > 2$ hops, we find the $F_k(s,d)$ values with $m' = 2, 3, ...m$ hops by considering the first $m'-1$ hops (from node $s$ to $j$) as one hop, and the last hop as another hop (from node $j$ to $j+1$), then, $F_k(s,j+1) = \sum_{a=0}^{W}\sum_{b=0}^{W} U(k|a,b)F_a(s,j)F_b(j,j+1)$.

Note that the reduced load approximation is also used in Independence Model.

### 6.5 Numerical Results

We now validate the models by comparing model results with simulation results. We also conduct a detailed performance evaluation of the three OEO allocation policies (Reach and Wavelength (RW), Wavelength Only (WO), and Reach Only (RO)) in a variety of scenarios. For the simulation, unidirectional requests for connections are assumed to arrive to the network according to a Poisson process. The source and destination of each connection are randomly selected (from a uniform distribution). For each data point in the graphs, we simulated several instances of 10,000 to 100,000 connection arrivals, and obtained 95% confidence intervals. The TR value $\Omega = 3600$ km (according to the physical layer model in [17] for QPSK 100 Gbps signal with 50GHz channel spacing), and the number of wavelengths per fiber $W = 32$.

We present results for three network topologies, the European Optical Network (EON), NSFNET, and a ring network shown in Figs. 6.4-6.6, respectively. The numbers on the links are link distances (in hundreds of kms), and the shaded nodes are 3R nodes. We select the 3R nodes according to the following algorithm. First, find the shortest path for each pair of nodes, and count the number of times a node is traversed by these paths. Nodes are sorted in descending order of this number. For each topology, the first 5 nodes in this order are selected as 3R nodes.

Results comparing the three algorithms are shown in Figs. 6.7 - 6.9. The loads were selected so that blocking probabilities are typically in the $10^{-5}$ to $10^{-1}$ range. First, notice the excellent agreement between simulation and analytical results. The

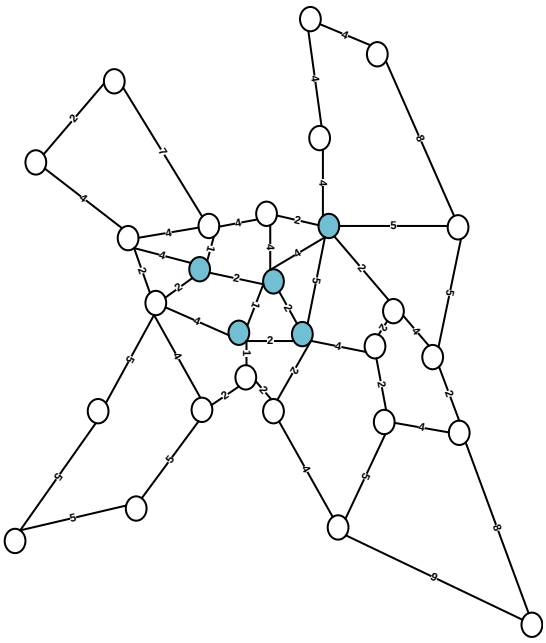

Figure 6.4: The 28 node EON.

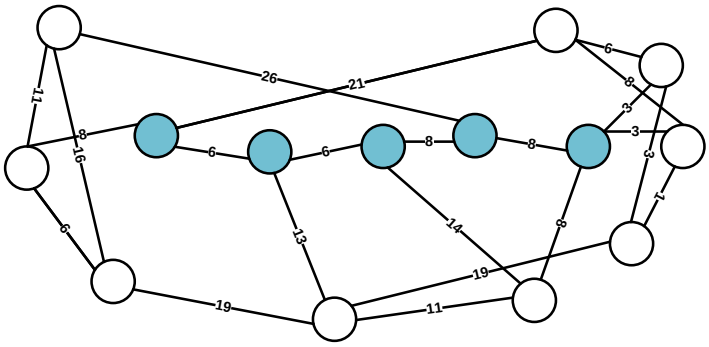

Figure 6.5: The 14 node NSFNET.

blocking probability for the WO policy is several orders of magnitude higher than that of the other two policies, especially at low loads. For example, for EON, at a load of 100 Erlangs, the blocking probability for the WO policy is about $10^5$ times the value for the RW policy. This shows that it is very important to consider the TR when allocating OEO converters. The almost flat behavior of blocking for the WO policy is interesting; we will explain the reason for this shortly.

Results for the RW and RO policies are shown in Figs. 6.10 - 6.15, with 10 OEOs per 3R node. The two-link model's accuracy can be easily seen from the excellent match with simulation results, while the much simpler "Independence" model greatly

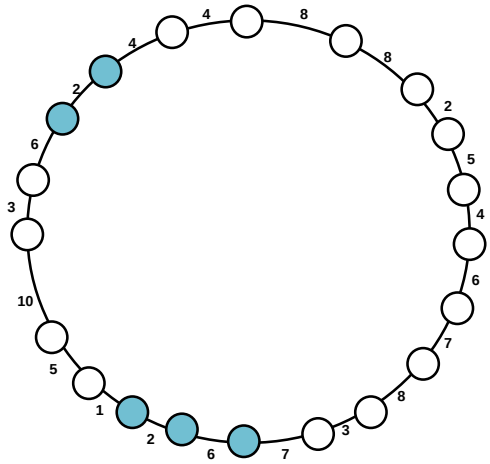

Figure 6.6: The 20 node ring network.

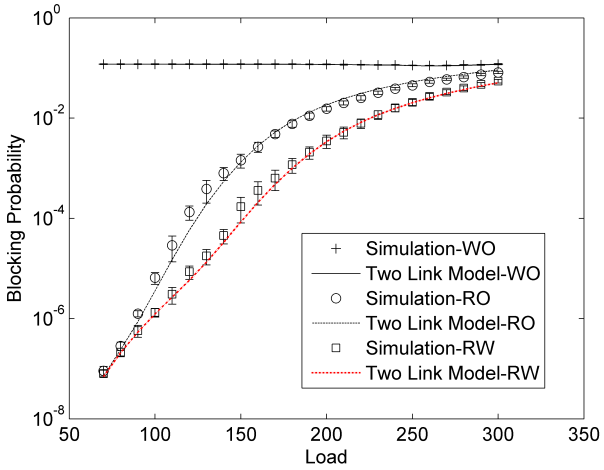


Figure 6.7: Comparison of the three OEO allocation policies in the EON; 10 OEOs per 3R node.

overestimates the blocking in the ring network.

Results for the WO policy are shown in Figs. 6.16 - 6.18, with 10 OEOs per 3R node. Quite surprisingly, the blocking probability actually *decreases* as load increases initially, and then starts to increase. This can be explained as follows. Recall that OEO converters are allocated by considering only wavelength availability and not QoT. Therefore, there is a high probability that the TR requirement is not satisfied, and hence the connection is blocked. When the load increases, a wavelength-continuous path from source to destination becomes harder to find, and therefore, OEO converters are allocated to the connection for performing wavelength conver-

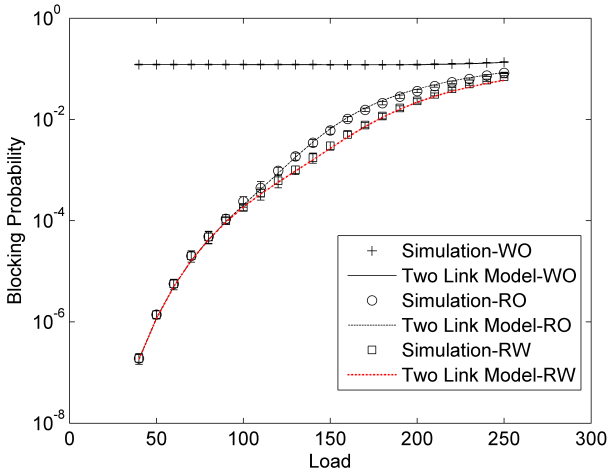


Figure 6.8: Comparison of the three OEO allocation policies in the NSFNET; 10 OEOs per 3R node.

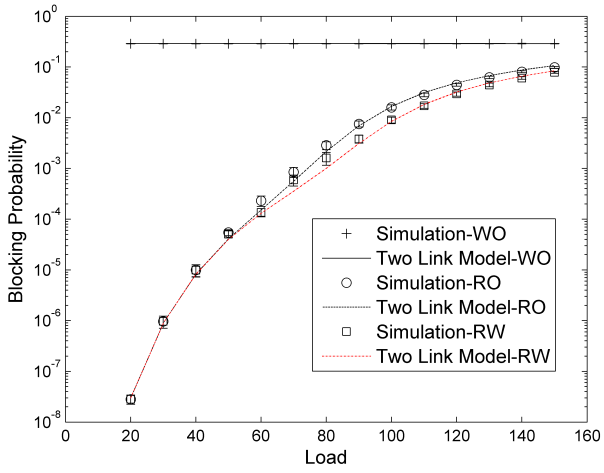


Figure 6.9: Comparison of the three OEO allocation policies in the Ring; 10 OEOs per 3R node.

sion. Since these OEO nodes also perform 3R regeneration, the probability that the selected path will be rejected due to poor QoT does not increase at low loads. But at somewhat high loads, the lack of wavelengths begins to dominate, and the blocking probability starts to increase. Remarkably, the Two-link Model captures this complex trend quite accurately. These results also demonstrate the importance of considering link load correlation (Two-link Model) even in relatively dense mesh topologies such as the NSFNET and EON. Notice that the blocking probabilities predicted by the

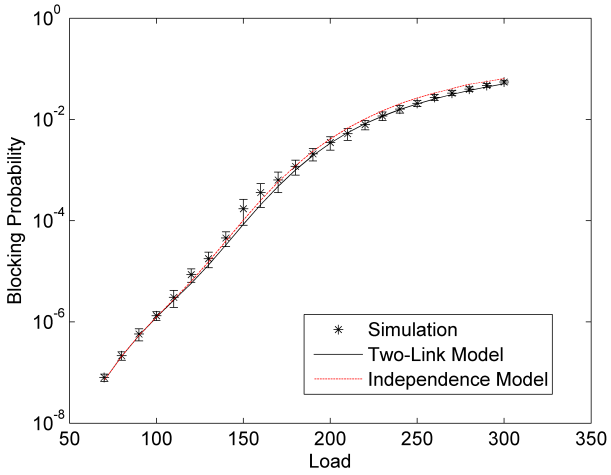


Figure 6.10: Model validation and comparison of Two-link and Independence models: EON; RW Policy.

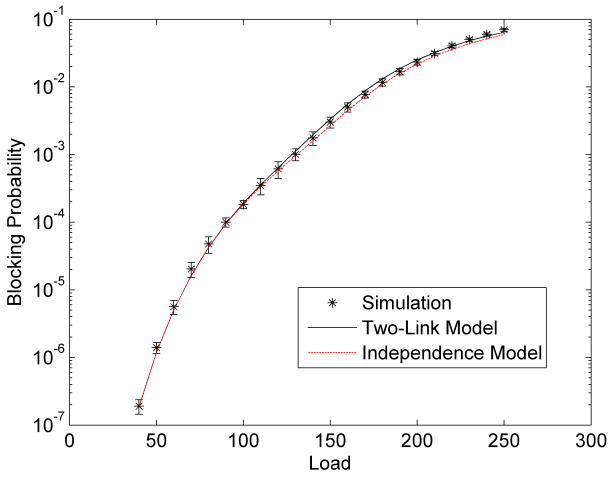


Figure 6.11: Model validation and comparison of Two-link and Independence models: NSFNET; RW Policy.

Independence Model are much higher than those obtained through simulation.

Results with three different numbers of OEO converters per 3R node for the NSFNET are shown in Figs. 6.19 - 6.21 (the performance has similar trends for the other two topologies, and are therefore omitted). Once again, notice the excellent match between analytical and simulation results. Further, it is interesting to see that the blocking is reduced significantly as the number of OEO converters is increased for the RW and RO policies, especially at low loads, whereas this effect is not seen for the

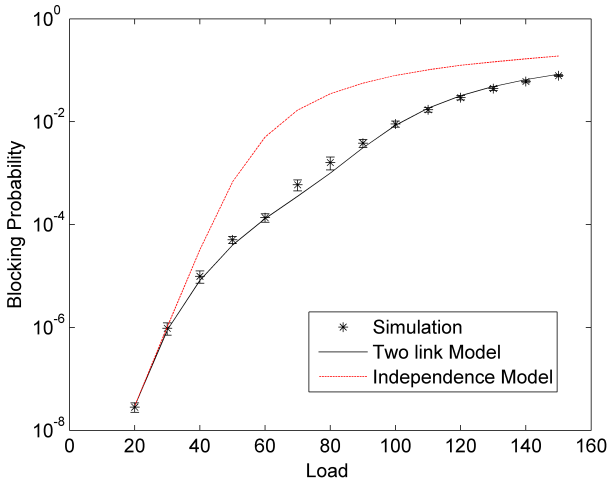


Figure 6.12: Model validation and comparison of Two-link and Independence models: Ring; RW Policy.

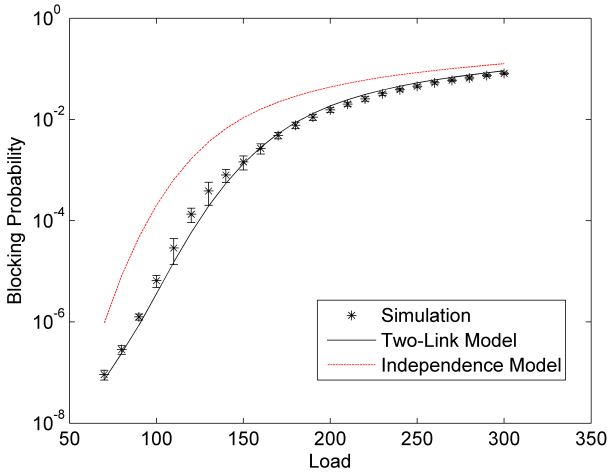


Figure 6.13: Model validation and comparison of Two-link and Independence models: EON; RO Policy.

WO policy. This is because the WO policy allocates OEOs only when wavelengths need conversion. Therefore many long wavelength-continuous paths are eventually blocked due to poor QoT, because the WO policy fails to allocate OEOs even when they are available.

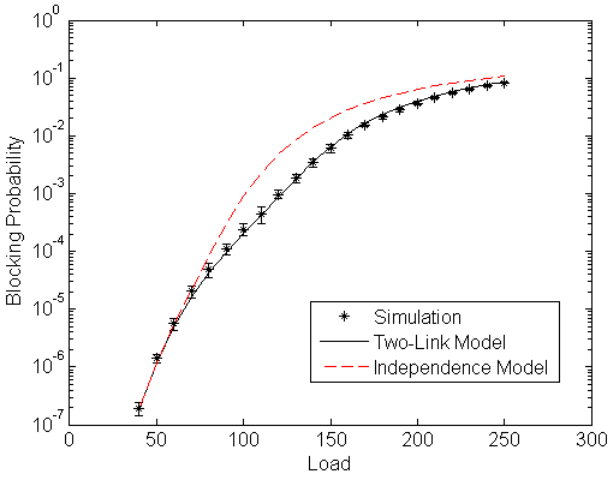


Figure 6.14: Model validation and comparison of Two-link and Independence models: NSFNET; RO Policy.

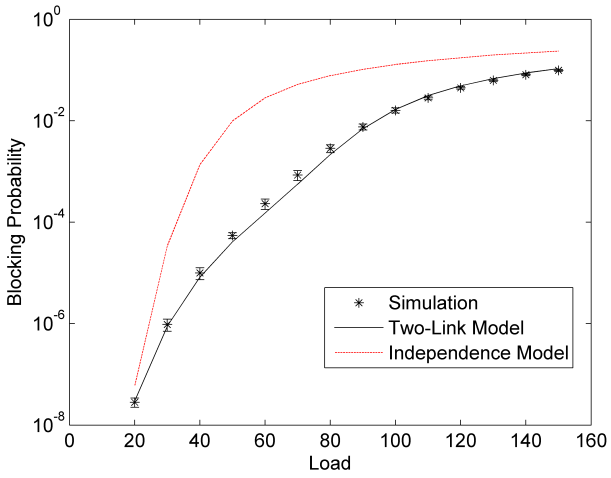


Figure 6.15: Model validation and comparison of Two-link and Independence models: Ring; RO Policy.

## 6.6 Conclusions

Transnational and transcontinental optical networks are translucent – they are mostly optically switched but have sparsely located 3R regenerators (with a limited number of OEO converters) that help to mitigate physical layer impairments and/or perform wavelength conversion. Given their wide applicability, analyzing the performance of such networks is an important issue. In this chapter, we present the first

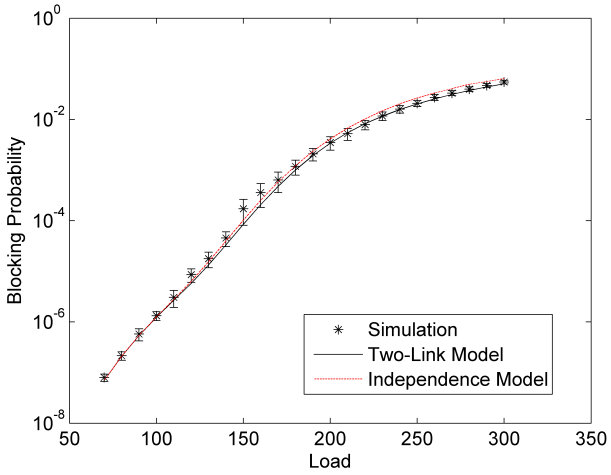


Figure 6.16: Model validation and comparison of Two-link and Independence models: EON; WO Policy.

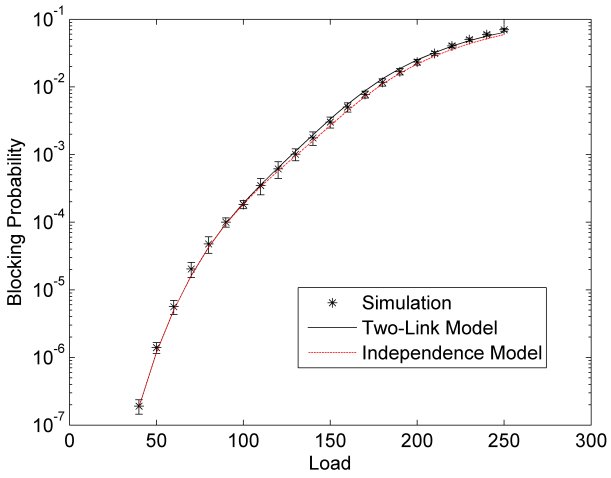


Figure 6.17: Model validation and comparison of Two-link and Independence models: NSFNET; WO Policy.

analytical models for calculating the connection blocking probability in translucent optical networks. Three OEO allocation policies – RW, WO, and RO – are analyzed. Our models are rigorously constructed and maintain a balance between accuracy and computational complexity. The models are shown to predict blocking performance extremely well as demonstrated by extensive simulation results for a variety of topologies and parameter settings. Our results also confirm what is well-known in the literature – it is important to consider physical layer impairments when setting up connections,

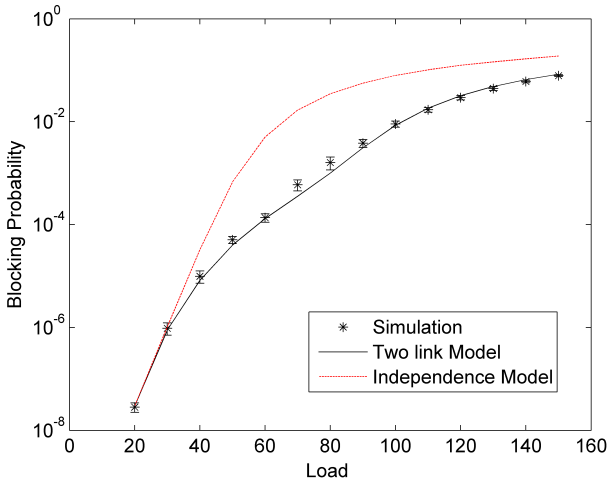


Figure 6.18: Model validation and comparison of Two-link and Independence models: Ring; WO Policy.

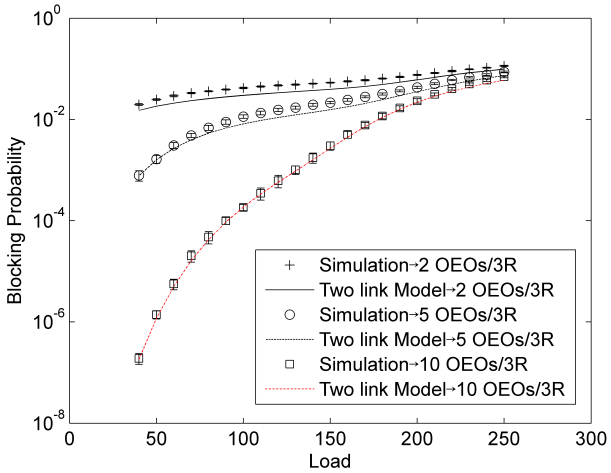


Figure 6.19: Blocking vs. load, RW Model.

because otherwise the connection could have poor QoT and be blocked. In this work, we assumed fixed paths and random wavelength assignment for connections. Future extensions can consider alternate paths, First-Fit wavelength assignment, grooming, and other OEO sharing models.

## 6.7 Appendix A

The probability $P(\alpha, K, \mathcal{C}_r, \mathcal{C}_w, \mathcal{C}_c, \mathcal{C}_e, \mathcal{C}_f)$ in Equation (6.17) is defined as the joint probability of the following events: there are $W - \mathcal{C}_c - \mathcal{C}_e - \mathcal{C}_w$ available wavelengths on

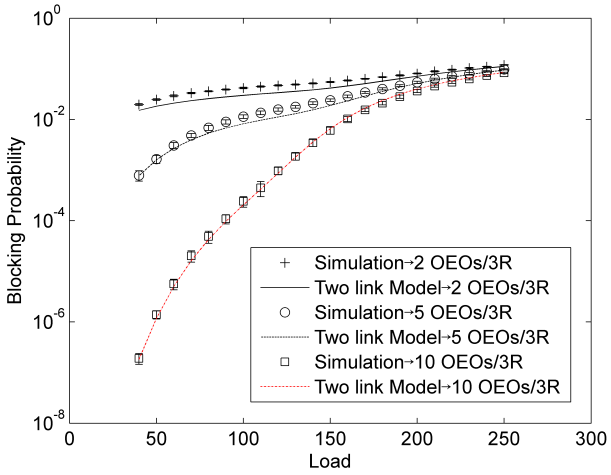


Figure 6.20: Blocking vs. load, RO Model.

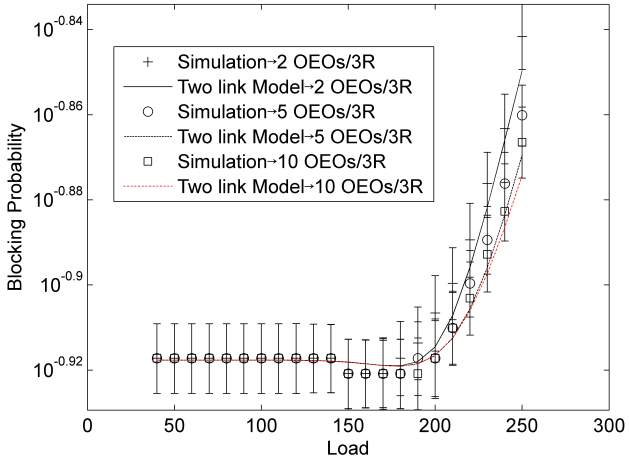


Figure 6.21: Blocking vs. load, WO Model.

the first link, $W-\mathcal{C}_c-\mathcal{C}_f-\mathcal{C}_w$ on the second link, $K$ available (common) wavelengths on both links, and when $\mathcal{C}_r$ wavelengths are randomly chosen from the available wavelengths on each of the two links, $\alpha$ (of the $\mathcal{C}_r$) are identical on both links. To find this probability, let us define $P(\alpha, \mathcal{C}_r|K, \mathcal{C}_w, \mathcal{C}_c, \mathcal{C}_e, \mathcal{C}_f)$ as follows. Suppose there are $W-\mathcal{C}_c-\mathcal{C}_e-\mathcal{C}_w$ available wavelengths on the first link, $W-\mathcal{C}_c-\mathcal{C}_f-\mathcal{C}_w$ available wavelengths on the second link, there are $K$ available (common) wavelengths on both links; then we randomly choose $\mathcal{C}_r$ wavelengths from the available wavelengths on each link ($\mathcal{C}_r$ from the first link and, independently, $\mathcal{C}_r$ from the second link). Then, the probability that $\alpha$ wavelength pairs of $\mathcal{C}_r$ have the same wavelength on the two

links is denoted by $P(\alpha, \mathcal{C}_r|K, \mathcal{C}_w, \mathcal{C}_c, \mathcal{C}_e, \mathcal{C}_f)$.

In order to find $P(\alpha, \mathcal{C}_r|K, \mathcal{C}_w, \mathcal{C}_c, \mathcal{C}_e, \mathcal{C}_f)$, we first find $Y(a, b, m, u, v)$ defined as follows. Given there are $u$ available wavelengths on the first link, $v$ available wavelengths on the second link, and $m$ available (common) wavelengths on both links; then randomly choose $a+b$ wavelengths from the available wavelengths on each link. Then $Y(a, b|m, u, v)$ is the number of ways that $a$ wavelength-pairs have the same wavelengths on the two links, while $b$ wavelength-pairs have different wavelengths on the two links, for $m \leq u, v; a+b \leq u, v; a \leq m$. We show how to calculate $Y(a, b|m, u, v)$ in Appendix D.

Now, we can write

$$\begin{aligned} &P(\alpha, \mathcal{C}_r|K, \mathcal{C}_w, \mathcal{C}_c, \mathcal{C}_e, \mathcal{C}_f) = \\ &\frac{Y(\alpha, \mathcal{C}_r - \alpha|K, W - \mathcal{C}_c - \mathcal{C}_e - \mathcal{C}_w, W - \mathcal{C}_c - \mathcal{C}_f - \mathcal{C}_w)}{\binom{W-\mathcal{C}_c-\mathcal{C}_e-\mathcal{C}_w}{\mathcal{C}_r}\binom{W-\mathcal{C}_c-\mathcal{C}_f-\mathcal{C}_w}{\mathcal{C}_r}}. \end{aligned} \tag{6.40}$$

Using the law of total probability, we then have

$$\begin{aligned} &P(\alpha, K, \mathcal{C}_r, \mathcal{C}_w, \mathcal{C}_c, \mathcal{C}_e, \mathcal{C}_f) \\ &= P(\alpha, \mathcal{C}_r|K, \mathcal{C}_w, \mathcal{C}_c, \mathcal{C}_e, \mathcal{C}_f) P(K, \mathcal{C}_w, \mathcal{C}_c, \mathcal{C}_e, \mathcal{C}_f) \\ &= P(\alpha, \mathcal{C}_r|K, \mathcal{C}_w, \mathcal{C}_c, \mathcal{C}_e, \mathcal{C}_f) P(K|\mathcal{C}_w, \mathcal{C}_c, \mathcal{C}_e, \mathcal{C}_f) \sum_{\mathcal{C}_r} \boldsymbol{\pi}(\mathcal{C}_e, \mathcal{C}_f, \mathcal{C}_c, \mathcal{C}_r, \mathcal{C}_w) \end{aligned} \tag{6.41}$$

where,

$$\begin{aligned} &P(K|\mathcal{C}_w, \mathcal{C}_c, \mathcal{C}_e, \mathcal{C}_f) \\ &= \frac{\binom{W}{\mathcal{C}_c}\binom{W-\mathcal{C}_c}{\mathcal{C}_e+\mathcal{C}_w}\binom{W-\mathcal{C}_c-\mathcal{C}_e-\mathcal{C}_w}{K}\binom{\mathcal{C}_e+\mathcal{C}_w}{W-\mathcal{C}_c-\mathcal{C}_f-\mathcal{C}_w-K}}{\binom{W}{\mathcal{C}_c}\binom{W-\mathcal{C}_c}{\mathcal{C}_e+\mathcal{C}_w}\binom{W-\mathcal{C}_c}{\mathcal{C}_f+\mathcal{C}_w}} \\ &= \frac{\binom{W-\mathcal{C}_c-\mathcal{C}_e-\mathcal{C}_w}{K}\binom{\mathcal{C}_e+\mathcal{C}_w}{W-\mathcal{C}_c-\mathcal{C}_f-\mathcal{C}_w-K}}{\binom{W-\mathcal{C}_c}{W-\mathcal{C}_c-\mathcal{C}_f-\mathcal{C}_w}}. \end{aligned} \tag{6.42}$$

## 6.8 Appendix B

In this appendix, we calculate $M(i, j, d)$ and $M'(i, j, d, k)$.

### 6.8.1 Calculation of $M(i, j, d)$

Recall that $M(i, j, d)$ denotes the probability that there is no blocking from $i$ to $d$, given that there are available OEOs at node $j$, the previously allocated 3R node is node $i$ (if there is no previously allocated 3R node, node $i$ is source node $s$), and there are available wavelengths on $p_{i,j}$, i.e.,

$$M(i, j, d) = \Pr\{G_{i,d} = 1 \mid E_{i,j} = 1, H_j = 1, \text{the previously allocated 3R node is node } i.\}$$

We need to consider the cases $D(p_{i,j+1}) \leq \Omega$ and $D(p_{i,j+1}) > \Omega$ separately when calculating $M(i, j, d)$, since in the case $D(p_{i,j+1}) > \Omega$, OEOs at node $j$ are allocated to meet the TR requirement. However, in the case $D(p_{i,j+1}) \leq \Omega$, the OEOs at node $j$ are allocated only when there is no available wavelengths from node $i$ to $j + 1$.

*Case 1: $D(p_{i,j+1}) \leq \Omega$ and $j \neq h$*

Based on the availability of OEOs at node $j+1$, and the availability of wavelengths on path $p_{i,j+1}$, we have three subcases. When $E_{i,j+1} = 0$, the 3R node $j$ is allocated to convert wavelengths.

$$\begin{aligned}
&M(i, j, d) \\
&= \Pr\{H_{j+1} = 1, E_{i,j+1} = 1 \mid E_{i,j} = 1\}\Pr\{G_{i,d} = 1 \mid E_{i,j+1} = 1, H_{j+1} = 1\} + \Pr\{H_{j+1} = 1, \\
&E_{j,j+1} = 1, E_{i,j} = 1, E_{i,j+1} = 0 \mid E_{i,j} = 1\}\Pr\{G_{j,d} = 1 \mid E_{j,j+1} = 1, H_{j+1} = 1\} + \Pr\{H_{j+1} = 0, \\
&G_{i,d} = 1 \mid E_{i,j} = 1, H_j = 1\} \\
&= (1 - b^l_{j+1})\frac{F(i, j+1)}{F(i, j)}M(i, j+1, d) + (1 - b^l_{j+1})\frac{F'(i, j, j+1)}{F(i, j)}M(j, j+1, d) + b^l_{j+1} \\
&M'(i, j+1, d, j).
\end{aligned}$$

*Case 2: $D(p_{i,j+1}) > \Omega$ and $j \neq h$*

In this case, the 3R node $j$ is allocated to regenerate the signal, no matter the availability of wavelengths on path $p_{i,j+1}$. Based on the availability of OEOs at node $j + 1$, we have two subcases.

$M(i,j,d)$

$= \Pr\{H_{j+1}=1, E_{j,j+1}=1 \,|E_{i,j}=1\}\Pr\{G_{j,d}=1 \,|E_{j,j+1}=1, H_{j+1}=1\} + \Pr\{H_{j+1}=0\}$

$\Pr\{G_{i,d}=1 \,|E_{i,j}=1, H_{j+1}=0, H_j=1\}$

$= (1-b_{j+1}^l)F(j,j+1)M(j,j+1,d) + b_{j+1}^l M'(i,j+1,d,j).$

*Case 3:* $j=h$

$M(i,j,d) = \frac{F(i,d)}{F(i,j)} + \frac{F'(i,j,d)}{F(i,j)}$ if $D(p_{i,d}) \le \Omega$; $M(i,j,d) = F(j,d)$ if $D(p_{i,d}) > \Omega$.

### 6.8.2 Calculation of $M'(i,j,d,k)$

Recall that $M'(i,j,d,k)$ denotes the probability that there is no blocking from $i$ to $d$, given that there are no available OEOs at node $j$, the previously allocated 3R node is node $i$ (if there is no previously allocated 3R node, node $i$ is source node $s$), and the previous 3R node with available OEOs, but not yet allocated is node $k$, there are available wavelengths on $p_{i,k}$. (Node $k$ is set as 0 if there is no such $k$, e.g., $j=i+1$; in this case, there is no condition that there are available wavelengths on $p_{i,k}$.).

$M'(i,j,d,k) = \Pr\{G_{i,d}=1 \,|E_{i,k}=1, H_j=0, H_k=1,$ the previously allocated 3R node is node $i$, 3R node $k$has not been allocated yet.$\}$

For the case $k=0, j\neq h, D(p_{i,j+1}) \le \Omega$, depending on the availability of OEOs at node $j+1$, we have $M'(i,j,d,k) = (1-b_{j+1}^l)F(i,j+1)M(i,j+1,d) + b_{j+1}^l M'(i,j+1,d,k)$. If $k=0$, $j=h$, and $D(p_{i,d}) \le \Omega$, $M'(i,j,d,k) = F(i,d)$. Otherwise, $M'(i,j,d,0) = 0$.

Suppose now that $k \neq 0$.

*Case 1:* $D(p_{i,j+1}) \le \Omega$ *and* $j \neq h$

Similar to $M(i,j,d)$, based on the availability of OEOs at node $j+1$, and the availability of wavelengths on path $p_{i,j+1}$, we have three subcases. When $E_{i,j+1}=0$, the 3R node $k$ is allocated to convert wavelengths.

$M'(i,j,d,k)$

$= \Pr\{H_{j+1}=1, E_{i,j+1}=1 \,|E_{i,k}=1\}\Pr\{G_{i,d}=1 \,|E_{i,j+1}=1, H_{j+1}=1\} + \Pr\{H_{j+1}=1,$

$E_{k,j+1}=1, E_{i,k}=1, E_{i,j+1}=0 \,|E_{i,k}=1\}\Pr\{G_{k,d}=1 \,|E_{k,j+1}=1, H_{j+1}=1\} + \Pr\{H_{j+1}=0,$

$G_{i,d}=1 \,|E_{i,k}=1, H_k=1\}$

$= (1-b^l_{j+1})\dfrac{F(i,j+1)}{F(i,k)}M(i,j+1,d) + (1-b^l_{j+1})\dfrac{F'(i,k,j+1)}{F(i,k)}M(k,j+1,d) + b^l_{j+1}$

$M'(i,j+1,d,k).$

*Case 2:* $D(p_{i,j+1}) > \Omega$, $D(p_{k,j+1}) \le \Omega$, *and* $j \neq h$

In this case, the 3R node $k$ is allocated to regenerate the signal, no matter the availability of wavelengths on path $p_{i,j+1}$. Based on the availability of OEOs at node $j+1$, we have two subcases.

$M'(i,j,d,k)$

$= \Pr\{H_{j+1}=1, E_{k,j+1}=1 \,|E_{i,k}=1\}\Pr\{G_{k,d}=1 \,|H_{j+1}=1, \quad E_{k,j+1}=1\} + \Pr\{H_{j+1}=0,$

$G_{i,d}=1 \,|E_{i,k}=1, H_k=1\}$

$= (1-b^l_{j+1})F(k,j+1)M(k,j+1,d) + b^l_{j+1}M'(i,j+1,d,k).$

*Case 3:* $j = h$

If $D(p_{i,d}) \le \Omega$, $M'(i,j,d,k) = \frac{F(i,d)}{F(i,k)} + \frac{F'(i,k,d)}{F(i,k)}$. If $D(p_{i,d}) > \Omega, D(p_{k,d}) \le \Omega$, $M'(i,j,d,k) = F(k,d)$.

## 6.9 Appendix C

In this appendix, we calculate several variables defined in Table 6.3. From the definitions in Table 6.3, we can write:

$$\bar{F}(u,v,t) = \begin{cases} 0, & \text{if } D(P_{u,v}) > \Omega \text{ or } D(P_{v,t}) > \Omega, \\ F_0(u,t) - F_0(u,v), & \text{otherwise.} \end{cases} \tag{6.43}$$

$$F'(u,v,t) = \begin{cases} 0, & \text{if } D(P_{u,v}) > \Omega \text{ or } D(P_{v,t}) > \Omega, \\ F_0(u,t) - F_0(u,v) - F(u,v)F_0(v,t), & \text{otherwise.} \end{cases} \tag{6.44}$$

Now, let us consider the path $p$. Assume the source $s$ and destination $d$ of the path are dummy 3R nodes, and let $b_s^l = 0$ and $b_d^l = 0$. Fig. 6.1 shows the positions of nodes $s$, $q$, $h$, $i$, $g$, $d$. Suppose the current 3R node under consideration is node $i$.

We will first find $X(s,i,g)$, the probability that the next 3R node (from $s$) with free OEOs is node $g$ (which means that all the 3R nodes $j$ between $i$ and $g$ have no free OEOs), there are available wavelengths on $p_{s,i}$, but there is no wavelength available on $p_{s,g}$. So we have,

$$X(s,i,g) = \begin{cases} (1-b_g^l)\prod_{j=i+1}^{g-1} b_j^l \bar{F}(s,i,g), & \text{if } D(P_{s,g}) \leq \Omega \\ 0. & \text{otherwise} \end{cases} \tag{6.45}$$

$X'(s,i,g)$ is the same as $X(s,i,g)$ except that it requires that there are available wavelengths on $p_{i,g}$ also; so by replacing $\bar{F}(s,i,g)$ in the previous equation with $F'(s,i,g)$, we have,

$$X'(s,i,g) = \begin{cases} (1-b_g^l)\prod_{j=i+1}^{g-1} b_j^l F'(s,i,g), & \text{if } D(P_{s,g}) \leq \Omega \\ 0. & \text{otherwise} \end{cases} \tag{6.46}$$

Now, we show the equations corresponding to the general case that the previously allocated 3R node is some node $h$ (as opposed to the source $s$). This implies that node $h$ has free OEOs, and this happens with probability $(1-b_h^l)$. Similar to $X(s,i,g)$, there are free OEOs at 3R node $g$, and no free OEOs at the 3R nodes $j$ between $i$ and $g$. Thus, we need to find the probability that there is no blocking from $s$ to $i$, and

there are available wavelengths on $p_{h,i}$, but there is no wavelength available on $p_{h,g}$. Assume the 3R node allocated before node $h$ is node $q$, and the first 3R node after $h$ with free OEOs is node $m$ ($m$ can be $i$). Now, note that node $h$, the previously allocated 3R node, may be allocated either to convert wavelengths, or to regenerate signals, depending on the distance of the path $p_{q,m}$. $X'(q,h,m)$ and $Z'(q,h,m)$ reflect these two cases, respectively. We thus have:

$$X(h,i,g) = (1-b_h^l)(1-b_g^l)\prod_{j=i+1}^{g-1} b_j^l \sum_{q=s}^{h-1}\left(\sum_{\substack{h+1\le m\le i,\\ D(p_{q,m})\le\Omega}} X'(q,h,m) + \sum_{\substack{h+1\le m\le i,\\ D(p_{q,m})>\Omega\\ D(p_{h,m})\le\Omega}} Z'(q,h,m)\right)$$

$$\begin{aligned}&\Pr\{E_{h,i}=1, E_{h,g}=0\,|E_{h,m}=1\}\\ &= (1-b_h^l)(1-b_g^l)\prod_{j=i+1}^{g-1} b_j^l \sum_{q=s}^{h-1}\left(\sum_{\substack{h+1\le m\le i,\\ D(p_{q,m})\le\Omega}} X'(q,h,m) + \sum_{\substack{h+1\le m\le i,\\ D(p_{q,m})>\Omega\\ D(p_{h,m})\le\Omega}} Z'(q,h,m)\right)\frac{\bar{F}(h,i,g)}{F(h,m)}.\end{aligned} \tag{6.47}$$

To find $X'(h,i,g)$, besides replacing $\bar{F}(h,i,g)$ with $F'(h,i,g)$, we also need to consider the case when $m=i$, since the value of $X'(h,i,g)$ will be used for the calculation of $X'(i,g,z)$ (or $Z'(i,g,z)$), which includes the probability that there are free OEOs at node $i$, that is $(1-b_i^l)$. However, if $m=i$, this probability is already included in $X'(q,h,m)$ and $Z'(q,h,m)$, and we need to subtract that probability from $X'(h,i,g)$. Let $I=1$ if $D(p_{q,i})\le\Omega$. We have,

$$\begin{aligned}X'(h,i,g) = (1-b_h^l)(1-b_g^l)\prod_{j=i+1}^{g-1} b_j^l \sum_{q=s}^{h-1}\Bigg(&\sum_{\substack{h+1\le m\le i-1,\\ D(p_{q,m})\le\Omega}} X'(q,h,m) + \frac{X'(q,h,i)}{1-b_i^l}I +\\ &\sum_{\substack{h+1\le m\le i-1,\\ D(p_{q,m})>\Omega\\ D(p_{h,m})\le\Omega}} Z'(q,h,m) + \frac{Z'(q,h,i)}{1-b_i^l}(1-I)\Bigg)\frac{F'(h,i,g)}{F(h,m)}.\end{aligned} \tag{6.48}$$

Then we consider $Z$ and $Z'$. $Z(s,i,g)$ is the probability that the next 3R node having free OEOs is node $g$, and there are available wavelengths on $p_{s,i}$. So we have,

$$Z(s,i,g) = \begin{cases} (1-b_g^l)\prod_{j=i+1}^{g-1} b_j^l F(s,i), & \text{if } D(P_{s,g}) > \Omega \\ 0. & \text{otherwise} \end{cases} \tag{6.49}$$

$Z'(s,i,g)$ is the same as $Z(s,i,g)$ except that it requires that there are available wavelengths on $p_{i,g}$ also. (Note that for $Z$, we don't care whether there are free wavelengths on $p_{s,g}$ as with $X$.) So we have,

$$Z'(s,i,g) = \begin{cases} (1-b_g^l)\prod_{j=i+1}^{g-1} b_j^l F(s,i)F(i,g), & \text{if } D(P_{s,g}) > \Omega \\ 0. & \text{otherwise} \end{cases} \tag{6.50}$$

Now we show the equations corresponding to the general case that the previously allocated 3R node is node $h$. As in finding $X(h,i,g)$, we also need the values of $X'(q,h,m)$ and $Z'(q,h,m)$, the difference being that we only need to include the probability that there are available wavelengths on $p_{h,i}$, without consideration of $p_{h,g}$.

$$Z(h,i,g) = (1-b_h^l)(1-b_g^l)\prod_{j=i+1}^{g-1} b_j^l \sum_{q=s}^{h-1}\left(\sum_{\substack{h+1\le m\le i,\\ D(p_{q,m})\le\Omega}} X'(q,h,m) + \sum_{\substack{h+1\le m\le i,\\ D(p_{q,m})>\Omega}} Z'(q,h,m)\right)$$

$$\begin{aligned}&\Pr\{E_{h,i}=1 \mid E_{h,m}=1\}\\ &= (1-b_h^l)(1-b_g^l)\prod_{j=i+1}^{g-1} b_j^l \sum_{q=s}^{h-1}\left(\sum_{\substack{h+1\le m\le i,\\ D(p_{q,m})\le\Omega}} X'(q,h,m) + \sum_{\substack{h+1\le m\le i,\\ D(p_{q,m})>\Omega\\ D(p_{h,m})\le\Omega}} Z'(q,h,m)\right)\frac{F(h,i)}{F(h,m)}.\end{aligned} \tag{6.51}$$

The difference between $Z'(h,i,g)$ and $Z(h,i,g)$ is that it includes the probability that there are available wavelengths on $p_{i,g}$ and we also need to consider the case $m=i$ as we did when finding $X'(h,i,g)$.

$$\begin{aligned}Z'(h,i,g) = (1-b_h^l)(1-b_g^l)\prod_{j=i+1}^{g-1} b_j^l \sum_{q=s}^{h-1}\Bigg(&\sum_{\substack{h+1\le m\le i-1,\\ D(p_{q,m})\le\Omega}} X'(q,h,m) + \frac{X'(q,h,i)}{1-b_i^l}I + \\ &\sum_{\substack{h+1\le m\le i-1,\\ D(p_{q,m})>\Omega\\ D(p_{h,m})\le\Omega}} Z'(q,h,m) + \frac{Z'(q,h,i)}{1-b_i^l}(1-I)\Bigg)\frac{F(h,i)F(i,g)}{F(h,m)}.\end{aligned} \tag{6.52}$$

## 6.10 Appendix D

In this Appendix, we show how to calculate $Y(a,b|m,u,v)$. $Y(a,b|m,u,v)$ can be computed by first picking the $a$ common wavelength-pairs from the $m$ common available wavelengths, and then selecting the $b$ different wavelengths from the remaining wavelengths. It is given by the following expression:

$$Y(a,b|m,u,v) = \binom{m}{a} Y(0,b|m-a,u-a,v-a). \tag{6.53}$$

If $b=0$, we have $Y(a,0|m,u,v) = \binom{m}{a}$.

Then,

$$\begin{aligned} &Y(0,b|m-a,u-a,v-a) \\ &= \binom{u-a}{b}\binom{v-a}{b} - \sum_{i=1}^{\min(b,m-a)} Y(i,b-i|m-a,u-a,v-a) \\ &= \binom{u-a}{b}\binom{v-a}{b} - \sum_{i=1}^{\min(b,m-a)} \binom{m-a}{i} Y(0,b-i|m-a-i,u-a-i,v-a-i). \end{aligned} \tag{6.54}$$

The above is derived as follows. We want $b$ different wavelength-pairs to be selected on the two links. To get this, we find the total number of ways of selecting $b$ wavelengths on each link from the set of available wavelengths, respectively (the first term), and then subtract from it the number of ways in which there are one or more common wavelength-pairs on the two links (the second term of the first equation). Now, notice that the second term is equal to what we are seeking, but with a smaller number wavelengths. We can thus compute $Y(\cdot)$ recursively, provided we know how to compute the base case. The base case is:

$$Y(0,1|m',u',v') = \begin{cases} \binom{m'}{1}\binom{v'-1}{1} + \binom{u'-m'}{1}\binom{v'}{1} & \text{if } v' \geq 2, u' \geq m'+1, m' \geq 1 \\ \binom{u'-m'}{1} & \text{if } v'=1, u' \geq m'+1 \\ \binom{u'}{1}\binom{v'}{1} & \text{if } m'=0 \\ \binom{m'}{1}\binom{v'-1}{1} & \text{if } m'=u', v' \geq 2. \end{cases} . \tag{6.55}$$

Here, $\binom{m'}{1}\binom{v'-1}{1}+\binom{u'-m'}{1}\binom{v'}{1}$ means if one wavelength on the first link is selected from a set of $m'$ wavelengths ($\binom{m'}{1}$ ways), then that wavelength cannot be selected on the second link ($\binom{v'-1}{1}$ ways). If the wavelength on the first link is not selected from the set of $m'$ wavelengths ($\binom{u'-m'}{1}$ ways), then the wavelength selected on the second link can be any one of the available wavelengths on the second link ($\binom{v'}{1}$ ways).

## 6.11 Appendix D

The probability $P(\alpha, K, \mathcal{C}_r, \mathcal{C}_c, \mathcal{C}_e, \mathcal{C}_f)$ in equation (6.35) is defined as the probability that there are $W-\mathcal{C}_c-\mathcal{C}_e$ available wavelengths on the first link, $W-\mathcal{C}_c-\mathcal{C}_f$ available wavelengths on the second link, there are $K$ available wavelengths on the both links, then randomly choose $\mathcal{C}_r$ wavelengths from the available wavelengths of each link, $\alpha$ wavelength pairs of $\mathcal{C}_r$ have the same wavelength of the two links, its calculation is in Appendix E.

To find it, let us define $P(\alpha, \mathcal{C}_r|K, \mathcal{C}_c, \mathcal{C}_e, \mathcal{C}_f)$ as follows. Suppose there are $W-\mathcal{C}_c-\mathcal{C}_e$ available wavelengths on the first link, $W-\mathcal{C}_c-\mathcal{C}_f$ available wavelengths on the second link, there are $K$ available (common) wavelengths on both links; then we randomly choose $\mathcal{C}_r$ wavelengths from the available wavelengths on each link ($\mathcal{C}_r$ from the first link and, independently, $\mathcal{C}_r$ from the second link). Then, the probability that $\alpha$ wavelength pairs of $\mathcal{C}_r$ have the same wavelength on the two links is denoted by $P(\alpha, \mathcal{C}_r|K, \mathcal{C}_c, \mathcal{C}_e, \mathcal{C}_f)$.

Now, we can write

$$P(\alpha, \mathcal{C}_r|K, \mathcal{C}_c, \mathcal{C}_e, \mathcal{C}_f) = \frac{Y(\alpha, \mathcal{C}_r-\alpha, K, W-\mathcal{C}_c-\mathcal{C}_e, W-\mathcal{C}_c-\mathcal{C}_f)}{\binom{W-\mathcal{C}_c-\mathcal{C}_e}{\mathcal{C}_r}\binom{W-\mathcal{C}_c-\mathcal{C}_f}{\mathcal{C}_r}}. \tag{6.56}$$

Using the law of total probability, we then have

$$\begin{aligned} &P(\alpha, K, \mathcal{C}_r, \mathcal{C}_c, \mathcal{C}_e, \mathcal{C}_f) \\ &= P(\alpha, \mathcal{C}_r|K, \mathcal{C}_c, \mathcal{C}_e, \mathcal{C}_f)P(K, \mathcal{C}_c, \mathcal{C}_e, \mathcal{C}_f) \\ &= P(\alpha, \mathcal{C}_r|K, \mathcal{C}_c, \mathcal{C}_e, \mathcal{C}_f)P(K|\mathcal{C}_c, \mathcal{C}_e, \mathcal{C}_f)\sum_{\mathcal{C}_r}\boldsymbol{\pi}(\mathcal{C}_e, \mathcal{C}_f, \mathcal{C}_c, \mathcal{C}_r) \end{aligned} \tag{6.57}$$

where,

$$P(K|\mathcal{C}_c,\mathcal{C}_e,\mathcal{C}_f) = \frac{\binom{W}{\mathcal{C}_c}\binom{W-\mathcal{C}_c}{\mathcal{C}_e}\binom{W-\mathcal{C}_c-\mathcal{C}_e}{K}\binom{\mathcal{C}_e}{W-\mathcal{C}_c-\mathcal{C}_f-K}}{\binom{W}{\mathcal{C}_c}\binom{W-\mathcal{C}_c}{\mathcal{C}_e}\binom{W-\mathcal{C}_c}{\mathcal{C}_f}}$$
$$= \frac{\binom{W-\mathcal{C}_c-\mathcal{C}_e}{K}\binom{\mathcal{C}_e}{W-\mathcal{C}_c-\mathcal{C}_f-K}}{\binom{W-\mathcal{C}_c}{W-\mathcal{C}_c-\mathcal{C}_f}}. \tag{6.58}$$

Table 6.1: Basic Notation

| **Symbol** | **Meaning** |
|---|---|
| $n$ | an arbitrary node |
| $l$ | an arbitrary link ( $l_{a,b}$ is a link from node $a$ to node $b$) |
| $p$ | an arbitrary path ( $p_{s,d}$ is the path from node $s$ to node $d$) |
| $D(p)$ | the length of path $p$ |
| $R$ | the total number of OEOs per 3R node's outgoing link |
| $W$ | the total number of wavelengths per link per direction |
| $\Omega$ | the transmission reach (TR) |
| $\lambda_{s,d}$ | the arrival rate of connection $s, d$ |
| $\lambda_p$ | the arrival rate on path $p$, $\lambda_{p_{s,d}} = \lambda_{s,d}$ |
| $B_{s,d}$ | the blocking probability of connection $s, d$ |
| $A_{s,d}$ | the acceptance probability of connection $s, d$ |
| $B_N$ | the network blocking probability, $B_N = \frac{\sum_{s,d} \lambda_{s,d} B_{s,d}}{\sum_{s,d} \lambda_{s,d}}$ |
| $b_n^l$ | the probability that there is no available OEOs at 3R node $n$ on outgoing link $l$ |
| $\rho_l$ | the offered load of link $l$ |
| $\mu$ | $= 1$, the average duration of each connection |
| $E_{u,v}$ | an indicator function; =1 if there are available wavelengths on path $p_{u,v}$ without OEO converter allocation |
| $H_n$ | an indicator function; =1 if there are available OEOs at node $n$ |
| $G_{u,v}$ | an indicator function; =1 if there is no blocking on path $p_{u,v}$ (some OEO converters maybe allocated to make it true) |
| $F_k(u, v)$ | the probability that there are exactly $k$ available wavelengths on the path $p_{u,v}$ without OEO converter allocation |
| $F(u, v)$ | $= \sum_{k=1}^{W} F_k(u, v)$, the probability that there are available wavelengths on path $p_{u,v}$ without OEO converter allocation |

Table 6.2: Notation for paths with two or more links

| **Symbol** | **Meaning** |
|---|---|
| $\mathcal{C}_e$ | the number of connections that use link $a$-$b$ only |
| $\mathcal{C}_f$ | the number of connections that use link $b$-$c$ only |
| $\mathcal{C}_c$ | the number of connections that use both links $a$-$b$ and $b$-$c$, but do not use OEOs at node $b$ |
| $\mathcal{C}_r$ | the number of connections that use both links $a$-$b$ and $b$-$c$, and OEOs at node $b$ are allocated to regenerate signals |
| $\mathcal{C}_w$ | the number of connections that use both links $a$-$b$ and $b$-$c$, and OEOs at node $b$ are allocated to convert wavelengths |
| $\rho_e$ | the offered load for $\mathcal{C}_e$ type connections |
| $\rho_f$ | the offered load for $\mathcal{C}_f$ type connections |
| $\rho_c$ | the offered load for $\mathcal{C}_c$ type connections |
| $\rho_r$ | the offered load for $\mathcal{C}_r$ type connections |
| $\rho_w$ | the offered load for $\mathcal{C}_w$ type connections |
| $\mathcal{P}_1(h\|i,j,k)$ | the probability that there are $h$ available wavelengths on a two-hop path given that there are $i$ available wavelengths on the first hop, there are $j$ available wavelengths on the second hop and $k$ connections use the same wavelengths on both hops |
| $\mathcal{P}_2(i)$ | the probability that there are $i$ available wavelengths on a link |
| $\mathcal{P}_3(j\|i)$ | the probability that there are $j$ available wavelengths on a link of a path given that there are $i$ available wavelengths on the previous link of the path |
| $\mathcal{P}_4(k\|i,j)$ | the probability that there are $k$ connections that use the same wavelengths on the current link and the previous link of a path given that there are $i$ available wavelengths on previous link, and $j$ available wavelengths on current link |
| $T^m(h,e)$ | the probability that there are $h$ available wavelengths on a path with $m$ hops, and there are $e$ available wavelengths on the last hop of the path |
| $\hat{x}_n^l(p)$ | the offered load to 3R node $n$ on outgoing link $l$ for path $p$ to convert wavelengths |

Table 6.3: Notation to calculate $\rho_r$ and $\rho_w$

| **Symbol** | **Meaning** |
|---|---|
| $\hat{F}(u,v)$ | $= 0$, if $D(P_{u,v}) > \Omega$; otherwise, $\hat{F}(u,v) = F(u,v)$ |
| $\bar{F}(u,v,t)$ | $= 0$, if $D(P_{u,v}) > \Omega$ or $D(P_{v,t}) > \Omega$; otherwise, it is the probability that $E_{u,v} = 1$ and $E_{u,t} = 0$ |
| $F'(u,v,t)$ | $= 0$, if $D(P_{u,v}) > \Omega$ or $D(P_{v,t}) > \Omega$; otherwise, it is the probability that $E_{u,v} = 1$, $E_{v,t} = 1$, and $E_{u,t} = 0$ |
| $X(u,v,t)$ | given $D(p_{u,t}) \leq \Omega$, the probability that $G_{s,v} = 1$, the previously allocated 3R node of the path is node $u$, the next 3R node with available OEOs on the path is node $t$, and $E_{u,v} = 1$, $E_{u,t} = 0$ |
| $X'(u,v,t)$ | given $D(p_{u,t}) \leq \Omega$, the probability that $G_{s,v} = 1$, the previously allocated 3R node of the path is node $u$, the next 3R node with available OEOs on the path is node $t$, $E_{u,v} = 1$, $E_{v,t} = 1$, and $E_{u,t} = 0$ |
| $Z(u,v,t)$ | given $D(p_{u,t}) > \Omega$, $D(p_{u,v}) \leq \Omega$ and $D(p_{v,t}) \leq \Omega$, the probability that $G_{s,v} = 1$, the previously allocated 3R node of the path is node $u$, the next 3R node with available OEOs on the path is node $t$, and $E_{u,v} = 1$ |
| $Z'(u,v,t)$ | given $D(p_{u,t}) > \Omega$, $D(p_{u,v}) \leq \Omega$ and $D(p_{v,t}) \leq \Omega$, the probability that $G_{s,v} = 1$, the previously allocated 3R node of the path is node $u$, the next 3R node with available OEOs on the path is node $t$, $E_{u,v} = 1$, and $E_{v,t} = 1$ |

# Chapter 7 Conclusions and Future Directions

## 7.1 Conclusions

This dissertation investigated several problems of resource allocation in translucent optical networks with physical layer impairments. The research objective was to minimize the blocking probability for dynamic traffic by effectively allocating the limited OEO converters and frequency resources, while considering the transmission reach limit resulting from the physical layer impairments.

In Chapters 2 and 3, we investigated the QoT-aware routing and wavelength assignment problem in translucent optical networks for both intra-domain connections and inter-domain connections, respectively. A novel algorithm based on Dynamic Programming, called DP, was proposed. The simulation results showed that the DP algorithm outperformed all existing algorithms in the literature in terms of blocking probability. For inter-domain connections, we used the Backward Recursive Path Computation (BRPC) framework to develop new algorithms that require different pieces of information to be exchanged between domains. Our results suggested that some pieces of information were more critical than others.

In Chapter 4, we studied the QoT-aware grooming, routing and wavelength assignment problem in Mixed-Line-Rate translucent optical networks. An effective heuristic called LG was proposed, which was based on logical graphs. By comparison with other heuristics, LG could achieve lower blocking probability. The simulation results also showed that serving a connection using multiple paths can improve the performance considerably.

In Chapter 5, we addressed the virtual network mapping and OOFDM subcarrier assignment problem in OOFDM-based elastic optical networks for both static and

dynamic traffic. Two heuristics called LL and FF based on list scheduling were proposed. Simulation results showed that LL achieved better performance than FF.

In Chapter 6, we developed analytical models for calculating connection blocking probabilities in physically-impaired translucent networks for three regenerator allocation methods. The models were thoroughly validated using extensive simulation results for both mesh and ring networks. We developed models that assumed both link load independence and load correlation between adjacent links on a path. Our results suggested that the independence model was not accurate enough, even though it was considerably less complex than the correlation model. Further, our results confirmed that ignoring the transmission reach when allocating regenerators could affect the performance drastically.

## 7.2 Future Directions

Our work can be extended in a number of directions, and we point out a few below.

### 7.2.1 Advanced Reservation

This dissertation was focused on the immediate reservation (IR) case, where a connection is required to be set up as soon as it arrives. This scheme is usually used for delay-sensitive applications. There are a number of applications, e.g., scheduled file transfers, where the connection is not required to be set up immediately; for instance, the connection may only have to be set up within a specified time window. In this case, called as Advance Reservation (AR), one has the flexibility of allocating resources as well as scheduling the connections, and resource utilization can potentially been improved. Many papers exist in the literature on AR [60–65]. However, there does not appear to exist any work on impairment-aware RWA for AR in translucent optical networks with dynamic traffic. An interesting direction is to extend our work for the AR case.

### 7.2.2 Survivable Translucent Optical Networking

Yet another direction for future research is impairment-aware resource allocation for survivable translucent optical networks. Survivability is a critical issue in high-capacity optical networks. A short disconnection can result in terabits of data being lost. There are two main methods to address failures in optical networks. One is protection, where backup resources are allocated to each connection; if some failures occur, the source and destination are still connected by using these backup resources. The protection can be path protection, wherein there is an end-to-end backup path (e.g., a path that is disjoint from the primary path) assigned to the connection. Alternatively, the protection can be applied to links; in this case, each link is assigned a backup path, and any traffic transiting a failed link is switched over to the backup path. Protection can guarantee recovery from failures for which the methods are designed, but it generally requires a significant amount of resources that may never need to be used, if there are no failures.

In contrast to protection, restoration does not reserve any resources and relies on the network control algorithms to dynamically find backup resources when failures occur. Obviously, restoration requires no dedicated backup resources, but does not guarantee recovery. Much work exists in the literature on survivable optical networks [66–71]. Recently, survivability methods for networks with impairments have begun to be explored [72–77]. However, to the best of our knowledge, we are not aware of any RWA algorithms for survivable translucent networks with impairments, multiple failures, and availability considerations for dynamic traffic. A significant extension of our work is to develop algorithms for such networks.

High capacity optical connections have long holding times and are typically provisioned through a contract. A Service Level Agreement (SLA), which is usually part of the contract, typically specifies the desired availability of the connection (for instance, the connection's availability must be 99.99% of the time, e.g., one month (30 days), which translates to a maximum of 4.32 minutes of downtime). An interesting optimization objective is to allocate resources judiciously so that each connection's

SLA requirement can be met (with high probability, since failures are random events) while maximizing the network's utilization.

### 7.2.3 Analytical Models

Future extensions for the analytical performance models can consider alternate paths, such as $K$ shortest paths; other wavelength assignment methods, such as First-Fit; grooming; multiple paths and the share-per-node OEO sharing model. Moreover, analytical performance models for Mixed Line Rate networks and elastic networks are yet to be developed.

# Bibliography


[1] A. Pontes, A. Drummond, N. da Fonseca, and A. Jukan, "PCE-based inter-domain lightpath provisioning," in *Proc. ICC*. IEEE, 2012, pp. 3073–3078.

[2] G. Hernndez-Sola, J. Perell, F. Agraz, S. Spadaro, J. Comellas, and G. Junyent, "Scalable hybrid path computation procedure for pce-based multi-domain WSON networks," in *International Conference on Transparent Optical Networks (ICTON)*. IEEE, 2011.

[3] R. Nejabati, E. Escalona, P. Shuping, and D. Simeonidou, "Optical network virtualization," in *Optical Network Design and Modeling (ONDM)*, Feb. 2011.

[4] I. B. Djordjevic and B. Vasic, "Orthogonal frequency division multiplexing for high-speed optical transmission," *Optics Express*, vol. 14, no. 9, pp. 3767–3775, 2006.

[5] W. Wei, J. Hu, D. Qian, P. Ji, T. Wang, X. Liu, and C. Qiao, "PONIARD: A programmable optical networking infrastructure for advanced research and development of future internet," *J. Lightwave Technol.*, vol. 27, no. 3, pp. 233 – 242, Feb. 2009.

[6] M. Jinno, B. Kozicki, H. Takara, A.Watanabe, Y. Sone, T. Tanaka, and A. Hirano, "Distance-adaptive spectrum resource allocation in spectrum-sliced elastic optical path network," vol. 48, no. 8, pp. 138 – 145, Aug. 2010.

[7] K. Manousakis, P. Kokkinos, K. Christodoulopoulos, and E. Varvarigos, "Joint online routing, wavelength assignment and regenerator allocation in translucent

optical networks," *J. Lightwave Technol.*, vol. 28, no. 8, pp. 1152–1163, Apr. 2010.

[8] X. Yang and B. Ramamurthy, "Dynamic routing in translucent WDM optical networks: the intradomain case," *J. Lightwave Technol.*, vol. 23, no. 3, pp. 955–971, Mar. 2005.

[9] S. Pachnicke, N. Luck, and P. M. Krummrich, "Online physical-layer impairment-aware routing with quality of transmission constraints in translucent optical networks," in *International Conference on Transparent Optical Networks (ICTON)*, 2009.

[10] F. Kuipers, A. Beshir, A. Orda, and P. V. Mieghem, "Impairmentaware path selection and regenerator placement in translucent optical networks," in *the 18th IEEE International Conference on Network Protocols (ICNP)*, 2010.

[11] N. Sambo, N. Andriolli, A. Giorgetti, L. Valcarenghi, F. Cugini, and P. Castoldi, "Accounting for shared regenerators in GMPLS-controlled translucent optical networks," *J. Lightwave Technol.*, vol. 27, no. 19, pp. 4338–4347, Oct. 2009.

[12] R. Martínez, R. Casellas, R. Muñoz, and T. Tsuritani, "Experimental translucent-oriented routing for dynamic lightpath provisioning in GMPLS-enabled wavelength switched optical networks," *J. Lightwave Technol.*, vol. 28, no. 8, pp. 1241–1255, Apr. 2010.

[13] S. Rai, S. Ching-Fong, and B. Mukherjee, "On provisioning in alloptical networks: An impairment-aware approach," *IEEE/ACM Trans. Networking*, vol. 17, no. 6, pp. 1989–2001, Dec. 2009.

[14] V. Chava, E. Salvadori, A. Zanardi, S. Dalsass, G. Galimberti, A. Tanzi, G. Martinelli, and O. Gerstel, "Impairment and regenerator aware lightpath setup using distributed reachability graphs," in *Proc. Infocom*, 2011.

[15] E. Tordera, R. Martinez, R. Munoz, R. Casellas, and J. Sole-Pareta, "Improving IA-RWA algorithms in translucent networks by regenerator allocation," in *International Conference on Transparent Optical Networks (ICTON)*, 2009.

[16] P. Poggiolini, "The GN model of non-linear propagation in uncompensated coherent optical systems," *J. Lightwave Technol.*, 2012.

[17] A. Carena, V. Curri, G. Bosco, P. Poggiolini, and F. Forghieri, "Modeling of the impact of nonlinear propagation effects in uncompensated optical coherent transmission links," *J. Lightwave Technol.*, vol. 30, no. 10, May 2012.

[18] J. Zhao, S. Subramaniam, and M. Brandt-Pearce, "Cross layer RWA in translucent optical networks," in *Proc. ICC*. IEEE, 2012.

[19] ——, "Inter-domain QoT-aware RWA for translucent optical networks," in *Proc. International Conference on Computing, Networking and Communications (ICNC)*, 2013.

[20] J. Y. Yen, "Finding the K shortest loopless paths in a network," *Management Science*, vol. 17, no. 11, pp. 712–716, July 1971.

[21] R. Casellas, R. Martinez, R. Munoz, and S. Gunreben, "Enhanced backwards recursive path computation for multi-area wavelength switched optical networks under wavelength continuity constraint," *IEEE/ACM Trans. Networking*, vol. 1, no. 2, pp. A180–A193, July 2009.

[22] S. Spadaro, J. Perelló, G. Hernández-Sola, A. Moreno, F. Agraz, J. Comellas, and G. Junyent, "Analysis of traffic engineering information dissemination strategies in PCE-based multi-domain optical networks," in *International Conference on Transparent Optical Networks (ICTON)*, 2010.

[23] F. Cugini, F. Paolucci, L.Valcarenghi, P. Castoldi, and A. Welin, "PCE communication protocol for resource advertisement in multi-domain BGP-based networks," in *Proc. OFC*, 2009.

[24] L. Liu, R. Casellas, T. Tsuritani, I. Morita, R. Martínez, and R. Muñoz, "Lab trial of PCE-based OSNR-aware dynamic restoration in multi-domain GMPLS-enabled translucent WSON," in *European Conference and Exhibition on Optical Communication (ECOC)*, 2011.

[25] R. Casellas, R. Martínez, R. Muñoz, L. Liu, T. Tsuritani, I. Morita, and M. Tsurusawa, "Dynamic virtual link mesh topology aggregation in multi-domain translucent WSON with hierarchical-PCE," in *European Conference and Exhibition on Optical Communication (ECOC)*, 2011.

[26] X.Yang and B. Ramamurthy, "Interdomain dynamic wavelength routing in the next-generation translucent optical internet," *Optical Communications and Networking, IEEE/OSA Journal of*, vol. 3, no. 3, pp. 169–187, 2004.

[27] M. Yannuzzi, E. Marín-Tordera, R. Serral-Gracià, X. Masip-Bruin, O. González, J. Jiménez, and D. Verchere, "Modeling physical-layer impairments in multidomain optical networks," in *Optical Network Design and Modeling (ONDM)*, 2011.

[28] M. Batayneh, D. A. Schupke, M. Hoffmann, A. Kirstaedter, and B. Mukherjee, "On routing and transmission-range determination of multi-bit-rate signals over mixed-line-rate WDM optical networks for carrier ethernet," *IEEE/ACM Trans. Networking*, vol. 19, no. 5, pp. 1304–1316, 2011.

[29] A. Nag, M. Tornatore, and B. Mukherjee, "Optical network design with mixed line rates and multiple modulation formats," *J. Lightwave Technol.*, vol. 28, no. 4, pp. 466–475, 2010.

[30] J. Santos, J. Pedro, P. Monteiro, and J. Pires, "Cost-optimized planning for supporting 100 Gb/s and 40 Gb/s services over channel count-limited optical transport networks," in *Proc. ICC*, 2011.

[31] K. Christodoulopoulos, K. Manousakis, and E. Varvarigos, "Reach adapting algorithms for mixed line rate WDM transport networks," *J. Lightwave Technol.*, vol. 29, no. 21, pp. 3350–3363, 2011.

[32] M. Liu, M. Tornatore, and B. Mukherjee, "New strategies for connection protection in mixed-line-rate optical WDM networks," *Optical Communications and Networking, IEEE/OSA Journal of*, vol. 3, no. 9, pp. 641– 650, 2011.

[33] P. Chowdhury, M. Tornatore, A. Nag, T. W. E. Ip, and B. Mukherjee, "On the design of energy-efficient mixed-line-rate (MLR) optical networks," *J. Lightwave Technol.*, vol. 30, no. 1, pp. 130–139, 2012.

[34] A. Klekamp, U. Gebhard, and F. Ilchmann, "Energy and cost efficiency of adaptive and mixed-line-rate IP over DWDM networks," *J. Lightwave Technol.*, vol. 30, no. 2, pp. 215 –221, 2012.

[35] M. Batayneh, B. Mukherjee, D. A. Schupke, M. Hoffmann, and A. Kirstaedter, "Carrier-grade ethernet: Etherpath protection vs. ethertunnel protection," *IEEE Network*, vol. 23, no. 3, pp. 10–17, 2009.

[36] C. Taunk, S. Bidkar, C. V. Saradhi, and A. Gumaste, "Impairment aware RWA based on a K-shuffle edge-disjoint path solution(IA-KS-EDP)," in *Proc. OFC*, 2011.

[37] N. Sambo, M. Secondini, F. Cugini, G. Bottari, P. Iovanna, F. Cavaliere, and P. Castoldi, "Modeling and distributed provisioning in 10-40-100Gb/s multirate wavelength switched optical networks," *J. Lightwave Technol.*, vol. 29, no. 9, pp. 1248–1257, 2011.

[38] F. Paolucci, N. Sambo, F. Cugini, A. Giorgetti, and P. Castoldi, "Experimental demonstration of impairment-aware PCE for multi-bit-rate WSONs," *J. Lightwave Technol.*, vol. 3, no. 8, pp. 610–619, 2011.

[39] Y. Chen, N. Hua, X. Zheng, and H. Zhang, "Dynamic connection provisioning in mixed-line-rate optical networks," in *Communications and Photonics Conference and Exhibition (ACP)*, 2010.

[40] X. Wang, M. Brandt-Pearce, and S. Subramaniam, "Grooming and RWA in

translucent dynamic mixed-line-rate WDM networks with impairments," in *Proc. OFC*, 2012.

[41] G. Shen and R. S. Tucker, "Sparse traffic grooming in translucent optical networks," *J. Lightwave Technol.*, vol. 27, no. 20, pp. 4471–4479, Oct. 2009.

[42] S. Chen, I. Ljubi, and S. Raghavan, "The regenerator location problem," *Networks - Network Optimization*, vol. 55, no. 3, pp. 205–220, May 2010.

[43] O. Rival and A. Morea, "Resource requirements in mixed-line rate and elastic dynamic optical networks," in *Proc. OFC*, 2012.

[44] M. Yu, Y. Yi, J. Rexford, and M. Chiang, "Rethinking virtual network embedding: substrate support for path splitting and migration," in *ACM SIGCOMM*, April 2008.

[45] N. G. Duffield, P. Goyal, and A. Greenberg, "A flexible model for resource management in virtual private networks," in *ACM SIGCOMM*, Aug. 1999.

[46] B. Kozicki, H. Takara, T. Yoshimatsu, K. Yonenaga, and M. Jinno, "Filtering characteristics of highly-spectrum efficient spectrum-sliced elastic optical path (SLICE) network," in *Proc. OFC*, March 2009.

[47] S. Blouza, J. Karaki, N. Brochier, E. L. Rouzic, E. Pincemin, and B. Cousin, "Multi-band OFDM networking concepts," in *Conference on telecommunications*, April 2011.

[48] K. Christodoulopoulos, I. Tomkos, and E. A. Varvarigos, "Elastic bandwidth allocation in flexible OFDM-based optical networks," *J. Lightwave Technol.*, vol. 29, no. 9, pp. 1354 – 1366, May 2011.

[49] X. Chu, B. Li, and Z. Zhang, "A dynamic RWA algorithm in a wavelength-routed all-optical network with wavelength converters," in *Proc. Infocom*, Apri 2003.

[50] M. Kovacevic and A. Acampora, "Benefits of wavelength translation in all-optical clear-channel networks," *IEEE J. Select. Areas Commun.*, vol. 14, no. 5, pp. 868–880, 1996.

[51] A. Birman, "Computing approximate blocking probabilities for a class of all-optical networks," *IEEE J. Select. Areas Commun.*, vol. 14, no. 5, pp. 852– 857, 1996.

[52] J. P. Lang, V. Sharma, and E. A. Varvarigos, "An analysis of oblivious and adaptive routing in optical networks with wavelength translation," *IEEE/ACM Trans. Networking*, vol. 9, no. 4, pp. 503–517, 2001.

[53] H. Harai, M. Murata, and H. Miyahara, "Performance of alternate routing methods in all-optical switching networks," in *Proc. Infocom*, Apri 1997.

[54] J. Triay, C. Cervello-Pastor, and V. M.Vokkarane, "Analytical blocking probability model for hybrid immediate and advance reservations in optical WDM networks," *IEEE/ACM Trans. Networking*, vol. PP, no. 99, p. 1, 2013.

[55] T. Onur and S. Subramaniam, "Performance of optical networks with limited reconfigurability," *IEEE/ACM Trans. Networking*, vol. 17, no. 6, pp. 2002–2013, 2009.

[56] P. Yvan, B.-P. Maite, and S. Subramaniam, "Analysis of blocking probability in noise- and cross-talk-impaired all-optical networks," vol. 1, no. 6, pp. 543 –554, 2009.

[57] J. He, M. Brandt-Pearce, and S. Subramaniam, "Analysis of blocking probability for first-fit wavelength assignment in transmission-impaired optical networks," vol. 3, no. 5, pp. 411 –425, 2011.

[58] S. Subramaniam, M. Azizoglu, and A. K. Somani, "All-optical networks with sparse wavelength conversion," *IEEE/ACM Trans. Networking*, vol. 4, no. 4, pp. 544–557, 1996.

[59] A. Girard, *Routing and Dimensioning in Circuit-Switched Networks, Chapter 4*, 1990.

[60] E. Varvarigos, V. Sourlas, and K. Christodoulopoulos, "Routing and scheduling connections in networks that support advance reservations," in *Broadband Communications, Networks and Systems (BROADNETS)*, 2008.

[61] A. Patel and J.Jue, "Routing and scheduling for variable bandwidth advance reservation," *Optical Communications and Networking, IEEE/OSA Journal of*, vol. 3, no. 12, pp. 912–923, Dec. 2011.

[62] N. Charbonneau and V. Vokkarane, "Static routing and wavelength assignment for multicast advance reservation in all-optical wavelength-routed WDM networks," *Optical Communications and Networking, IEEE/OSA Journal of*, vol. 20, no. 1, pp. 1–14, Feb. 2012.

[63] C. Xie, F. Xu, N. Ghani, E. Chaniotakis, C. Guok, and T. Lehman, "Load-balancing for advance reservation connection rerouting," *IEEE Commun. Lett.*, vol. 14, no. 6, 2010.

[64] S. Steven, W. Lee, A. Chen, and M. C. Yuang, "A lagrangean relaxation based near-optimal algorithm for advance lightpath reservation in WDM networks," *Photonic Network Communications*, vol. 19, no. 1, pp. 103–109, Feb. 2010.

[65] T. Entel, A. Gadkar, and V. M. Vokkarane, "Static manycast advance reservation in split-incapable optical networks," in *Proc. ICC*, 2013.

[66] Y. Yamada, H. Hasegawa, and K. Sato, "Survivable hierarchical optical path network design with dedicated wavelength path protection," *J. Lightwave Technol.*, vol. 21, no. 29, pp. 3196–3209, Nov. 2011.

[67] X. Shao, Y. Bai, X. Cheng, Y.-K. Yeo, L. Zhou, and L. H. Ngoh, "Best effort SRLG failure protection for optical WDM networks," *Optical Communications and Networking, IEEE/OSA Journal of*, vol. 3, no. 9, pp. 739–749, Sept. 2011.

[68] M. Liu, M. Tornatore, and B. Mukherjee, "New strategies for connection protection in Mixed-Line-Rate optical WDM networks," *Optical Communications and Networking, IEEE/OSA Journal of*, vol. 3, no. 9, pp. 641–650, Sept. 2011.

[69] P. Soproni, P. Babarczi, J.Tapolcai, and T. C. an Pin-Han Ho, "A meta-heuristic approach for non-bifurcated dedicated protection in WDM optical networks," in *Design of Reliable Communication Networks (DRCN)*, 2011.

[70] J. Lopez, Y. Ye, V. Lopez, F. Jimenez, R. Duque, F. Musumeci, A. Pattavina, and P. Krummrich, "Differentiated quality of protection to improve energy efficiency of survivable optical transport networks," in *Proc. OFC*, 2013.

[71] C. Cavdar, M.Tornatore, F. Buzluca, and B. Mukherjee, "Shared-path protection with delay tolerance (SDT) in optical WDM mesh networks," *J. Lightwave Technol.*, vol. 29, no. 14, pp. 2068–2076, 2010.

[72] C. P. Lai, F. Fidler, P. J. Winzer, M. K. Thottan, and K. Bergman, "Cross-layer proactive packet protection switching," *Optical Communications and Networking, IEEE/OSA Journal of*, vol. 4, no. 10, pp. 847–857, Oct. 2012.

[73] A. Askarian, Y. Zhai, S. Subramaniam, Y. Pointurier, and M. Brandt-Pearce, "Cross-layer approach to survivable DWDM network design," *Optical Communications and Networking, IEEE/OSA Journal of*, vol. 2, no. 6, pp. 319–331, June 2010.

[74] C. Gao, H. C. Cankaya, A. N. Patel, J. P. Jue, X. Wang, Q. Zhang, P. Palacharla, and M. Sekiya, "Survivable impairment-aware traffic grooming and regenerator placement with connection-level protection," *Optical Communications and Networking, IEEE/OSA Journal of*, vol. 4, no. 3, pp. 259–270, Feb. 2012.

[75] A. Manolov, I. Cerutti, R. Muoz, S. Ruepp, A. Giorgetti, N. Andriolli, N. Sambo, P. Castoldi, R. Martnez, and R. Casellas, "Distributed sharing of functionalities and resources in survivable GMPLS-controlled WSONs," *Optical Communica-*

*tions and Networking, IEEE/OSA Journal of*, vol. 4, no. 3, pp. 219–228, Feb. 2012.

[76] S. Azodolmolky, M. Klinkowski, Y. Pointurier, M. Angelou, D. Careglio, J. Sole-Pareta, and I. Tomkos, "A novel offline physical layer impairments aware RWA algorithm with dedicated path protection consideration," *J. Lightwave Technol.*, vol. 28, no. 20, pp. 3029–3040, Oct. 2010.

[77] J. Perello, S. Spadaro, F. Agraz, M. Angelou, S. Azodolmolky, Y. Qin, R. Nejabati, D. Simeonidou, P. Kokkinos, E. Varvarigos, S. A. Zahr, M. Gagnaire, and I. Tomkos, "Experimental demonstration of a GMPLS-enabled impairment-aware lightpath restoration scheme," *Optical Communications and Networking, IEEE/OSA Journal of*, vol. 4, no. 5, pp. 344–355, May 2012.